

University of Southern Queensland  
Faculty of Engineering and Surveying

# **Experimental Investigation into the Uplift Capacity of Ground Anchors in Sand**

A dissertation submitted by

**Jotham Ariel Kennedy**

In fulfilment of the requirements of

**Courses ENG4111 and ENG4112 Research Project**

towards the degree of

**Bachelor of Engineering (CIVIL)**

Submitted: November, 2010

---

# Abstract

Many modern engineering structures require a foundation system that provides adequate support by resisting loads that are imposed on the foundation of the structure or vertical and horizontal pullout forces. Stability and support of structures is provided by transferring foundational loads from the structures foundation through some form of anchors and then onto the surrounding soil and terrain. In many cases these loads and forces that are transmitted through anchors to surrounding terrain can cause the anchor to experience subsequent uplift forces. As a result, ground anchors have been developed so as to be fixed to structures and are embedded to sufficient ground depths to provide adequate amounts of support within required safety limits. It is therefore the primary focus of this project and subsequent dissertation to investigate the uplift capacity of various ground anchors in sand.

Ground anchors have in fact been utilised for thousands of years in many different forms. Predominantly the use of these early anchors was to support lightweight structures only and it was not until recent times with the invention of suspension bridges that anchors were used to transfer very large loads. As a result, during the last 50 years there have been a number of studies conducted to investigate the design and use of these ground anchors. A number of theories have been developed to estimate the ultimate uplift capacity of different ground anchors in sand and it is the aim of this investigation to take a predominantly physical approach to further investigate and test this pullout phenomenon. A Basic two-dimensional situation shall provide the primary focus of this investigation, however some initial investigation into three-dimensional effects shall be conducted and will therefore provide opportunity for further works in this area.

The primary focus of the project is the physical of plate anchors, buried pipelines in sand and pile anchors in sand. The focus of these physical investigations shall include investigation into the failure mechanism, the load-displacement relationship, variation of peak uplift load with changing embedment ratio and variation of the break-out factor with the embedment ratio. This results shall be compared to existing results in this field. Finally, this research project will be run in cooperation with a PIV investigation and will therefore include some PIV results for these investigations.

---

University of Southern Queensland  
Faculty of Engineering and Surveying

**ENG4111 Research Project Part 1 &  
ENG4112 Research Project Part 2**

**Limitations of Use**

The Council of the University of Southern Queensland, its Faculty of Engineering and Surveying, and the staff of the University of Southern Queensland, do not accept any responsibility for the truth, accuracy or completeness of material contained within or associated with this dissertation.

Persons using all or any part of this material do so at their own risk, and not at the risk of the Council of the University of Southern Queensland, its Faculty of Engineering and Surveying or the staff of the University of Southern Queensland.

This dissertation reports an educational exercise and has no purpose or validity beyond this exercise. The sole purpose of the course "Project and Dissertation" is to contribute to the overall education within the student's chosen degree programme. This document, the associated hardware, software, drawings, and other material set out in the associated appendices should not be used for any other purpose: if they are so used, it is entirely at the risk of the user.



**Prof Frank Bullen**

Dean  
Faculty of Engineering and Surveying

---

## **Certification**

I certify that the ideas, designs and experimental work, results, analyses and conclusions set out in this dissertation are entirely my own effort, except where otherwise indicated and acknowledged.

I further certify that the work is original and has not been previously submitted for assessment in any other course of institution, except where specifically stated.

**Jotham Ariel Kennedy**

**Student Number: 0050073423**

---

Signature

---

Date

---

# Acknowledgements

I would like to thank Dr. Jim Shiau for his support and professional advice whilst completing this research paper. His knowledge and guidance was extensive and was always made available to myself. Jim has helped myself gain a far better understanding of geotechnical topics within and surpassing the scope of this project.

I would like to thank Michael Hobson for his help throughout the entire year. Michael has made many of the experiments and understandings required for this project topic throughout the year so much easier. I would especially like to thank Michael with his aid in PIV analysis, computer knowledge and formatting associated with this dissertation.

I would also like to thank to USQ Engineering workshop staff. In particular Daniel Eising & Dean Beliveau for their technical support throughout the year.

Finally I would like to thank my family for their support and guidance over the past four years. I would especially like to thank them for their patience, particularly through out this final year.

---

# Table of Contents

<b>Abstract</b> .....	ii
<b>Limitations of Use</b> .....	iii
<b>Certification</b> .....	iv
<b>Acknowledgements</b> .....	v
<b>Table of Contents</b> .....	vi
<b>List of Figures</b> .....	ix

<b>1 Introduction</b> .....	<b>1-1</b>
1.1 Introduction .....	1-1
1.2 Background .....	1-2
1.2.1 Ground Anchors .....	1-2
1.2.2 Plate Anchors .....	1-2
1.2.3 Buried Pipelines .....	1-3
1.2.4 Pile Anchors .....	1-3
1.3 Research Objectives .....	1-4
1.3.1 Overview .....	1-4
1.3.2 Initial Research Objectives .....	1-4
1.3.3 Update Research Objectives .....	1-5
1.4 Overview of Dissertation .....	1-6
1.4.1 Overview .....	1-6
1.4.2 Chapter 1: Introduction .....	1-6
1.4.3 Chapter 2: Literature Review .....	1-6
1.4.4 Chapter 3: USQ Physical Testing Facilities .....	1-6
1.4.5 Chapter 4: Experimental Material .....	1-7
1.4.6 Chapter 5: Plate Anchor .....	1-7
1.4.7 Chapter 6: Buried Pipeline .....	1-7
1.4.8 Chapter 7: Pile Anchor .....	1-7
1.4.9 Chapter 8: Conclusions and Future Work .....	1-8
1.5 Summary .....	1-8

<b>2 Literature Review</b> .....	<b>2-1</b>
2.1 Introduction .....	2-1
2.2 Horizontal Plate Anchors .....	2-1
2.2.1 Theory .....	2-1

2.2.2	Failure Mechanisms	2-5
2.2.3	Related Equations and Break-out Factor	2-6
2.2.4	Embedment Ratio	2-7
2.2.5	Existing Investigations	2-9
2.2.6	Uplift Capacity of Inclined Plate Anchors	2-18
2.2.7	Uplift Capacity of Group Anchor Plates	2-21
2.3	Buried Pipelines	2-26
2.3.1	Background	2-26
2.3.2	Failure Mechanisms	2-28
2.3.3	Limit Equilibrium Solutions	2-29
2.3.4	Deformation Mechanisms	2-30
2.3.5	Load-Displacement Relationship	2-31
2.3.6	Infilling Mechanism	2-32
2.4	Pile Anchors	2-33
2.4.1	Background	2-33
2.4.2	Failure Mechanisms	2-34
2.4.3	Existing Investigations	2-35

<b>3</b>	<b>USQ Physical Testing Facilities</b>	<b>3-1</b>
3.1	Introduction	3-1
3.2	Testing Equipment	3-1
3.2.1	Soil Loading Machine	3-1
3.2.2	Load Frame Software	3-3
3.2.3	Shear Box Test Equipment	3-5
3.3	Summary	3-6

<b>4</b>	<b>Experimental Material</b>	<b>4-1</b>
4.1	Introduction	4-1
4.2	Density & Unit Weight of Soil	4-1
4.2.1	Background	4-1
4.2.2	Previous Works Control Methods	4-2
4.2.3	Implemented Control Methods	4-3
4.2.4	Results	4-4
4.3	Moisture Content	4-4
4.3.1	Background	4-4
4.3.2	Methodology	4-5
4.3.3	Results	4-6
4.4	Shear Box Test	4-6
4.4.1	Background	4-6
4.4.2	Experimental Set-up	4-7
4.4.3	Experimental Procedure	4-8
4.4.4	Results	4-8

<b>5</b>	<b>Plate Anchor</b> .....	<b>5-1</b>
	5.1 Introduction .....	5-1
	5.2 Methodology .....	5-1
	5.2.1 Background .....	5-1
	5.2.2 Experimental Set-up .....	5-2
	5.2.3 Experimental Procedure .....	5-4
	5.3 Testing Results .....	5-5
	5.3.1 Introduction .....	5-5
	5.3.2 Results of Failure Mechanism .....	5-5
	5.3.3 Load-Displacement Behaviour .....	5-7
	5.3.4 Variation of Peak Uplift Load with Embedment Ratio .....	5-8
	5.3.5 Variation of Break-out Factor with Embedment Ratio .....	5-9
	5.3.6 Comparison to Existing Studies .....	5-10
	5.3.7 PIV Analysis .....	5-14
<b>6</b>	<b>Buried Pipeline</b> .....	<b>6-1</b>
	6.1 Introduction .....	6-1
	6.2 Methodology .....	6-1
	6.2.1 Background .....	6-1
	6.2.2 Experimental Set-up .....	6-2
	6.2.3 Experimental Procedure .....	6-3
	6.3 Test Results .....	6-4
	6.3.1 Results of Failure Mechanism .....	6-4
	6.3.2 Load-Displacement Behaviour .....	6-6
	6.3.3 Variation of Peak Uplift Load with Embedment Ratio .....	6-8
	6.3.4 PIV Analysis .....	6-8
<b>7</b>	<b>Pile Anchor</b> .....	<b>7-1</b>
	7.1 Introduction .....	7-1
	7.2 Methodology .....	7-1
	7.2.1 Background .....	7-1
	7.2.2 Experimental Set-up .....	7-2
	7.2.3 Experimental Procedure .....	7-3
	7.3 Test Results .....	7-4
	7.3.1 Results of Failure Mechanism .....	7-4
	7.3.2 Load-Displacement Behaviour .....	7-6
	7.3.3 Variation of Peak Uplift Load with Embedment Ratio .....	7-8
	7.3.4 PIV Analysis .....	7-9

---

<b>8</b>	<b>Conclusion &amp; Future Work</b> .....	<b>8-1</b>
	8.1 Conclusions .....	8-1
	8.1.1 Failure Mechanisms .....	8-1
	8.1.2 Load-Displacement Behaviour .....	8-1
	8.1.3 Variation of Peak Uplift Load with Embedment Ratio .....	8-2
	8.1.4 Variation of Break-out Factor with Embedment Ratio .....	8-2
	8.1.5 PIV Analysis .....	8-2
	8.2 Future Work .....	8-3
	8.2.1 Plate Anchor .....	8-3
	8.2.2 Pile Anchor .....	8-3
<b>9</b>	<b>References</b> .....	<b>9-1</b>
<b>10</b>	<b>Appendices</b> .....	<b>10-1</b>
	10.1 Appendix A - Project Specification .....	10-1
	10.2 Appendix B - Plate Anchor Results .....	10-3
	10.3 Appendix C - Buried Pipeline Results .....	10-9
	10.4 Appendix D - Pile Anchor Results .....	10-13

# List of Figures

Figure 2-1.	Basic Horizontal Plate Anchor Scenario	2-2
Figure 2-2.	Simplified Ultimate Uplift Capacity of Horizontal Plate Anchor	2-3
Figure 2-3.	Mors' Simplified Cone Method	2-4
Figure 2-4.	Failure Mechanisms of Shallow Anchor	2-6
Figure 2-5.	Failure Mechanisms of Deep Anchor	2-6
Figure 2-6.	Immediate Breakaway Conditions	2-9
Figure 2-7.	Load vs. Displacement Diagram $H/B = 4$	2-11
Figure 2-8.	Load vs. Displacement Diagram $H/B = 9.5$	2-11
Figure 2-9.	Break-out Factor vs Embedment Ratio	2-12
Figure 2-10.	Ultimate Load vs Embedment Ratio	2-13
Figure 2-11.	Break-out Factors for Horizontal Anchors in Sand	2-14
Figure 2-12.	Break-out Factors for Horizontal Anchors in Sand	2-15
Figure 2-13.	Velocity Plots Produced from Numerical Investigation	2-16
Figure 2-14.	Comparison of Theoretical Break-out Factors Merifield & Sloan (2006) and Murray & Geddes (1987)	2-17
Figure 2-15.	Comparison of Theoretical Break-out Factors Merifield & Sloan (2006) and Smith (1998)	2-18
Figure 2-16.	Overview of Inclined Plate Anchors (Source: Merifield, Lyamin & Sloan 2005)	2-19
Figure 2-17.	Break-out Factor vs Embedment Ratio - Inclined Plate Anchors	2-20
Figure 2-18.	Inclination Factors vs Embedment Ratio- Incline Plate Anchors	2-20
Figure 2-19.	Failure Mechanisms for Inclined Anchors	2-21
Figure 2-20.	Anchor Groups Pulled Vertically in Sand Overview	2-22
Figure 2-21.	Uplift Load vs Displacement - Two Plate Group (Source: Geddes & Murray 1996)	2-22
Figure 2-22.	Uplift Load vs Displacement - Four Plate Group (Source: Geddes & Murray 1996)	2-23
Figure 2-23.	Group Efficiency vs Seperation/Breadth Ratio - Two Plate Group (Source: Geddes & Murray 1996)	2-24
Figure 2-24.	Group Efficiency vs Seperation/Breadth Ratio - Four Plate Group (Source: Geddes & Murray 1996)	2-24
Figure 2-25.	Group Efficiency vs Seperation/Breadth Ratio - Group Strip Anchors (Source: Kouzer & Kumar 2009)	2-25
Figure 2-26.	Load-Displacement Curves for Individual Plates (Source: Geddes & Murray 1996)	2-26
Figure 2-27.	Overview of Pipeline Failure Mechanisms (Source: Cheuk et al 2008)	2-28
Figure 2-28.	Assumed Mohr's Circles In Situ and at Peak Uplift Resistance (Source: White et al 2008)	2-30

Figure 2-29. Displacement Field for Pipeline Uplift (Source: Cheuk et al 2008) .....	2-30
Figure 2-30. Load-Displacement Diagram for Pipeline Uplift (Source: Cheuk et al 2008) .....	2-31
Figure 2-31. Simplified Failure Mechanism – Pile Anchor (Source: Shanker et al 2007) .....	2-34
Figure 2-32. Failure Mechanism – Pile Anchor (Source: Chattopadhyay& Pise 1986) .....	2-34
Figure 3-1. Overview of Soil Loading Machine .....	3-2
Figure 3-2. Linear Actuator, Load Cell, Transducer and Attachment Plate Configuration .....	3-3
Figure 3-3. Load Machine Software – User Interface .....	3-4
Figure 3-4. Shear Box Testing Equipment .....	3-5
Figure 3-5. Shear Box .....	3-6
Figure 4-1. Typical Configuration of Shear Box Testing Apparatus (Source: Gan, Fredlund & Rahardjo 1988) .....	4-7
Figure 4-2. Shear Stress vs Horizontal Displacement for Relative Normal Stresses .....	4-9
Figure 4-3. Shear Stress vs Vertical Pressure .....	4-1 0
Figure 5-1. Overview of Testing Tank (Source: Cole, A.J.S 2009) .....	5-3
Figure 5-2. Overview of Model Plate Anchors .....	5-3
Figure 5-3. Horizontal Plate Anchor Failure H/B = 2 .....	5-6
Figure 5-4. Horizontal Plate Anchor Failure H/B = 5 .....	5-6
Figure 5-5. Horizontal Plate Anchor Load vs Displacement Diagram ... 5-7	5-7
Figure 5-6. Horizontal Plate Anchor Peak Load vs Embedment Ratio ... 5-8	5-8
Figure 5-7. Horizontal Plate Anchor Break-out Factor vs Embedment Ra- tio .....	5-9
Figure 5-8. Horizontal Plate Anchor: Load vs Displacement Merifield et al (1999) H/B = 4 .....	5-11
Figure 5-9. Horizontal Plate Anchor: Load vs Displacement H/B = 4 Com- parison to Merifield et al (1999) .....	5-12
Figure 5-10. Horizontal Plate Anchor: Peak Uplift Load vs Displacement Compared to Merifield et al (1999) .....	5-13
Figure 5-11. Horizontal Plate Anchor: Break-out Factor vs Embedment Ratio Compared to Merifield et al (1999) .....	5-14
Figure 5-12. PIV Analysis Vector Plot – Plate Anchor H/B = 5 (Source: Hobson 2010) .....	5-15
Figure 5-13. PIV Analysis Superimposed Image – Plate Anchor H/B = 5 (Source: Hobson 2010) .....	5-15
Figure 6-1. Overview of Pipeline Test Layout .....	6-2
Figure 6-2. Buried Pipeline Failure H/B = 2 .....	6-5
Figure 6-3. Buried Pipeline Failure H/B = 4 .....	6-5
Figure 6-4. Buried Pipeline H/B = 2 Before Downward Soil Movement ... 6-5	6-5
Figure 6-5. Buried Pipeline H/B = 2 After Downward Soil Movement ... 6-6	6-6
Figure 6-6. Buried Pipeline Load vs Displacement Diagram .....	6-6
Figure 6-7. Buried Pipeline Peak Uplift Load vs Embedment Ratio	6-8
Figure 6-8. PIV Analysis Pipeline H/B = 4 Vector Plot .....	6-9

Figure 6-9.	PIV Analysis Pipeline H/B = 4 Superimposed	6-9
Figure 7-1.	Overview of Pile Anchor Test Layout	7-2
Figure 7-2.	Pile Anchor Observed Failure	7-5
Figure 7-3.	Pile Anchor Observed Failure	7-5
Figure 7-4.	Smooth Pile Anchor Load vs Displacement Diagram	7-6
Figure 7-5.	Rough Pile Anchor Load vs Displacement Diagram	7-6
Figure 7-6.	Smooth Pile Anchor Peak Load vs Embedment Ratio	7-8
Figure 7-7.	Rough Pile Anchor Peak Load vs Embedment Ratio	7-8
Figure 10-1.	Horizontal Plate Anchor Failure H/B = 2	10-3
Figure 10-2.	Horizontal Plate Anchor Failure H/B = 2 - Highlighted Failure Plane	10-3
Figure 10-3.	Horizontal Plate Anchor Failure H/B = 3	10-4
Figure 10-4.	Horizontal Plate Anchor Failure H/B = 3 - Highlighted Failure Plane	10-4
Figure 10-5.	Horizontal Plate Anchor Failure H/B = 4	10-5
Figure 10-6.	Horizontal Plate Anchor Failure H/B = 4 - Highlighted Failure Plane	10-5
Figure 10-7.	Horizontal Plate Anchor Failure H/B = 5	10-6
Figure 10-8.	Horizontal Plate Anchor Failure H/B = 5 - Highlighted Failure Plane	10-6
Figure 10-9.	Horizontal Plate Anchor Load vs Displacement Diagram H/B = 2	10-7
Figure 10-10.	Horizontal Plate Anchor Load vs Displacement Diagram H/B = 3	10-7
Figure 10-11.	Horizontal Plate Anchor Load vs Displacement Diagram H/B = 4	10-8
Figure 10-12.	Horizontal Plate Anchor Load vs Displacement Diagram H/B = 5	10-8
Figure 10-13.	Horizontal Plate Anchor Load vs Displacement Diagram Combined Results	10-9
Figure 10-14.	Buried Pipeline Failure H/B = 2	10-9
Figure 10-15.	Buried Pipeline Failure H/B = 2 - Highlighted Failure	10-10
Figure 10-16.	Buried Pipeline Failure H/B = 3	10-10
Figure 10-17.	Buried Pipeline Failure H/B = 3 - Highlighted Failure	10-10
Figure 10-18.	Buried Pipeline Failure H/B = 4	10-11
Figure 10-19.	Buried Pipeline Failure H/B = 4 - Highlighted Failure	10-11
Figure 10-20.	Buried Pipeline Load vs Displacement Diagram H/B = 2	10-11
Figure 10-21.	Buried Pipeline Load vs Displacement Diagram H/B = 3	10-12
Figure 10-22.	Buried Pipeline Load vs Displacement Diagram H/B = 4	10-12
Figure 10-23.	Buried Pipeline Load vs Displacement Diagram Combined Results	10-13
Figure 10-24.	Smooth Pile Anchor Load vs Displacement H/B = 5	10-14
Figure 10-25.	Smooth Pile Anchor Load vs Displacement H/B = 10	10-14

---

Figure 10-26.	Smooth Pile Anchor Load vs Displacement $H/B = 13$	10-15
Figure 10-27.	Smooth Pile Anchor Load vs Displacement Combined . . .	10-15
Figure 10-28.	Rough Pile Anchor Load vs Displacement $H/B = 5$ .	10-16
Figure 10-29.	Rough Pile Anchor Load vs Displacement $H/B = 7.5$	10-16
Figure 10-30.	Rough Pile Anchor Load vs Displacement $H/B = 10$	10-17
Figure 10-31.	Rough Pile Anchor Load vs Displacement $H/B = 13$	10-17
Figure 10-32.	Rough Pile Anchor Load vs Displacement Combined	10-18

---

# Introduction



## 1.1 Introduction

Many modern engineering structures require a foundation system that provides adequate support by resisting loads that are imposed on the foundation of the structure or vertical and horizontal pullout forces. Stability and support of structures is provided by transferring foundational loads from the structures foundation through some form of anchors and then onto the surrounding soil and terrain. In many cases these loads and forces that are transmitted through anchors to surrounding terrain can cause the anchor to experience subsequence uplift forces. As a result, ground anchors have been developed so as to be fixed to structures and are embedded to sufficient ground depths to provide adequate amounts of support within required safety limits. It is therefore the primary focus of this project and subsequent dissertation to investigate the uplift capacity of various ground anchors in sand.

Ground anchors have in fact been utilised for thousands of years in many different forms. Predominantly the use of these early anchors was to support lightweight structures only and it was not until recent times with the invention of suspension bridges that anchors were used to transfer very large loads. As a result, during the last 50 years there have been a number of studies conducted to investigate the design and use of these ground anchors. A number of theories have been developed to estimate the ultimate uplift capacity of different ground anchors in sand and it is the aim of this investigation to take a predominantly physical approach to further investigate and test this pullout phenomenon. A Basic two-dimensional situation shall provide the primary focus of this investigation, however some initial

investigation into three-dimensional effects shall be conducted and will therefore provide opportunity for further works in this area.

## **1.2 Background**

### **1.2.1 Ground Anchors**

As mentioned ground anchors are generally designed and constructed to resist the forces that are applied to foundations of structures. The primary function of these anchors is to transmit the forces acting on the foundations of a structure to the surrounding soil or terrain. This simple form of buried anchors have been around for thousands of years and used to stabilise structures. An early example of this is the use of anchors or stakes that are buried to stabilise a tent.

Initially ground anchors were only used to stabilise small or lightweight structures such as transmission towers, radar towers or tents as explained in the above example. It was not until the mid 19th century when the creation of large suspension bridge structures introduced the need of ground anchors to bear and transmit very large loads to the earth. From this point in time forward, anchors began to form an important component of many civil engineering projects and in many of these cases be required to resist some form of uplift forces.

Ground anchors have been developed since this time into a number of different forms each with its own strengths and specific applications. Generally anchors can be classified into five different forms of ground anchor that are currently in use in industry and they are as follows: plate anchors, direct embedment anchors, helical anchors, grouted anchors, and anchor piles and drilled shafts. This project shall primarily focus on the plate anchor, pile anchors and shall further investigate buried pipelines in sand.

### **1.2.2 Plate Anchors**

Plate anchors can be constructed using a many number of materials and can be constructed in numerous shapes. For example plate anchors may be made of steel plates, precast concrete slabs, poured reinforced concrete slabs or timber sheets just to name a few of the most common construction materials. Plate anchors may also be put into location in a number of ways, the two most common methods utilised today are backfilled plate anchors or excavated trench plate anchors. Backfilled plate anchors are put into position by excavating the ground to the required depth, placing the anchor in position then backfilling and compacting with good quality soil. The other popular method of deposition is to install

the plate anchor in excavated trench, then attach the anchor to tie rods that are either driven or placed through auger holes. (Das 1990). The methodology used throughout experimentation in regards to this project will replicate the deposition method of backfilled plate anchors.

### **1.2.3 Buried Pipelines**

Buried pipelines have become an essential part of the modern world for transportation of many assets such as oil and gas. Offshore oil and gas pipelines are commonly buried under sand to protect them from environmental effects and fishing activities, establish mechanical protection all whilst providing a stable platform and thermal insulation. It is now popular practice to transport high pressure and high temperature goods via small diameter insulated pipes through the seas. (Bransby et al 2001a) & (Bransby et al 2002b). Due to the use of small diameter pipes at high temperatures and high pressure, uplift of these pipes can occur as a result of change in either the temperature or pressure. "Upheaval buckling is promoted by the elevated temperatures (which lead to thermal expansion) and the high degree of lateral and axial soil restraint. The resulting compressive forces can result in the pipeline being forced upwards out of the trench: a phenomenon known as upheaval buckling." (Bransby et al 2002a). Failure of such pipelines can be very detrimental having numerous consequences, especially economical and environmental. Increasing the depth of burial for pipelines will of course increase the uplift resistance provided. However, burial represents a large portion of the overall construction cost of buried pipes and increases significantly with increased depths. It is therefore important that design of buried pipelines occurs so as to obtain a minimised amount of cover to create economically viable constructions whilst still providing adequate amounts of uplift resistance and protection. (Cheuk et al 2008).

### **1.2.4 Pile Anchors**

Anchor piles can be used to support both compressive loads or resist uplift loads, or in certain circumstances act as lateral restraints. Piles are used when the structure is subject to very large loads or in instances where surrounding soil conditions are poor and require footings to pass to great depths to reach acceptable soil conditions. "When the soil located immediately below a given structure is weak, the load of the structure may be transmitted to a greater depth by piles and drilled shafts" (Das 1999). "Some structures, like transmission towers, mooring systems for ocean surface or submerged platforms, tall chimneys, jetty structures, etc., are constructed on pile foundations, which have to resist uplift loads" (Chattopadhyay and Pise 1986). Just as with plate anchors, piles can be made from many materials and be formed into numerous shapes. They too can be created from

steel, precast concrete, poured concrete or timber and may be formed into shapes such as square, circular or octagonal piles. Also, as with plate anchors, piles can be driven into place or excavated into position. Piles are often more expensive to use than a shallow anchor of most types, but in many cases when piles are utilised it is because they are 'required' for the specific situation. "Pile foundations, which are deep and which cost more than shallow foundations. Despite the cost, the use of piles often is necessary to ensure structural safety" (Das 2004).

## **1.3 Research Objectives**

### **1.3.1 Overview**

The research objectives have changed over time as the project has evolved and new directions are identified and looked into. This is an expected outcome and forms a known basis of research, i.e. that the initial ideas will not be the final product and ideas and areas will change over time as further exploration takes place.

### **1.3.2 Initial Research Objectives**

The initial direction of this dissertation was to investigate the uplift capacity of plate anchors in sand only. The creation of a numerical model would take place and the conducted physical experimentation would then be used to validate this model. Once the model is validated and known to be producing correct results, further numerical experimentation could take place to investigate the uplift capacity of the plate anchors with numerous combinations of variables. This would allow to investigate different variables including embedment ratio, sand density, soil cohesion and friction whilst not having to physically prepare each of the cases which can be time consuming and costly. Therefore the original research objectives as of January 2010 were as follows:

1. Research background information into uplift capacity of plate anchors in sand.
2. Experimentally investigate the uplift capacity of plate anchors in sand using laboratory tests. Primarily focussing on the effects different anchor depths have on the overall uplift capacity.
3. Undertake a numerical analysis of uplift capacity of ground anchors in sand using the computer analysis software FLAC. This numerical analysis is to be closely related to the physical experimentation and verify results.

4. Submit an academic dissertation on the research performed.

### **1.3.3 Update Research Objectives**

However, as mentioned above, due to the evolving nature of research and investigating further into topics as they arise as part of the research has led to the focus of this project and subsequent dissertation to change considerably. The primary focus of the project became physical experimentation and focused not only plate anchors but also expanded to include buried pipelines in sand and pile anchors in sand. This new direction was to include investigations into further applications such as 3 dimensional experimentation or uplift capacity of group anchors, however this is only if time permits. Another area of further investigation that has arisen due to project work is some brief discussion on footing on slope problem, the relationship between research and teaching applications and finally the changing or evolving methods of research. As a result of these changes, the research objectives as of June 2010 were as follows:

1. Demonstrate a sound understanding of the underlying theory and methods involved in the field of ground anchors.
2. Undertake a literature review to determine current theory, practices and results obtained in the field of ultimate uplift capacity of plate anchors, buried pipelines and pile anchors in sand.
3. Experimentally investigate the uplift capacity of plate anchors, buried pipelines and pile anchors in sand using scale laboratory experiments. These experiments are to primarily focus upon the effects of alternate anchor depths, and therefore embedment ratio, on the overall uplift capacity.
4. Compare these experimental results obtained with existing literature and results including discussion and understanding.
5. Undertake initial investigations into the three-dimensional effects acting upon anchors in an uplift situation.
6. Submit an academic dissertation on the research performed.

If time permits:

8. Perform uplift test on three-dimensional piles.

## **1.4 Overview of Dissertation**

### **1.4.1 Overview**

This dissertation will first investigate the existing theories, studies and understanding through a literature review. From here facilities and materials relating to the physical experimentation conducted as part of this research shall be investigated. This shall be followed by an overview of the methodologies used to conduct experiments, demonstrate results obtained and then include comparison and discussion with existing results for each of the three cases. Finally the dissertation will briefly discuss the topics of footing on a slope, the relationship between linking research with teaching and learning and the topic of how research aims and objects can evolve and change dramatically over time. At the end of the dissertation all conclusions will be stated and the lists of future work that have arisen as a result of this research shall also be listed.

### **1.4.2 Chapter 1: Introduction**

This chapter gives an overview to the dissertation as a whole. It provides some basic background information to ground anchors and then continues on to provide some further insight into each of the three specific anchor cases that are investigated within this research paper. This chapter also includes research objectives of this project and demonstrates what will be covered in each of the subsequent chapters.

### **1.4.3 Chapter 2: Literature Review**

This chapter gives an in depth review of existing studies conducted within similar manner to this research project. Primarily each of the three separate anchor cases is investigated where further detailed information on areas such as background, failure mechanisms, load-displacement relationships and existing results is explored and presented.

### **1.4.4 Chapter 3: USQ Physical Testing Facilities**

During the physical investigations conducted as part of this project, a number of testing facilities were utilised to conduct experimentation. The main testing equipment included the soil loading machine, the accompanying software and the shear box test equipment. The soil loading machine was used to induce required uplift loads whilst the computer and

appropriate software recorded the relevant data. Shear box tests were also conducted to determine the soil cohesion and soil friction angle. It is noted that other equipment was used throughout this investigation and is further mentioned in Chapter 4, however this chapter gives details of the ‘main’ components of experimentation.

#### **1.4.5 Chapter 4: Experimental Material**

Chapter 4 introduces the properties of the materials that were used for all of the experiments conducted as part of this research. This chapter introduces a brief background to each of the concepts and the methods employed to obtain reproducible material parameters for each of the experiments conducted.

#### **1.4.6 Chapter 5: Plate Anchor**

Chapter 5 presents the investigation conducted on the uplift of horizontal plate anchors. This chapter includes the methodology explanation for the set-up and preparation of the experiments. The experimental results are then presented including the observed failure mechanisms, load-displacement relationship, ultimate load compared to embedment ratio and the break-out factor in comparison to the embedment ratio. These results that are obtained are then compared with existing results in this field. Also included within the results section is some PIV analysis results conducted by fellow student Michael Hobson which provide further understanding of this topic.

#### **1.4.7 Chapter 6: Buried Pipeline**

Chapter 6 presents the investigation conducted on the uplift of buried pipelines. This chapter includes the methodology explanation for the set-up and preparation of the experiments. The experimental results are then presented including the observed failure mechanisms, load-displacement relationship and ultimate load compared to embedment ratio. Also included within the results section is some PIV analysis results conducted by fellow student Michael Hobson which provide further understanding of this topic.

#### **1.4.8 Chapter 7: Pile Anchor**

Chapter 7 presents the investigation conducted on the uplift of buried pipelines. This chapter includes the methodology explanation for the set-up and preparation of the experiments. The experimental results are then presented including the observed failure mechanisms, load-displacement relationship and ultimate load compared to embedment

ratio. Also included within the results section is some PIV analysis results conducted by fellow student Michael Hobson which provide further understanding of this topic.

#### **1.4.9 Chapter 8: Conclusions and Future Work**

This chapter provides closing observations on the research project and suggested directions for future research. The results obtained as part of this project include failure mechanism, the load-displacement relationship, variation of peak uplift load with changing embedment ratio and variation of the break-out factor with the embedment ratio. Also results are to be compared to existing results in this field. Finally, this research project was run in cooperation with a PIV investigation and will therefore includes some PIV results for these investigations.

### **1.5 Summary**

This chapter has demonstrated that anchors have been used by thousands of years and as time progresses structures become more and more dependant on suitable foundation and anchors systems to support large structures. Furthermore, it was seen how this project and subsequent dissertation will investigate the uplift capacity of ground anchors in sand, with a defining scope of objects and an overview of experimentation that is conducted. Finally, it is seen how the remainder of this dissertation will provide relevant information in regards to testing facilities and materials used during experimentation, results obtained and comparison with existing studies and presentation of conclusions and future works.

---

# Literature Review



## 2

### **2.1 Introduction**

The following chapter provides an in depth literature review into the uplift capacity of horizontal plate anchors, buried pipelines and pile anchors. The chapter focuses on introducing each of the ideas or background through horizontal plate anchors in depth and then secondly for buried pipelines and pile anchors. This is was done as most of the phenomena and methods presented for plate anchors are very similar to that of buried pipelines and pile anchors.

### **2.2 Horizontal Plate Anchors**

#### **2.2.1 Theory**

As briefly discussed earlier, horizontal plate anchors are used in the construction of structures that contain foundations that are subject to uplift forces. Since the late 1950's a number of investigations have been conducted that have led to the development of theories that predict the behaviour and capacity of anchors subject to these typical loading situations. Initially, ground anchors consisted of large mass concrete blocks and provided the uplift capacity required solely by the self-weight of the concrete and therefore supported structures. These large mass anchors were of course expensive to construct and therefore led to the investigations into alternate anchor design. As development into ground anchors further proceeded and the use of such anchors became more extensive, anchors have evolved to the point where they now provide an economical and competitive alternative to early mass anchors. (Das 1990) & (Merifield & Sloan 2006).

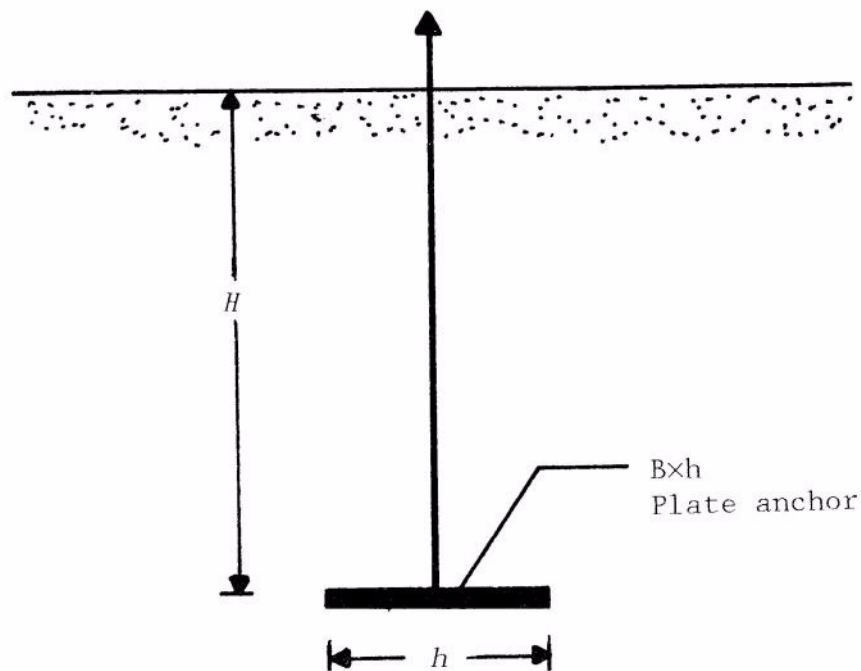


**Figure 2-1.** Basic Horizontal Plate Anchor Scenario  
(Source: Das 1990)

Figure 2-1 above demonstrates a typical overview of a simple plate anchor subject to uplift forces. Here it can be seen that  $H$  represents the depth at which the anchor is placed in relation to the soil surface and  $h$  represents the anchor width. In many cases  $h$  is also represented as  $B$  for the anchor width and shall be referred to as  $B$  from here onwards. The embedment ratio represents the ratio of the depth of the anchor to the width of the anchor, therefore  $H/B$ .

The most simplified definition of ultimate uplift capacity of a plate anchor is as follows:

$$Q_{u(g)} = Q_u + W_a \quad (2.1)$$

Where  $Q_{u(g)}$  = Gross ultimate uplift capacity.

$Q_u$  = Net ultimate uplift capacity.

$W_a$  = Effective selfweight of the anchor.

From equation 2.1 it can be seen that the gross ultimate uplift capacity of an anchor is subject to both the self-weight of the anchor and the net uplift capacity, which is subject to a number of other factors. The net uplift capacity is dependant on numerous factors but is heavily dependant on the surrounding soil conditions and the embedment ratio. The surrounding soil affects variables such as soil unit weight, soil cohesion and coefficient of friction whilst the depth and width of the anchor affect the embedment ratio. In the most simplest definition, the “net ultimate uplift capacity is the sum of the effective weight of

the soil located in the failure zone and the shearing resistance developed along the failure surface.” (Das 1990). This simple explanation of the uplift capacity of horizontal plate anchor can visualised and better understood by viewing Figure 2-2 below.

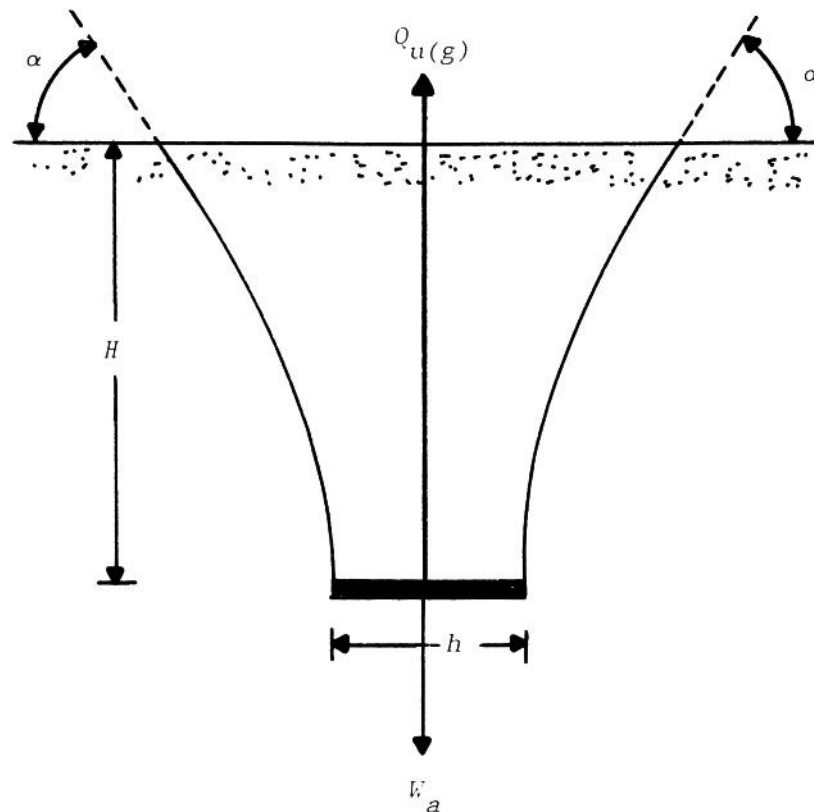


**Figure 2-2.** Simplified Ultimate Uplift Capacity of Horizontal Plate Anchor  
(Source: Das 1990)

Early theories related to ultimate uplift capacity are Soil Cone Method (Mors 1959) and Friction Cylinder Method (Downs and Chieurzzi 1966). It is from these two early methods that more recent methods are based upon. Both of these methods are fairly similar and work by relating the failure zone above the anchor as a simple cone. The ultimate uplift capacity of the anchor is then calculated as the volume of this cone above the anchor. The Soil Cone Method ignores the shearing resistance developed along the failure surface, whilst the Friction Cylinder Method includes this value in its calculations. There are many number of more recent theories developed from these early methods relating to uplift capacity of plate anchors involving Balla's Theory (1961), Back and Kondner's Empirical Relationship (1966), Mariupol'skii's Theory (1965), Meyerhof and Adams' Theory (1968). All of these listed theories are based on the fact that the ultimate uplift capacity of anchors is related

to the volume of soil within the failure area above the anchor, whilst some include frictional effects of the slope plane whilst some simply ignore this effect. Mors' simplified cone method can be seen below in Figure 2.3.

(Das 1990)

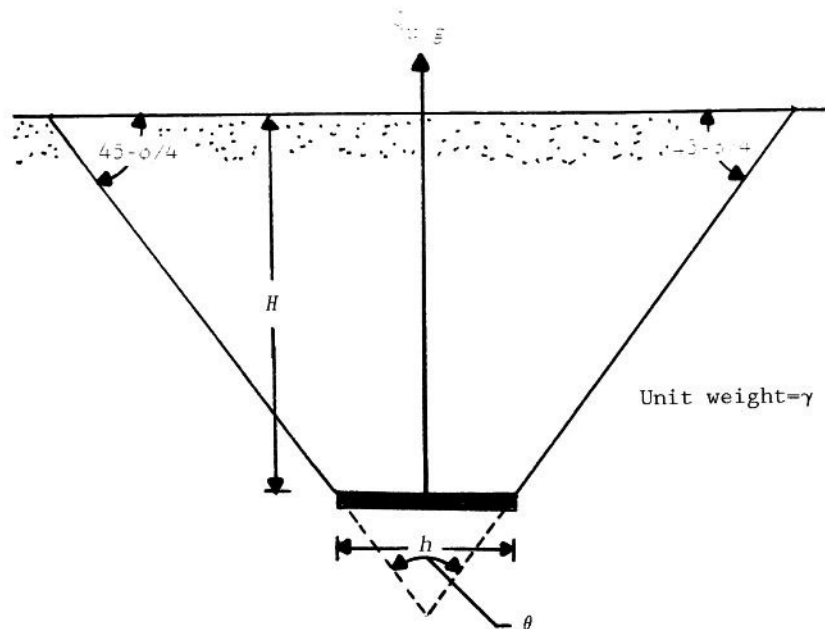


**Figure 2-3.** Mors' Simplified Cone Method  
(Source: Das 1990)

There are of course a further number of factors the effect the uplift capacity of an anchor; the theories mentioned above are the initial thoughts or simplified understandings of the situation. Rowe and Davis (1982) state that "Approaches involve the use of either equilibrium concepts or the method of characteristics, frequently combined with empirical corrections (e.g. Balla, 1961; Meyerhof & Adams, 1968; Vesic, 1971; Ovesen & Stroman, 1972; Neely, Stewart & Graham, 1973). All of those approaches involve some arbitrary assumptions regarding either the shape of the failure surface or the influence of the soil above the anchor on the field of characteristics. Previous investigators have generally not considered the possible effects of anchor roughness, initial stress state and soil dilatancy."

Rowe and Davis continue on to present the following formula:

$$q_u = \gamma h F_\gamma' \tag{2.2}$$

Where  $q_u =$  Average applied pressure  $= q_u = \frac{Q_u}{A_{plate}}$

$\gamma =$  Unit weight of soil

$h$  = Depth to the bottom of anchor

$F_{\gamma}'$  = Anchor capacity factor

The anchor capacity factor is a function of orientation, embedment ratio, angle of friction, dilatancy, initial stress state and anchor roughness. This formula is very similar to the formula presented by Merifield and Sloan (2006) and shall be discussed further on.

Calculating uplift capacities is a complicated process that is heavily dependant on what assumptions are to be made. All previous studies assume a different method for estimating the failure mechanism plane, and therefore assume a different final uplift capacity. This assumption may be simplified to linear cone shape, equations related to friction coefficient angle or complex exponential equations. However, “there is no entirely satisfactory theory for assessing the breakout capacity of anchors, mainly due to the difficulties in defining the shape of failure surface in terms of geometric and soil parameters.” (Ilamparuthi et al 2002). Bouazza et al (1996) noted that the uplift capacity for a circular plate anchor and for a rectangular plate anchor were the same as long as the total plate area was the same.

### **2.2.2 Failure Mechanisms**

Ilamparuthi et al (2002) comments on a various number of previous studies (Mors, 1959; Clemence & Veesaert, 1977; Sutherland, 1965; Balla, 1961; Sutherland et al, 1982; Saran et al, 1986) to describe the failure mechanism of plate anchors subject to uplift forces. It is noted that all these studies confirm that failure occurs in a truncated conical failure surface form. Also recognised is that “the pullout capacity is the sum of the weight of soil within this cone and the shearing resistance along the failure surface.” (Ilamparuthi et al 2002). Merifield & Sloan (2006) also comment on this topic “In the case of horizontal anchors, the failure mechanism is generally assumed to be a logarithmic spiral in shape (Murray and Geddes 1987), and the distribution of stress is obtained either by using Kotter’s equation (Balla 1961) or by making an assumption regarding the orientation of the resultant force acting on the failure plane.”

As mentioned earlier, the type of failure mechanism is also dependant whether the anchor is shallow or deep. This is therefore dependant on the embedment ratio, or the anchor depth and width. Below is an illustration of both shallow and deep failure mechanisms in figures 2-4 and 2-5 respectively. It can be seen in figure 2-4, that in the case of a shallow foundation, the failure plane formed is of a curved ‘cone’ type shape that extends to the soil surface. This is quite different in comparison to the deep anchor in figure 2-5 that forms a balloon shape failure surface that does not extend to the soil surface.

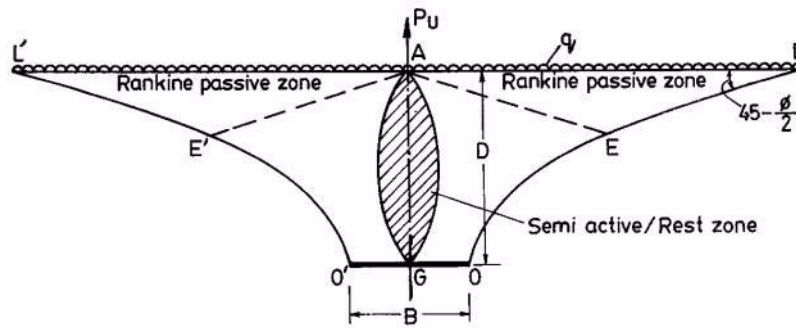


**Figure 2-4.** Failure Mechanisms of Shallow Anchor  
(Source: Kanakapura et al 1994)

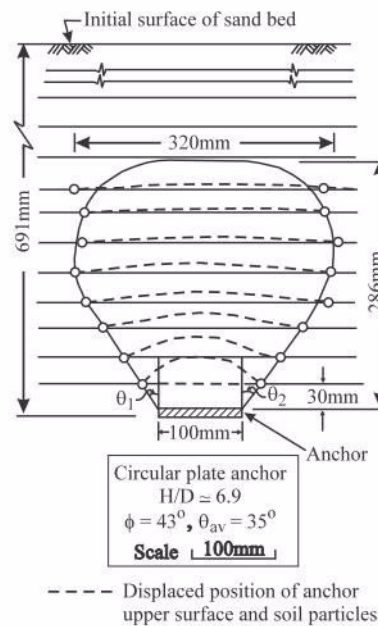


**Figure 2-5.** Failure Mechanisms of Deep Anchor  
(Source: Ilamparuthi et al 2002)

### 2.2.3 Related Equations and Break-out Factor

Merifield et al (1999) and Merifield & Sloan (2006) present two important formulae for uplift capacity of anchors in sand. The formulas are quite similar and are “in a analogous to Terzaghi’s equation” (Merifield & Sloan 2006).

$$Q_u = N_q \gamma A H \tag{2.3}$$

Where  $Q_u$  = Ultimate load  
 $N_q$  = Break-out factor  
 $\gamma$  = Unit weight of soil

$A$  = Area of anchor  
 $H$  = Depth of burial

(Merifield et al 1999)

$$q_u = \gamma H N_\gamma \quad (2.4)$$

Where  $q_u$  = Ultimate anchor capacity  
 $\gamma$  = Unit weight of soil  
 $H$  = Depth of anchor burial  
 $N_\gamma$  = Anchor break-out factor

(Merifield & Sloan 2006)

It should be noticed that these two formula bear a great resemblance to formula 1 presented earlier. It should also be noticed that these formula are in fact the same, just presented in alternate form as demonstrated in the equation below.

$$q_u = \frac{Q_u}{A_{plate}} \quad (2.5)$$

Where  $q_u$  = Ultimate capacity of anchor  
 $Q_u$  = Ultimate load  
 $A_{plate}$  = Area of plate anchor

The breakout factor presented in these formulae is a convenient way to compare results with existing studies and presents an aid when validating studies or experimentation. “The uplift capacity of anchors is typically expressed in terms of a bearing capacity/break-out factor which is a function of the anchor shape, embedment depth, overburden pressure and the soil properties.” (Merifield et al 1999). Merifield et al (1999) also comments and present trends of the breakout factor plotted against the embedment ratio and is generalised “as increasing steadily up to approximately  $H/B = 12$  at which point it plateaus out to an approximately constant value.” Typically, the above equation is utilised to back calculate the break-out factor from model anchor pullout tests.

#### 2.2.4 Embedment Ratio

Many textbooks, papers and investigations (Das, 1990; Ilamparuthi et al, 2002; Merifield & Sloan, 2006; Rowe & Davis, 1982; Su & Fragaszy, 1987) define a clear difference between deep and shallow anchors. The embedment ratio directly effects whether an anchor is shallow or deep, with increased depth the anchor will change from shallow to

deep. The embedment ratio at which this change occurs is known as the critical embedment ratio. Although there is no clear definition point of when an anchor changes from shallow condition to deep condition as it seems to be specific case sensitive. However, a general trend of commonalities can clearly be seen in numerous studies that at approximately  $H/B = 6$  is where anchors will change from shallow to deep properties. This is evident in both studies Merifield et al (1999) and Ilumparuthi et al (2002). Another determination of deep and shallow anchors is based upon the failure surface plane. It is said that for shallow anchors the failure plane will extend to the soil surface, whilst for deep anchors the failure plane will develop a balloon type shape and not extend to the soil surface. “An anchor is classified as shallow if, at ultimate collapse, the observed failure mechanism reaches the surface.” (Merifield et al 1999). Examples of typical shallow and deep anchor failure can be seen above in figures 2-4 and 2-5 respectively.

The relationship between ultimate capacity and embedment ratio forms a non-linear ‘exponential form’ relationship. Capacity of the anchor increases as the depth of the anchor increases. “Evidence suggest that anchors with embedment ratio of 8 or larger are capable of sustaining very high loads before collapse. In these cases actual performance will be dominated by contained plastic deformation before full collapse.” (Rowe & Davis 1982).

“For smooth anchors with a horizontal axis, the rate of increase in anchor capacity factor with embedment ratio is such that for a given depth  $h$  there is an optimum anchor width  $B$  for which the actual load carrying capacity of the anchor is maximum. For a wide range of friction angles ( $15^\circ \leq \phi \leq 45^\circ$ ) the optimum width is approximately  $0.5h$  and the provision of an anchor of width greater than  $0.5h$  will not increase the ultimate load carrying capacity.” (Rowe & Davis 1982).

The uplift behaviour of ground anchors can be divided into two separate categories of ‘immediate breakaway’ or ‘no breakaway.’ The immediate breakaway case demonstrates that soil-anchor contact interface does not sustain tension. Therefore when uplift loads act upon the anchor, the vertical stresses in the region immediately below the anchor reduce to zero and the anchor is no longer in contact with the underlying soil. This scenario represents the case where there is no suction or adhesion between the anchor and soil below. This immediate breakaway case is depicted below in figure 2-6. The no breakaway case can be described as the opposite of the breakaway case. The ‘no breakaway’ case assumes that the soil-anchor contact interface can support vertical stress below the anchor, therefore developing suction and adhesion forces. These suction or adhesion forces that are developed below the anchor will dependant on such variables as embedment depth, soil permeability, undrained shear strength and loading rate. As such, this ‘no breakaway’

assumption becomes quite complex and the actual magnitude of and suction or adhesion forces developed are difficult to estimate. (Merifield et al 1999).

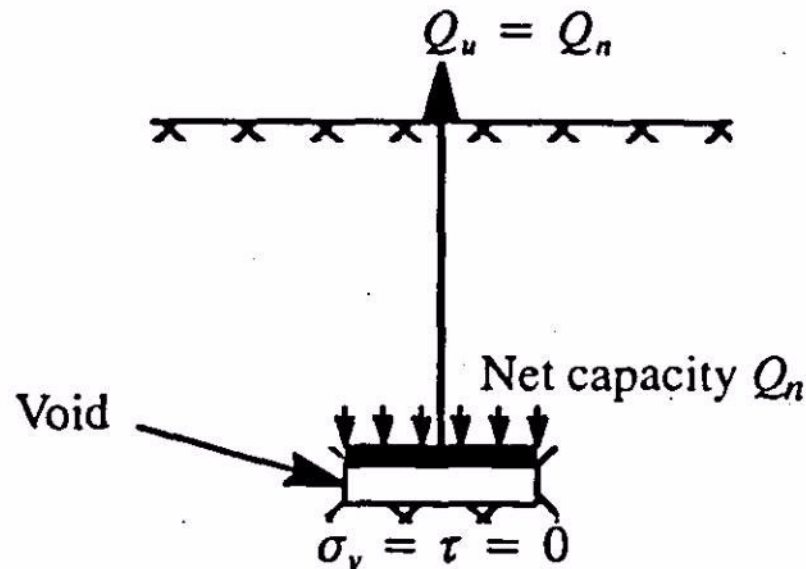


**Figure 2-6.** Immediate Breakaway Conditions  
(Source: Merifield et al 1999)

### 2.2.5 Existing Investigations

“Although there is no entirely adequate substitutes for full-scale field testing, tests at the laboratory scale have the advantage of allowing close control of at least some of the variables encountered in practice. In this way, trends and behaviour patterns observed in laboratory can be of value in developing an understanding of performance at larger scales” (Merifield & Sloan 2006).

Experimentation conducted by Merifield et al (1999) and Merifield & Sloan (2006) provide good examples of experimentation conducted on scale models using both physical and numerical investigations. These papers provide a good overview how to conduct similar uplift test and present results for both forms of testing; physical experimentation and numerical investigation.

Merifield et al (1999) conducted a laboratory physical investigation into the uplift capacity of anchors. These physical tests were conducted on circular plates pulled vertically in dense sand. Tests were conducted in large calibration chambers approximately 1m in height and 1m in diameter. The focus of these test was to investigate the effects of differing parameters such as anchor diameter, pullout rate and elasticity of loading systems has on the overall uplift capacity of the anchor.

This investigation involved the use of model anchors of diameter size  $d$  from 50mm to 125mm and were constructed of mild steel. “Larger diameter anchors were chosen compared with previous research, for a more realistic set-up and due to the recognised influence of scale effects on the break-out factor for anchors of diameters less than 50mm” (Merifield et al 1999). The sand used in this investigation was classified as a silty sand with the following properties: specific gravity = 2.65, compression index = 1.32, uniformity coefficient = 1.71  $kPa$  and density =  $17.87 \text{ kN/m}^3$ .

The experiments were conducted on different diameter anchors and relative depths therefore varying the embedment ratio  $H/B$  from 2 to 14.5. Thus investigating a range of anchors from shallow anchor conditions through to deep anchor positions. Also varied during this physical investigation was the pullout rate of the anchor which varied from  $1\text{mm}/\text{min}$  to  $6\text{mm}/\text{min}$  to assess the possible effects of the loading rate on the ultimate pullout load. Throughout the investigation the test chamber and anchor were simply placed directly underneath a hydraulic jack that applied the vertical load directly to the anchor, thus allowing a constant rate of displacement to be applied. Load was recorded using a load cell and the displacement was measured internally by the Instron - hydraulic jack.

Preparation of the chambers followed a strict method so as to produce uniform densities throughout all the tests completed. The following procedure was utilised to prepare each of the test chambers:

1. Sand was rained into the chamber using a hopper to predetermined height.
2. The anchor was then placed horizontally on a levelled out area of sand in the center of the chamber.
3. Sand was then rained into the chamber until the anchor was buried slightly deeper than the required depth.
4. The excess sand was then removed.

This preparation method allowed for uniform density to be provided throughout each of the test to be approximately equal to  $\gamma = 17.87\text{kN}/\text{m}^3$ .

(Merifield et al 1999)

The physical testing conducted by Merifield et al 1999 produced a number of interesting results and conclusions. The main data collected, load and displacement, can be presented in a number of ways to provide a good understanding of a number of phenomena. The load vs displacement diagrams obtained for a 75mm diameter anchor buried at different embedment ratios is presented below. The diagrams depict the anchor at an embedment ratio of  $H/B = 4$  and  $H/B = 9.5$  when tested at a pullout rate of  $3\text{mm}/\text{min}$ .

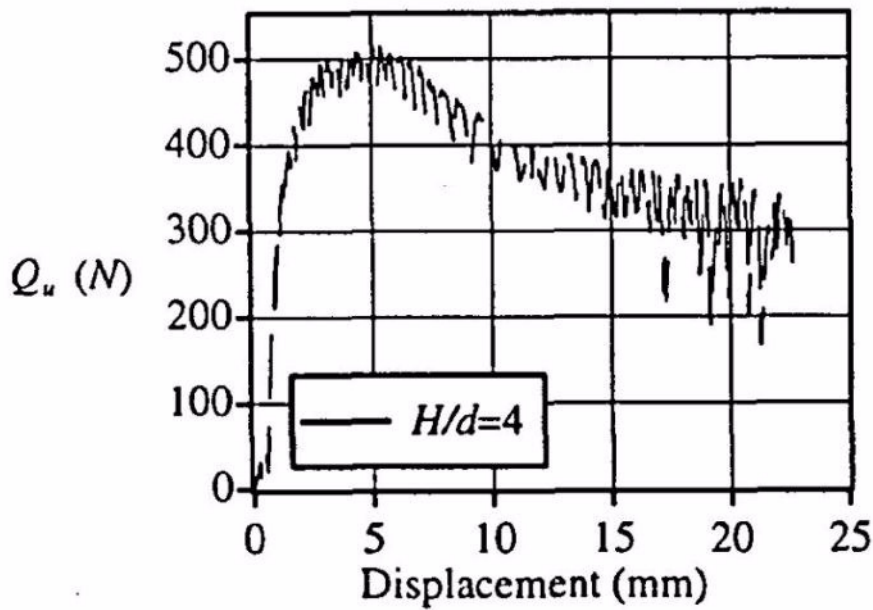


**Figure 2-7.** Load vs. Displacement Diagram  $H/B = 4$   
(Source: Merifield et al 1999)

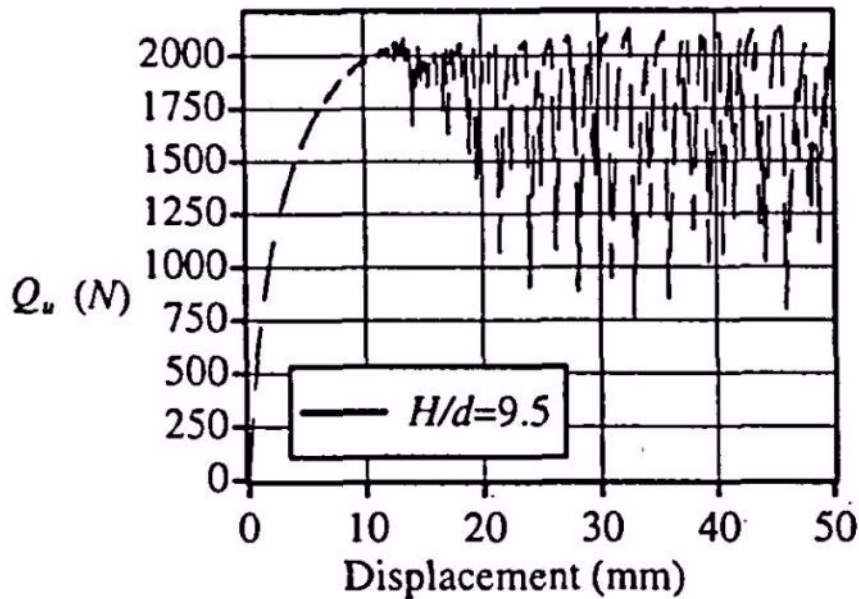


**Figure 2-8.** Load vs. Displacement Diagram  $H/B = 9.5$   
(Source: Merifield et al 1999)

From the above diagrams of Figure 2-7 and Figure 2-8 it can be seen that there is a clear difference between the load-displacement relationship for shallow and deep anchors. “Typically the load displacement response for shallow anchors (Figure 2-7) have a distinct ‘peak load hump’ where the load increases to a peak load, then quickly drops off and finally plateaus out to an approximately constraint load. In comparison, deep anchors (Figure 2-9)

exhibit no ‘peak load hump’, where instead the load increases to a constant peak load.” (Merifield et al 1999) It was discovered within this investigation that typically shallow behaviour of anchors is demonstrated for embedment ratios less than six ( $H/B \leq 6$ ) whilst deep anchor behaviour occurs above embedment ratios of 6 ( $H/B \geq 6$ ).

For each of the cases the effects of the break-out factor were also investigated. The break-out factor can be determined by using equation 2.3 above. The ultimate load  $Q_u$  is determined from the load cells results and therefore the corresponding load vs displacement diagram as represented above in Figure 2-7 and Figure 2-8 respectively. This ultimate load  $Q_u$  is taken to be maximum load reached for shallow anchors and the load just prior to a sudden change in oscillation behaviour for deep anchors. From the conducted experiments it was determined that the break-out factor “can be generalised as increasing steadily up to approximately  $H/B = 12$ , at which point it plateaus out to an approximately constant values.” (Merifield et al 1999). This observation can be seen below in Figure 2-9.

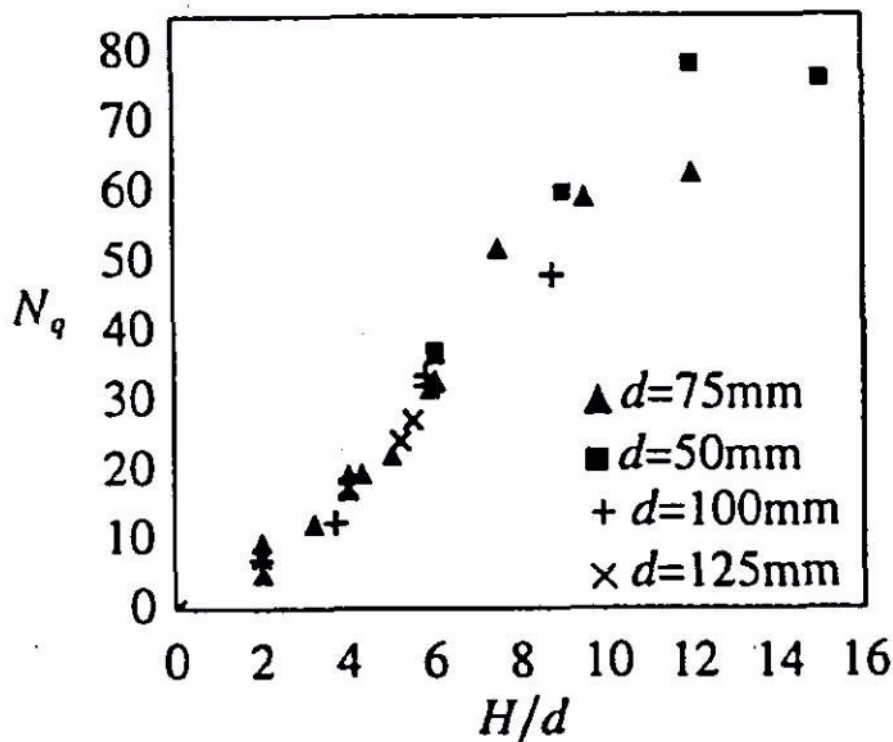


**Figure 2-9.** Break-out Factor vs Embedment Ratio  
(Source: Merifield et al 1999)

It was also determined by Merifield et al (1999) that ultimate loads increase in magnitude with an increase in anchor diameter and increased embedment ratio as would be expected. The increase in ultimate load with increased embedment ratio can be seen below in Figure 2-10. However, it was noted that the break-out factor appears to not be affected by anchor

size. These conclusions gives confidence in the results obtained during this investigation, meaning boundary effects did not affect the overall results.

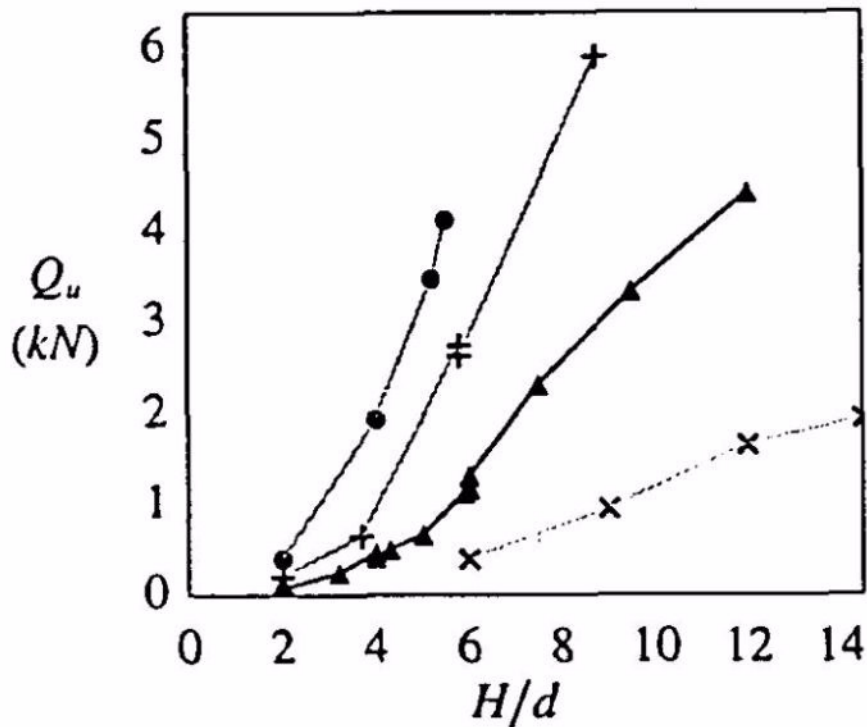


**Figure 2-10.** Ultimate Load vs Embedment Ratio  
(Source: Merifield et al 1999)

One final point that is highlighted in this paper was the effect the pullout rate has on the experimentation. “The rate of loading seems to have a significant effect on the load oscillation for each test.” (Merifield et al 1999) The oscillation phenomena has been previously observed in other studies including Murray and Geddes (1987) and Rowe and Davis (1982) and yet it is still not fully understood. One theory suggests that oscillation could represent localised failure around the anchor. This would therefore imply that the rate of pullout would have an affect on the oscillation results as suggested by Merifield et al (1999); “It was observed that by increasing the rate of loading from  $3\text{mm}/\text{min}$  to  $6\text{mm}/\text{min}$  the occurrence of oscillation was delayed to around the peak load for deep anchors, and until well after peak load for shallow anchors.” One interesting point involving the oscillation phenomena is that the rate of loading does not appear to affect the ultimate load  $Q_u$  and therefore does not effect the break-out factor  $N_q$ .

Merifield and Sloan (2006) takes another perspective into a similar problem by performing numerical investigations into horizontal anchors. “Although there are a variety of experimental results in the literature, very few rigorous numerical analyses have been performed to determine the pullout capacity of anchors in sand” (Merifield & Sloan 2006).

Numerical investigations provide a cost and time effective way to perform a number of investigations into different soil uplift resistance cases for the purpose of design. It is however essential that these theoretical investigation are verified through physical investigations. It is noted that the finite element formulation used within this numerical investigation is same as that presented by Abbo (1997) and Abbo & Sloan (1998).

Merifield & Sloan (2006) produce results for tests completed on plate anchors buried at embedment ratios of 1 to 10. Through this investigation it is reported that for any given embedment ratio  $H/B$ , the break-out factor increases almost linearly with an increase in the soil friction angle  $\phi$ . Through numerical investigation this trend is more apparent in lower bound results rather than in upper bound results. Figure 2-11 and 2-12 demonstrate the break-out factor  $N_\gamma$  plotted against differing coefficient of friction  $\phi$  values buried at differing embedment ratios  $H/B$ . It can be seen below that these tests demonstrate successful tests as only very small error bounds are observed between the upper and lower bound solutions. These graphs also demonstrate the usefulness of numerical investigations as the number of tests that can be completed, i.e. large number of embedment ratios and soil coefficient of friction investigations.

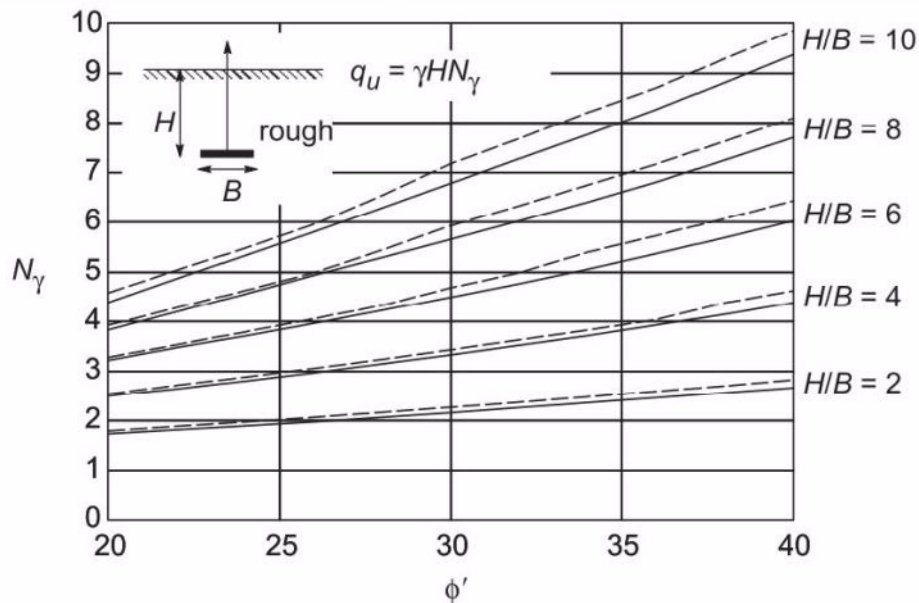


**Figure 2-11.** Break-out Factors  $N_\gamma$  for Horizontal Anchors in Sand. (Source: Merifield & Sloan 2006)

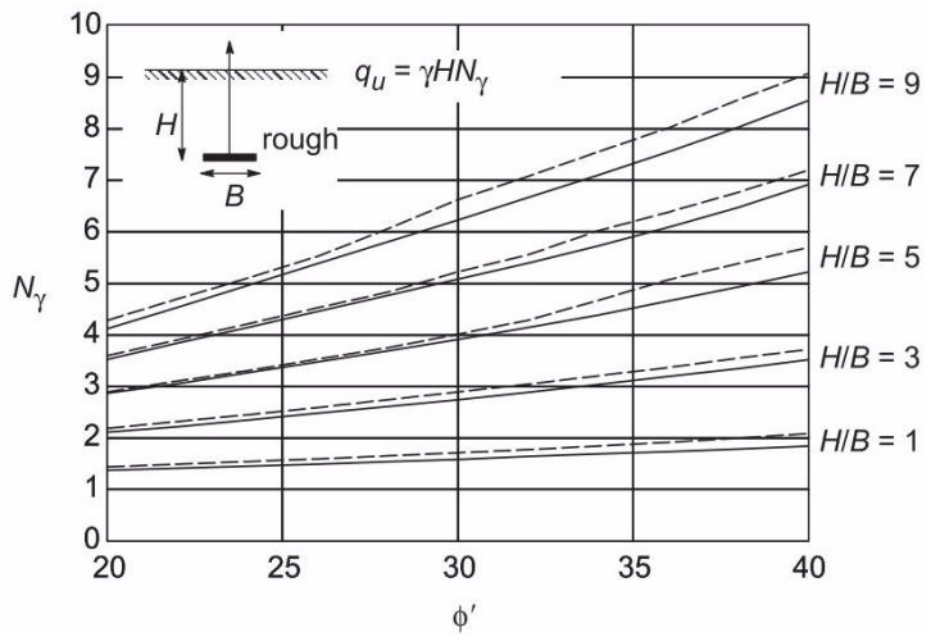


**Figure 2-12.** Break-out Factors  $N_\gamma$  for Horizontal Anchors in Sand.  
(Source: Merifield & Sloan 2006)

This investigation by Merifield & Sloan (2006) also provides insight into the failure mechanisms of plate anchors in sand. Failure properties are found in this numerical investigation to be quite similar to phenomena discovered in investigations by Rowe (1978). Velocity plots below demonstrate the failure that occurs during uplift.

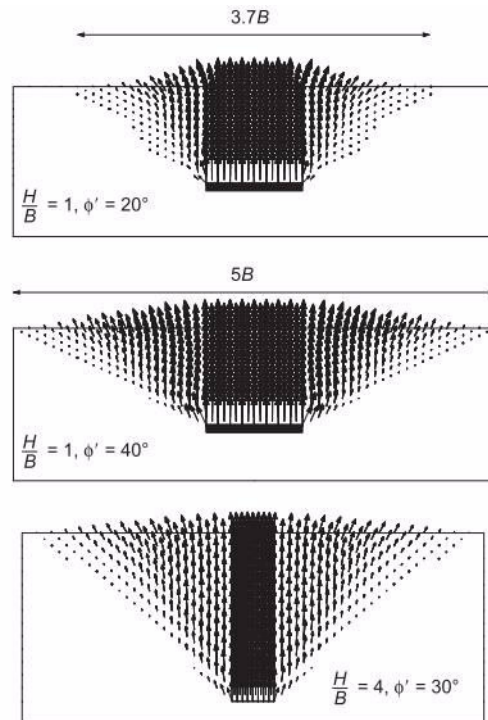


**Figure 2-13.** Velocity Plots Produced from Numerical Investigation  
(Source: Merifield & Sloan 2006)

Figure 2-13 above demonstrated the observed vector plots from this investigation and gives a good overview of the failure that occurs during uplift of plate anchors. It can be seen how the coefficient of friction of the soil affects the overall width of the error bound and are noticed to increase with increased friction angle. “The extent of lateral shearing was found to increase with an increase in the the friction angle at a given embedment depth.” (Merifield & Sloan 2006)

Merifield & Sloan (2006) explain the failure of the anchors to be “found that failure consists of the upwards movement of a rigid column of soil immediately above above the anchor, accompanied by lateral deformation extending out and upwards from the anchor edge. As the anchor is pulled vertically upwards, the material above the anchor tends to lock up as it attempts to dilate during deformation. As a consequence, to accommodate the rigid soil column movement, the observed plastic zone is forced to extend a large distance laterally outwards into the soil mass.”

It was observed that for relatively shallow anchors ( $H/B \leq 4$ ) this soil column directly above the anchor seems to remain nonplastic, whereas the lateral deformation at the extents of the soil profile plastic shearing is extensive. The extent of the nonplastic zone is seen to extend to the soil surface, however the vertical extent of the nonplastic zone is dependant on the friction angle of the soil. It is noted that “the vertical extent of the nonplastic zone

decreases with an increase in the friction angle... and no longer reaches the soil surface for friction angles greater than  $20^\circ$ " (Merifield & Sloan 2006).

Confidence can be taken that the results presented by Merifield & Sloan (2006) are accurate as a number of diagrams are provided comparing results to other existing investigations. Provided below in Figure 2-14 and 2-15 are examples of this numerical investigation compared to investigations by Murray & Geddes (1987) Smith (1998) respectively. It can be seen that these results are extremely accurately, especially in Figure 2-15 in comparison with Smith (1998) where it is difficult to distinguish the difference between results presented.

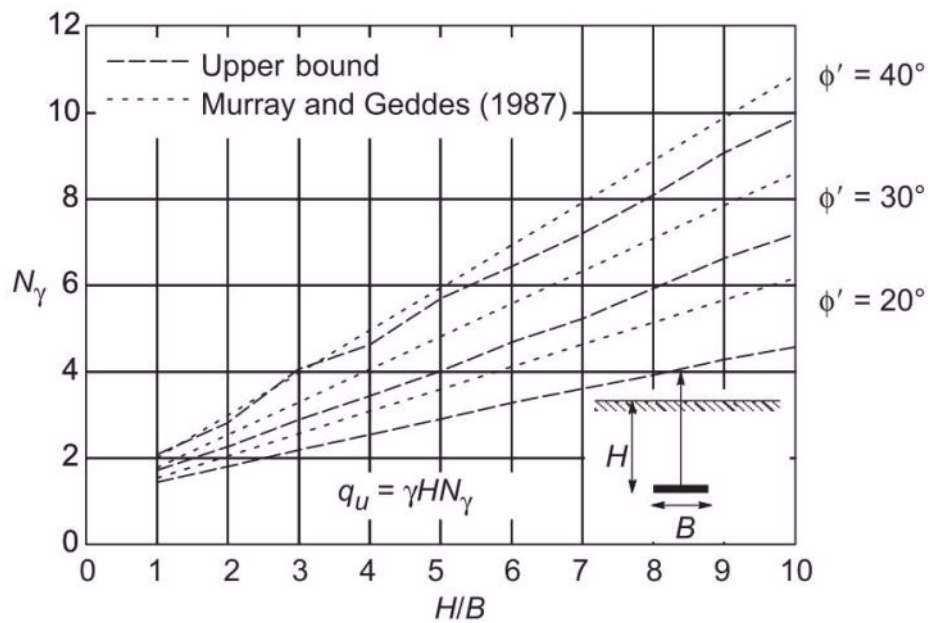


**Figure 2-14.** Comparison of Theoretical Break-out Factors Merifield & Sloan (2006) and Murray & Geddes (1987)  
(Source: Merifield & Sloan 2006)

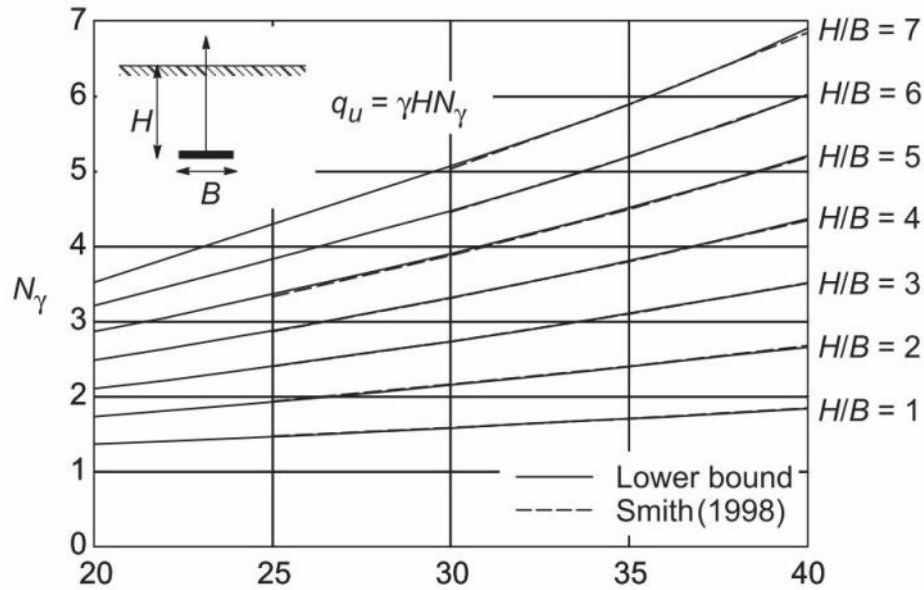


**Figure 2-15.** Comparison of Theoretical Break-out Factors Merifield & Sloan (2006) and Smith (1998)  
(Source: Merifield & Sloan 2006)

### 2.2.6 Uplift Capacity of Inclined Plate Anchors

An inclined plate anchor is defined as an anchor placed at an angle  $\beta$  to the vertical, whereas horizontal anchors can be defined as having an angle value of  $\beta = 0^\circ$  and a vertical anchor has an angle of  $\beta = 90^\circ$ . The direction of the pullout force is to act perpendicular to the face of the anchor whilst  $H'$ ,  $H_a$ , and  $H$  represent the depths to the top, middle and bottom of the anchor respectively measured from the soil surface. In the diagram below an overview of inclined plate anchors can be seen. Part (a) represents typical horizontal anchor, part (b) demonstrates the inclined anchors whilst part (c) shows the vertical anchor.

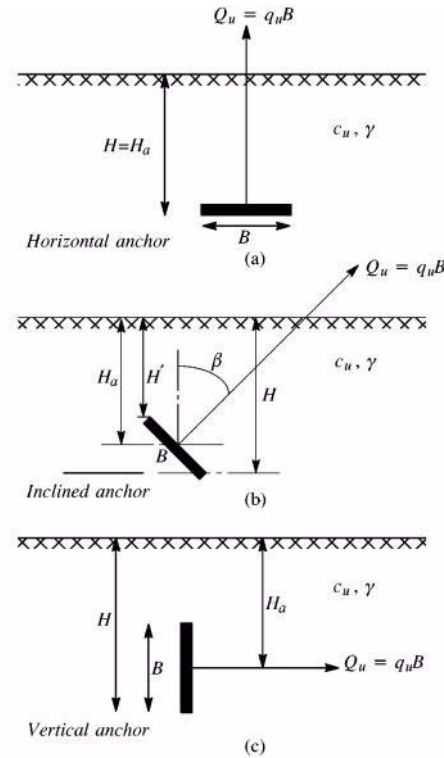


**Figure 2-16.** Overview of Inclined Plate Anchors  
(Source: Merifield, Lyamin & Sloan 2005)

As with horizontal plate anchors, it is relevant to present pullout capacities of inclined anchors in terms of a break-out factor. Merifield, Lyamin & Sloan (2005) demonstrate the capacity of inclined anchors using the break-out factor in two ways. The first is the break-out factor plotted against the embedment ratio and the second representation is the inclination factor versus the embedment ratio. The inclination factor is defined as the ratio of the break-out factor for an inclined anchor at an embedment ratio of  $H_a/B$  compared to a vertical anchor at the same embedment ratio of  $H_a/B$ . Presented below in figure 2-17 and 2-18 respectively are the results obtained from Merifield, Lyamin & Sloan (2005).

$$i = \frac{N_{co\beta}}{N_{co90}} \quad (2.7)$$

Where  $i$  = Inclination factor

$N_{co\beta}$  = Break-out factor for inclined anchor

$N_{co90}$  = Break-out factor for vertical anchor

(Merifield, Lyamin & Sloan 2005)

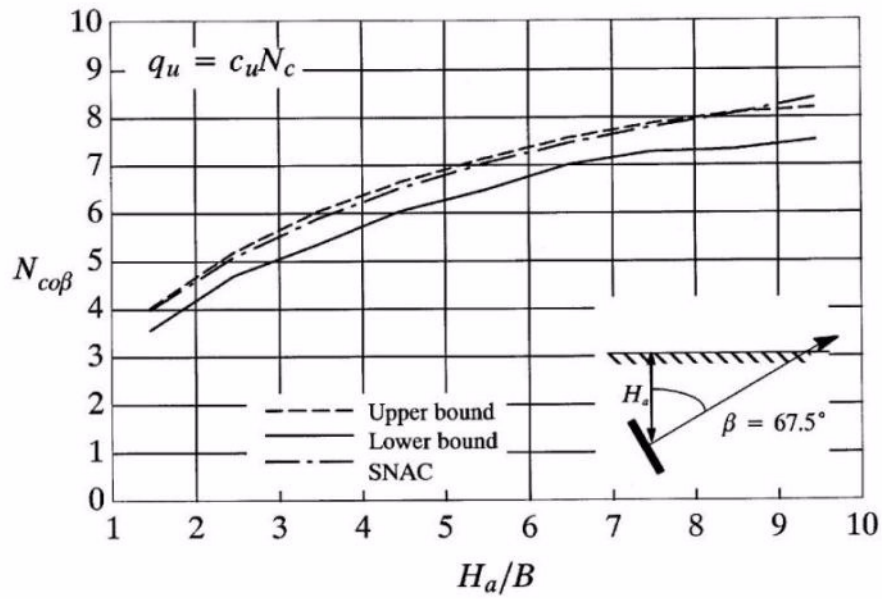


**Figure 2-17.** Break-out Factor vs Embedment Ratio - Inclined Plate Anchors (Source: Merifield, Lyamin & Sloan 2005).

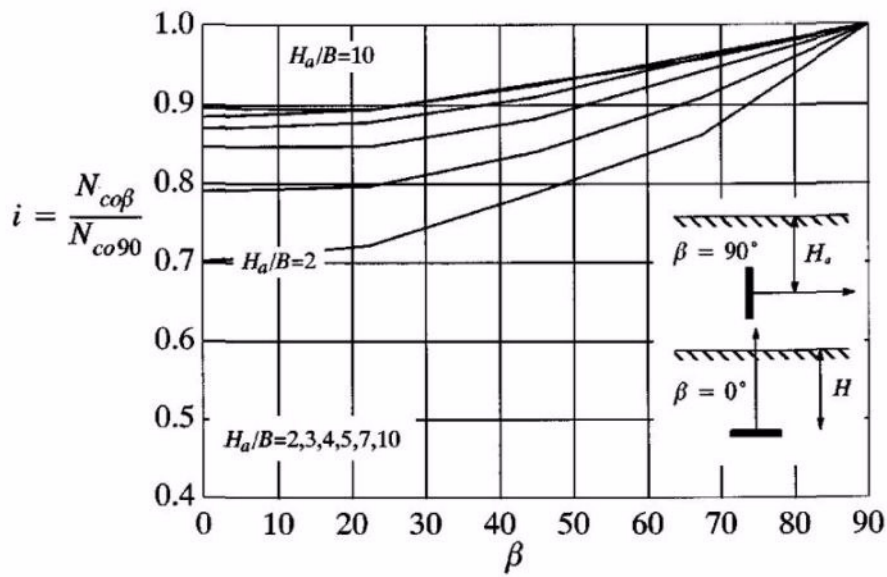


**Figure 2-18.** Inclination Factors vs Embedment Ratio- Incline Plate Anchors (Source: Merifield, Lyamin & Sloan 2005)

Figure 2-17 above demonstrates the break-out factor of an inclined anchor against the embedment ratio. The graph produced is similar to that of horizontal plate anchors as seen earlier in figure 2-11 and 2-12. As expected, the breakout factor increases with increased embedment ratio just as with horizontal plate anchors. It would appear from figure 2-17 as the graph begins to curve that eventually a peak value would be found where maximum break-out factor would be obtained above a certain embedment ratio. It is also noted that with an increase in embedment ratio there is an increase in inclination factor, this can be seen in figure 2-18. Merifield, Lyamin & Sloan (2005) note from observations “that there

is very little difference between the capacity of a horizontal anchor ( $\beta = 0$ ) and anchors inclined at  $\beta \leq 22.5^\circ$ . The greatest rate of increase in anchor capacity appears to occur once  $\beta \geq 30^\circ$ .

The failure mechanisms observed by Merifield, Lyamin & Sloan are depicted below. “The lateral extent of surface deformation increases with increasing embedment depth and inclination angle. This is consistent with the findings for both the horizontal and vertical anchor cases. As expected, the actual magnitude of the surface deformations decreases with the embedment ratio. ...In addition, very little plastic shearing was observed below the bottom edge of anchors inclined at  $\beta < 45^\circ$ .

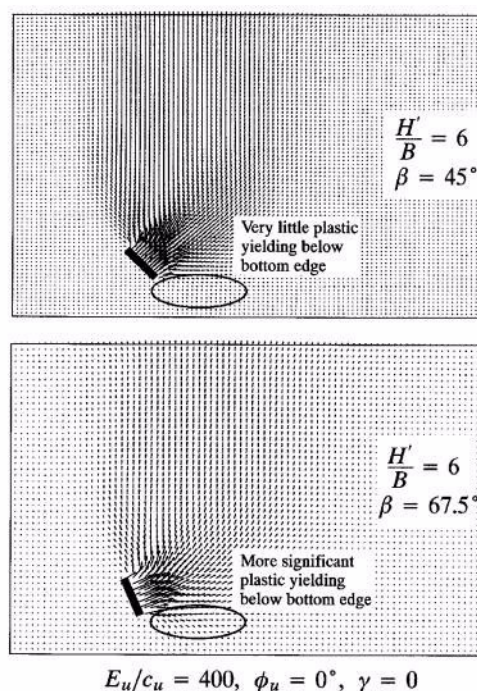


**Figure 2-19.** Failure Mechanisms for Inclined Anchors  
(Source Merifield, Lyamin & Sloan 2005)

### 2.2.7 Uplift Capacity of Group Anchor Plates

Both Geddes & Murray (1996) and Kouzer & Kumar (2009) make note that there is a number of studies and results conducted for the uplift of individual plate anchors, however anchor groups represent a considerably important field and yet there is very little published information on this topic. Anchor groups and spaced horizontal strip anchors represent a large portion of the field of anchors, especially in consideration for industry use. Testing in this field may represent concrete slab anchors, grilling anchors, pad footings and group anchors that are designed to resist wind loading, overturning of guyed structures or even resisting hydrostatic uplift of buried structures below the water table. Geddes & Murray (1996) presents a physical investigation of this situation whilst Kouzer & Kumar (2009)

compliment this study with a numerical investigation. Kouzer & Kumer (2009) make two points that can be drawn from existing investigations into groups anchors pulled vertically; 1. the vertical uplift capacity of the anchors reduces quite significantly with a decrease in the spacing between the anchors; 2. the magnitude of failure loads for a given spacing reduces continuously with an increase in the number of anchors in a group.

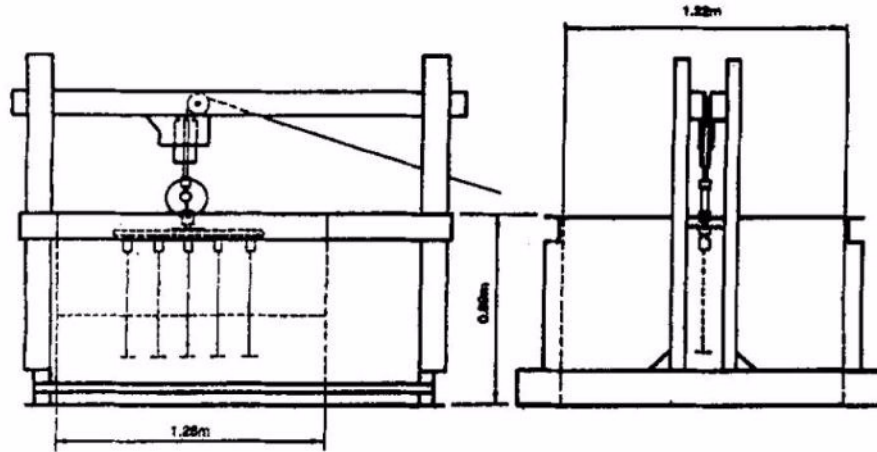


**Figure 2-20.** Anchor Groups Pulled Vertically in Sand Overview (Source: Geddes & Murray 1996)

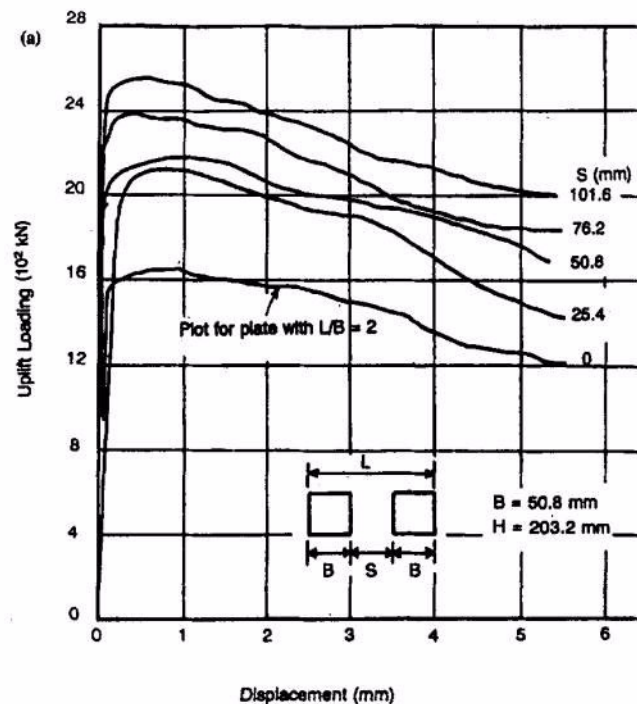


**Figure 2-21.** Uplift Load vs Displacement - Two Plate Group (Source: Geddes & Murray 1996)

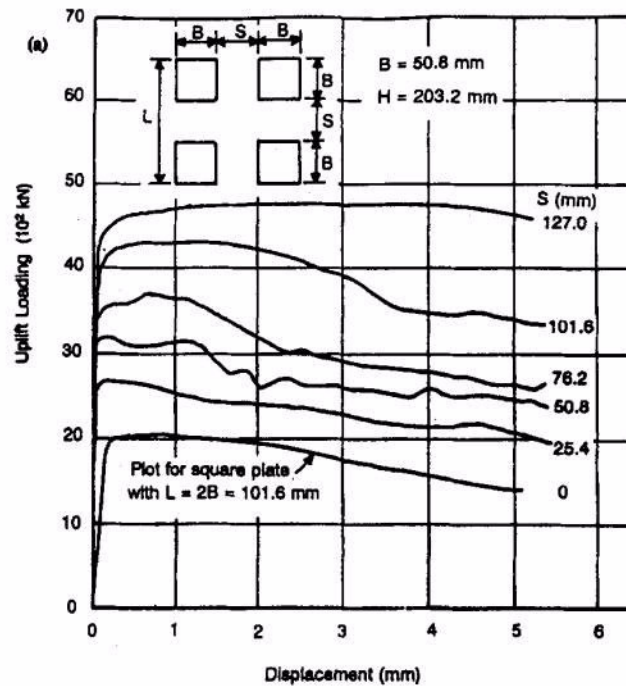


**Figure 2-22.** Uplift Load vs Displacement - Four Plate Group  
(Source: Geddes & Murray 1996)

Figure 2-20 and 2-21 demonstrate the load versus displacement curves for group anchor plates for groups of 2 and 4 plates respectively. The variable  $S$  represents the spacing between each of the plate anchors within the group, this can be better understood from viewing the accompanying diagram with the above graphs. Results are displayed for separation from  $S/B = 0$  to  $S/B = 2$ , where  $S/B = 0$  represents plates directly beside one another with no spacing. “The curves all display a rapid rise in resistance with displacement in the early stages, with a distinctive peak value at small displacement, followed by a progressive reduction as the displacement is increased.” (Geddes & Murray 1996) It is noted that the shape of the curve is very similar to the load-displacement curves produced by the uplift of single plate anchors in sand.

It is possible to express the uplift capacity of a group of anchors in terms of group efficiency represented as a percentage. This group efficiency represents the peak load of a group of anchors compared to the peak load of a single isolated plate. Kouzer & Kumar (2009) explain this efficiency factor as “the ratio of the magnitude of the collapse load for a strip anchor of given width  $B$  and placed at a depth  $H$  in a group of infinite of anchors, to that of an isolated strip anchor with the same values of  $B$  and  $H$ .” It is also appropriate to demonstrate this efficiency factor as a formula as follows:

$$\text{group efficiency (\%)} = \frac{\text{peak load of group of } N \text{ plates} \times 100}{N \times \text{peak load of a single isolated plate}} \quad (2.8)$$

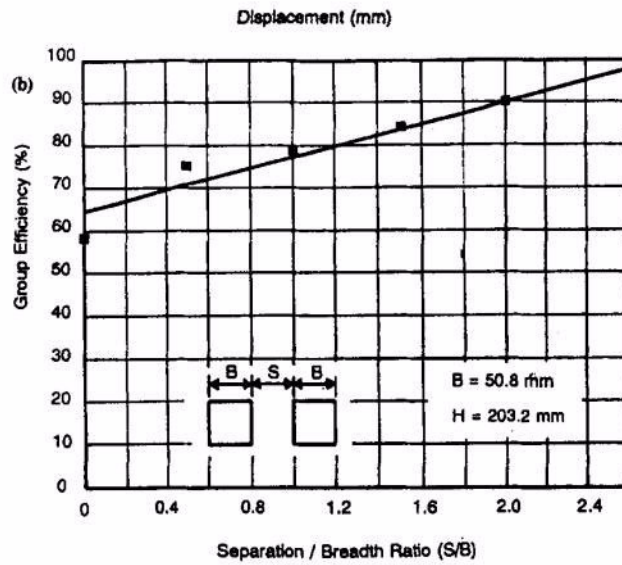


**Figure 2-23.** Group Efficiency vs Separation/Breadth Ratio - Two Plate Group (Source: Geddes & Murray 1996)

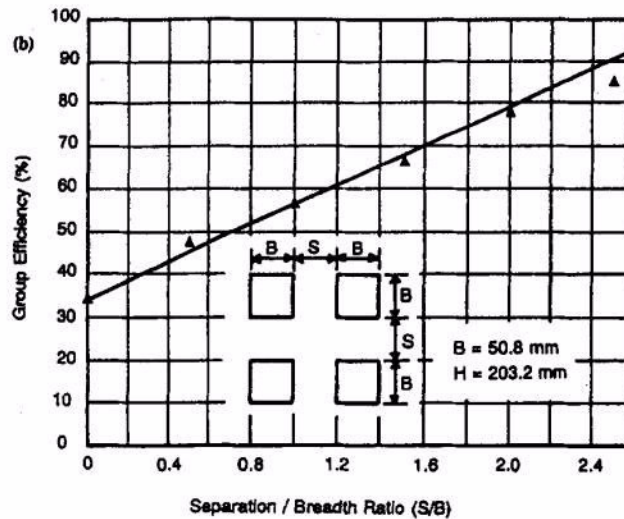


**Figure 2-24.** Group Efficiency vs Separation/Breadth Ratio - Four Plate Group (Source: Geddes & Murray 1996)

Figure 2-19 and 2-20 demonstrate the group efficiency described above versus the separation-breadth ratio of the anchors. Efficiency of the system increases with an increase in separation and can be related to an approximate linear relationship. Using this theology, it is therefore possible to assume that if this linear relationship continues there will be a point when the efficiency of the plates is at a maximum of 100% with an increased  $S/B$  ratio. At this point, 100% efficiency suggests that each of the plate anchors are working independently of each other and can be assumed to be individual plate anchors. Another observation from these above figures is that for low  $S/B$  ratios the group of four plates has significantly lower values of efficiency when compared to respective two plate group

anchors. Similar results were obtained in the numerical experimentation conducted by Kouzer & Kumar (2009) and can be seen below in Figure 2-21. Kouzer & Kumar (2009) make to observations in regards to the efficiency factor that agree with the results reported in Geddes & Murray (1996). “A decrease in spacing between the anchors the magnitude of the efficiency factor reduces continuously. For the value of  $S$  equal to or greater than  $2d \tan \phi$ , the magnitude of efficiency factor becomes almost equal to 1.0. This implies that for  $S \geq 2d \tan \phi$ , the uplift resistance of the anchors becomes equal to that of an isolated anchor... It can also be noticed that the magnitude of efficiency factor for given values of  $S/B$  and embedment ratio decreases continuously with an increase in  $\phi$ .

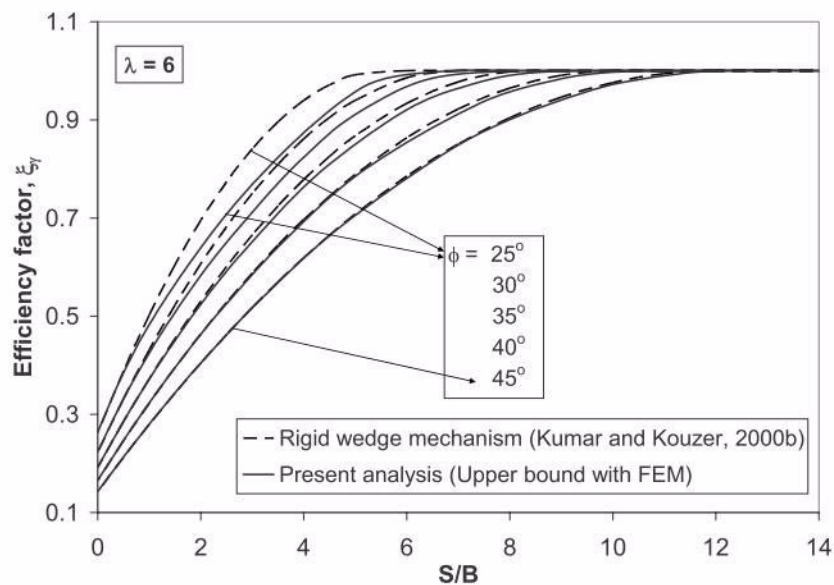


**Figure 2-25.** Group Efficiency vs Separation/Breadth Ratio - Group Strip Anchors  
(Source: Kouzer & Kumar 2009)

Figure 2-22 below demonstrates the loads on individual plates for a group of five anchors pulled vertically in a row configuration. It can be seen that “all plates do not reach their maximum resistance simultaneously. ...the three inner plates were found to reach their peak loads first, and then decline in their resistance as the end plates A and E moved to a maximum at substantially greater displacements. For all separations, the end plates reached individually higher ultimate loads than the inner plates. For all but the lowest separation ratio of 0.25, the center plate of the group carried the lowest ultimate load” (Geddes & Murray 1996).

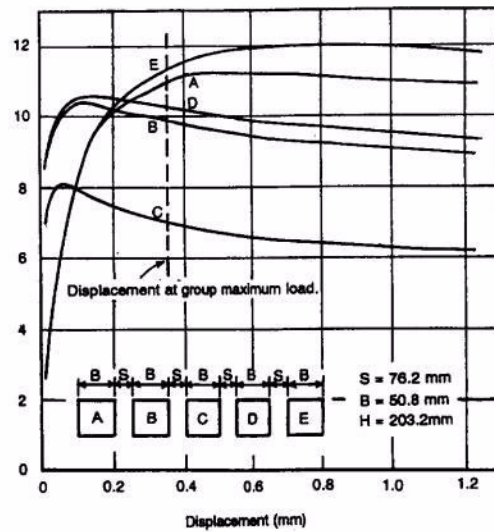


**Figure 2-26.** Load-Displacement Curves for Individual Plates  
(Source: Geddes & Murray 1996)

## 2.3 Buried Pipelines

### 2.3.1 Background

As mentioned earlier, it is becoming increasingly common to transport materials such as oil and gas via buried pipelines that may be subject to uplift forces. Failure of these buried pipelines via uplift forces can have many negative effects that include environmental, economic and social consequences. An increase in pipeline burial depth does increase levels of protection against physical disruption and uplift failure. However, burial depth represents one of the main contributing factors to the overall capital cost of buried pipelines. Thus careful design of such pipelines is required to allow adequate cover and protection to be provided in an economical and viable way.

A key form of failure for buried pipelines at sea is thermal buckling. As these underground pipelines often transfer contents such as liquids and gas at high temperatures ( $160^{\circ}\text{C}$ ) and high pressures ( $70\text{MPa}$ ). Under these operating conditions axial thermal expansion can occur and is restrained by the friction at the soil-pipe interface and end connections. If the expansion is great enough it is common for protrusion of the pipeline through the soil cover to occur and in extensive cases of expansion bending failure can occur.

“Stresses will therefore build up and a point may be reached where the axial load acting on a section of the pipe will be greater than the buckling load for a similar length of pipe. A buckle might occur if the pipe can overcome the resistance of the soil to lateral movement, with the pipe moving in direction of least resistance. In most cases

this will be the resistance of the remoulded soil above the pipe and so therefore the pipe will tend to move out of the ground and be prone to damage.” (Schupp et al 2006).

This form of failure is noted to be the most common reason for failure in pipeline applications in a number of papers including Cheuk et al (2008), Schupp et al (2006), Trautmann et al (1985) and White et al (2008). Therefore, as mentioned above it is important the design of pipelines allows for significant burial depth that can be provided in an economical fashion. Currently, the design approach for predicting peak uplift forces from existing soil type and cover depth are based on simple rigid block mechanisms and are compared against existing model tests as a form of check.

The pipelines are usually deposited into trenches to provide burial and protection. Burial of pipelines is normally achieved in one of two methods. The first involves ‘jetting’ the soil where the soil forms properties similar to a fluid. Whilst in this form the pipeline is able to be lowered into the soil as a result of sinking through the ‘quicksand’ soil. The second method involves mechanically removing the soil, placing the pipeline into position and then mechanically filling back over the pile. The problem with buried pipelines consists in the fact that even after following either of these deposition procedures the remoulded strength of the soil that is above and surrounding the buried pipe is significantly less than that of the soil before it was disturbed.

One way of combating this uplift phenomenon encountered by buried pipelines is to attempt to optimise the axial friction that occurs between the soil and the pipeline to reduce this possibility of buckling. It is important to avoid upheaval at all costs because if upheaval does occur it is an expensive process to repair the uplifted section through mechanical repair or rock dumping operations.

### 2.3.2 Failure Mechanisms

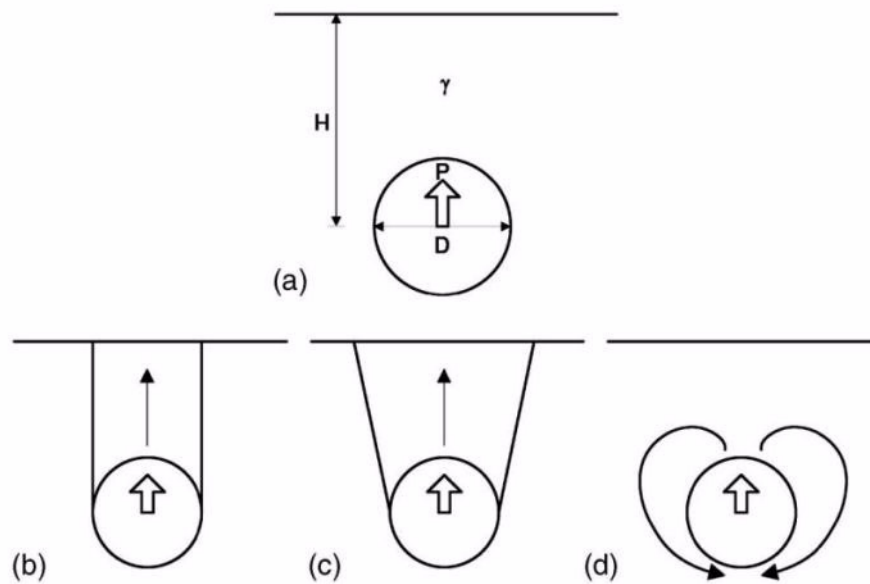


**Figure 2-27.** Overview of Pipeline Failure Mechanisms  
(Source: Cheuk et al 2008)

Figure 2-27 above provides a good overview of common understandings of the failure mechanisms of pipelines buried in sand. Section (a) provides an overview of the geometry associate with the buried pipeline problem, whilst (b) demonstrates the simplest form of failure understanding, (c) takes the understanding of (b) a little further to include angular slip planes, whilst part (d) highlights the flow around phenomena that is observed in pipeline failures. Figure 2-27(b) represents a simple load block mechanism that is bound by by a pair of shear bands, the capacity of which is the weight of soil above the anchor plus the shear stress of the planes. This is exactly the same theology as that applied to the uplift capacity of plate anchors in sand. Figure 2-27 (c) demonstrates further application of the simplified model of the vertical slip model presented in part (b). This failure mechanism recognises that the planes that form will occur at some inclination  $\theta$  to the vertical plane. Once more “the uplift resistance is equal to the lifted soil weight plus the resultant vertical force on the slip planes, which arises from both the shear and the normal stresses.” (White et al 2008). Figure 2-27(d) depicts the flow around phenomena that is observed to occur in pipeline investigations and shall be discussed further in section 2.3.8 Infilling Mechanism.

Typically there are two common ways of estimating expected uplift resistance of pipelines, they are limit equilibrium solutions and plastic solutions. Limit equilibrium solutions are based off figure 2-27 (b) and (c) above whilst plastic solutions are based on lower and upper-bound analysis and are more rigorous than the limit equilibrium solutions. The limit

equilibrium solution is discussed further below as it provides the best way to perform analysis on pipelines compared to the plastic solutions.

### 2.3.3 Limit Equilibrium Solutions

Physical experimentation determines that normality does not hold for pipeline uplift investigations and therefore leads to bound theorems to be of limited use. Although limit equilibrium solutions lack the rigour of bound theorem investigations they do allow for normality to be ignored and therefore the assumed failure mechanisms can be matched to experimental observations allowing for the introduction of parameters such as flow rules and soil dilatancy to be included within the investigation.

This method assumes that an inverted trapezoidal block of soil is lifted above the pipeline, similar to figure 2-27(c) and capacity is determined from the weight of soil contained in the block plus the shear stress developed along the slip planes. The angle of the trapezoid is assumed to be the angle of dilatancy of the soil, therefore in figure 2-27(c) above  $\theta = \psi$ . Calculation of the weight of soil is simple enough, however some assumptions are required to determine the shear stress. It is assumed that the shear resistance developed along the slip planes is equal to the in situ value that is determined from the factor  $K_0$  from the Mohr's circle depicted below in figure 2-28. "As a result, a realistic increase in vertical stress ahead of the pipe is permitted, as shown by the larger Mohr's circle representing the conditions at peak resistance." (White et al 2008). Therefore from the geometry of these two circles depicted below, the shear stress can be calculated as follows:

$$\tau = \gamma'z \tan \phi_{\text{peak}} \left[ \frac{(1 + K_0)}{2} - \frac{(1 - K_0) \cos 2\psi}{2} \right] \quad (2.9)$$

Where:  $\tau$  = Peak mobilised shear stress along the slip surface

$\gamma'$  = Unit weight of soil

$z$  = From Mohr's circle diagram below

$\phi_{\text{peak}}$  = Soil angle of friction at peak uplift load

$K_0$  = Factor determined from Mohr's circle

$\psi$  = Soil dilation angle

Therefore, "by integrating along the slip planes and equating the vertical forces acting on the sliding block, the peak uplift resistance per unit length, (White et al 2008),  $P$  is calculated as follows:

$$P = \gamma'HD + \gamma'H^2 \tan \psi + \gamma'H^2(\tan \phi_{\text{peak}} - \tan \psi) \times \left[ \frac{(1 + K_0)}{2} - \frac{(1 - K_0) \cos 2\psi}{2} \right] \quad (2.10)$$

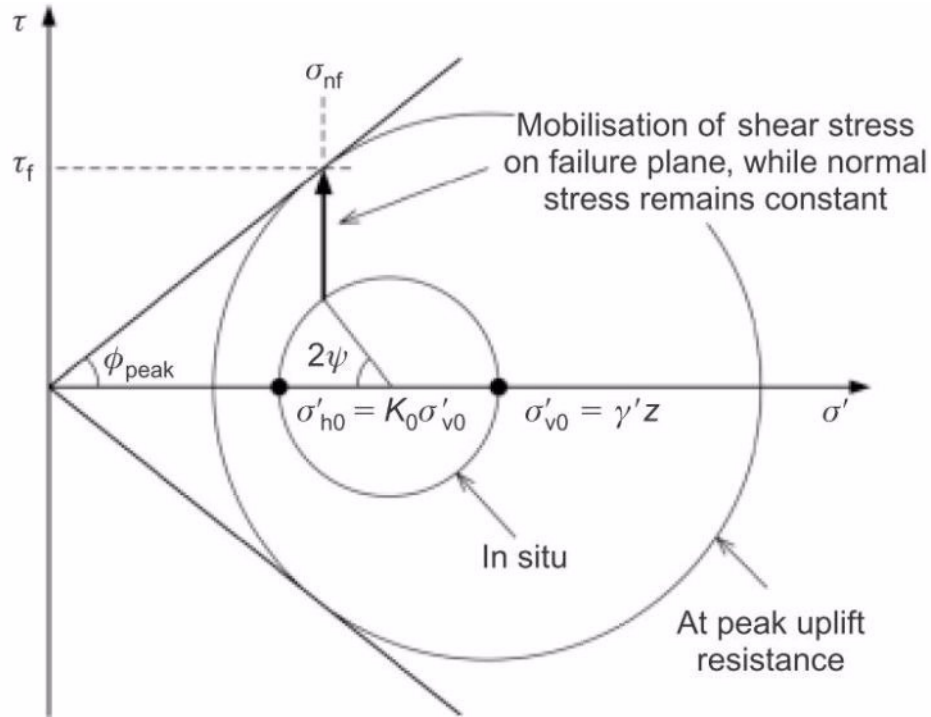


**Figure 2-28.** Assumed Mohr's Circles In Situ and at Peak Uplift Resistance (Source: White et al 2008)

**2.3.4 Deformation Mechanisms**

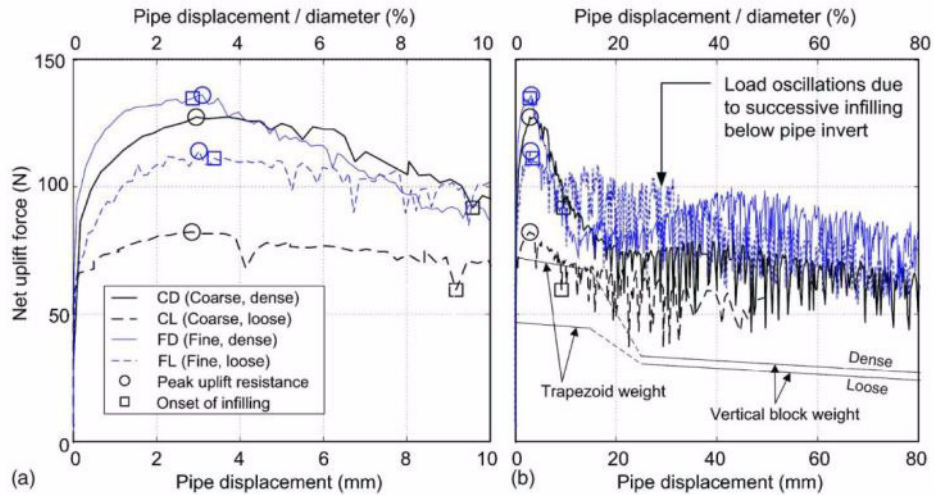


**Figure 2-29.** Displacement Field for Pipeline Uplift (Source: Cheuk et al 2008)

Figure 2-29 above demonstrates the displacement field obtained for a pipeline exposed to uplift forces where part (a) is the vector field at maximum load and part (b) is the vector field obtained at displacement of  $0.5B$  or half of the pipeline diameter. At peak load wide zones of distributed shear can be seen in section (A) whilst the the shear planes curve

outwards (*B*) and therefore displaying increased dilation near the soil surface. In figure 2-29(b) after peak load is reached the shear planes have become narrower as highlighted at point (*C*). Figure 2-29(b) also displays downwards soil movement at the very edges of the pipe. This is evidence of the flow around phenomena occurring and can be clearly seen at point (*D*).

Therefore Cheuk et al (2008) suggests that the deformation mechanisms during uplift experience four key stages:

1. Mobilisation of peak resistance.
2. Onset of infilling beneath the pipe invert.
3. Postpeak shear band formation.
4. Flow around.

A similar layout of key stages is also presented in Schupp et al (2006) confirming the above statement.

### 2.3.5 Load-Displacement Relationship

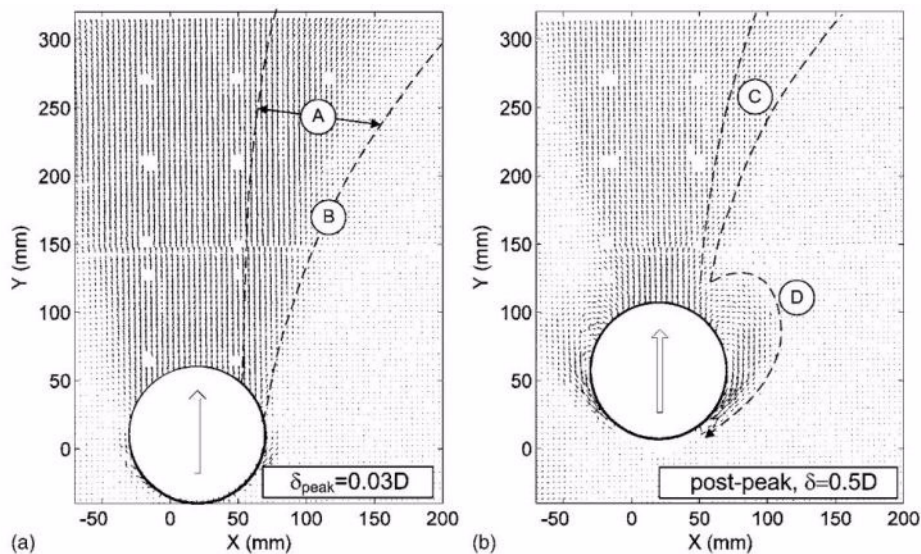


**Figure 2-30.** Load-Displacement Diagram for Pipeline Uplift  
(Source: Cheuk et al 2008)

Figure 2-30 above demonstrates a typical load-displacement response from an uplift investigation of pipelines buried in sand. It can be seen that a peak load is reached very quickly after a small amount of displacement, just as occurs with plate anchors. It is noted that after this peak load is reached and the load begins to drop with increased pipeline displacement that serious oscillation of load is noticed. These oscillations are also described in Trautmann et al (1985) and are proven to be caused by miniature slope failures as soil falls around the pipeline to fill the cavity below in Cheuf et al (2008).

The following passage from Cheuf et al (2008) best describes this observed phenomena. “These slope failures have significant implications for the up-heaval buckling behavior of the pipe. During cyclic thermal loading, the infilling at the pipe invert triggers upward ratcheting. If infilling occurs during a cycle of uplift, the pipeline cannot return to the original configuration upon cooling. This irrecoverable movement enlarges any overbend in the pipe, leading to a greater chance of buckle initiation in the next thermal cycle.”

### **2.3.6 Infilling Mechanism**

The infilling mechanism observed as part of buried pipelines has been introduced throughout the above paragraphs. Infilling contributes to the pipeline being subject to irreversible uplift as the pipeline cannot return to its original position that is then filled with soil. It is noted that this infilling phenomena is dependant on soil grain size. This noticed in Cheuk et al (2008) where large amounts of downward soil movement was observed for fine grained sand but little to none was observed for course sand. “In the fine sand, this infilling mechanism begins at the same moment as peak resistance is mobilised. In the coarse sand, inspection of the images show that no infilling occurred until [larger pipeline displacements occur]” (Cheuk et al 2008). It is also noted that although the infilling mechanism is dependant upon soil size it is not a linear relationship that describes this phenomena.

## 2.4 Pile Anchors

### 2.4.1 Background

A large number of studies existing for the investigation into pile anchors that are subject to compressible loads, however pile anchors that resist uplift forces has far less information available. Prediction of loads is a very important aspect of any form of civil engineering and is especially true for geotechnical aspects. Often load estimations will lead to actions being taken and it is therefore important that these estimates are accurate and reliable. Structures that are supported on pile foundations are normally subject to very large forces and often represent common foundations for super structures. It is therefore imperative that the estimations associated with pile loadings are correct as large loads can have very large consequences if incorrectly calculated.

Whilst most structures that utilise pile anchors for support are subject to compression forces, it is not uncommon practice for piles to be required to resist uplift forces. These uplift forces may be caused by large wind or wave loads and can induce tension within the pile. Typically structures that require pile anchors to resist uplift loads will be in a marine or offshore setting supporting structures such as mooring systems, submerged platforms or jetty structures. Other applications may include transmission towers, large chimneys, tall structures and buildings or large superstructures. With an increase in the use of pile anchors used to resist uplift forces, it is important that acceptable prediction methods are established.

The main contributing factor to the piles uplift capacity in sand is the friction created between the pile-soil profile. “The uplift resistance of straight shafted pile in sand is assumed to be dependent on the skin friction between the pile shaft and the soil.” (Chattopadhyay & Pise 1986). It is also noted that typically literature suggests that the skin frictional resistance of piles subject to uplift forces is lower than the mobilised in resistance of compressively load pile anchor counterpart.

## 2.4.2 Failure Mechanisms

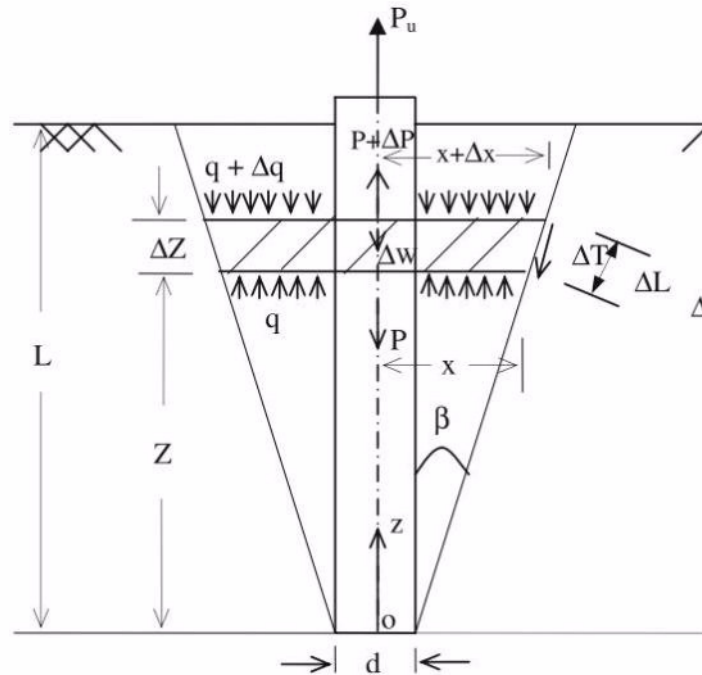


**Figure 2-31.** Simplified Failure Mechanism - Pile Anchor  
(Source: Shanker et al 2007)

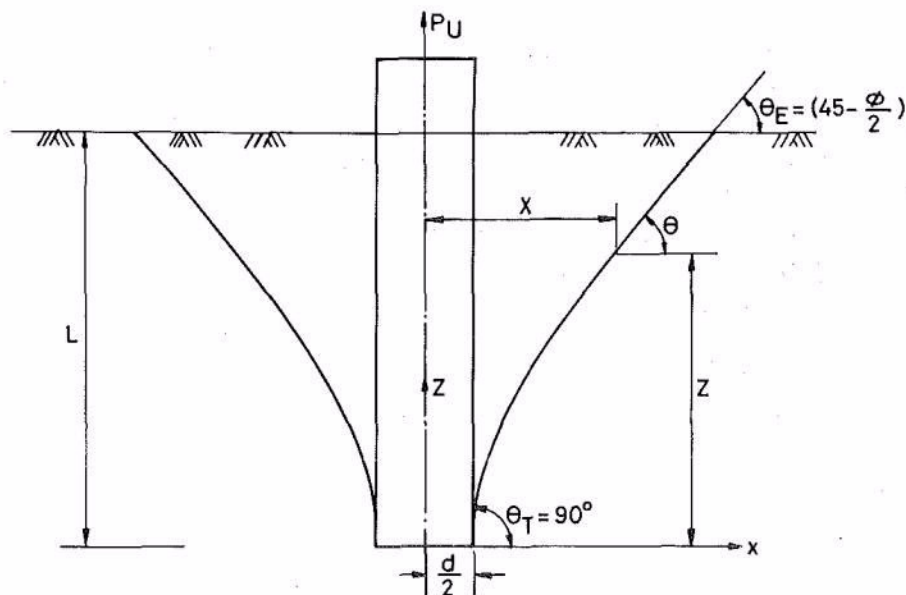


**Figure 2-32.** Failure Mechanism - Pile Anchor  
(Source: Chattopadhyay & Pise 1986)

Figures 2-31 and 2-32 demonstrate common failure mechanisms adopted for pile foundations subjected to uplift loading conditions. Figure 2-31 represents a simplified model that displays an inverted trapezoidal shape whilst figure 2-32 displays the common observed failure mechanism of shear planes extending to the soil surface in a conical shaped fashion. It is observed that both of these adopted failure mechanisms are very similar in

concept and exactly the same in general shape as the failure mechanisms for both horizontal plate anchors and buried pipelines.

“During uplift of a vertical circular pile embedded in sand, an axisymmetry solid body of revolution of soil along with the pile is assumed to be initiated to move up along the resulting surface, as shown in [Figure 2-32]. The movement is resisted by the mobilized shear strength of the soil along the failure surface and the weight of the soil and the pile. In the limiting equilibrium condition, ultimate uplift capacity of the pile is attained.” (Chattopadhyay & Pise 1986).

The shape and size of the shear planes are dependant on a number of parameters. These parameters include the slenderness ratio of the pile  $\lambda$ , the internal friction angle of the soil  $\phi$  and the pile friction angle  $\delta$ . Chattopadhyay & Pise (1986) make three observations in regards to the above factors and the relationship they have to failure planes created.

1. For a given slenderness ratio, the horizontal extent of the shear planes from center of the pile is greatest for pile friction angle is equal to the soil friction angle,  $\phi = \delta$ .
2. For piles with a pile friction angle greater than zero ( $\delta \geq 0$ ), the failure surface plane initiates at the tip of the pile and moves through the surrounding soil towards the soil surface.
3. For piles with a pile friction angle greater than zero ( $\delta \geq 0$ ), the angle created between the shear planes and the horizontal axis approaches  $(45 - \phi/2)$ . Whilst for pile anchors with a pile friction angle of 0 ( $\delta = 0$ ), the angle is  $90^\circ$ .

### 2.4.3 Existing Investigations

Shanker et al (2007) gives a good overview of the studies conducted thus far and the methods presented for determining the ultimate uplift capacity of the piles. This section shall now present these existing investigations as they prove appropriate.

Standard Model: Assumes that failure takes place on a cylindrical surface and introduce the  $K_s$  value to represent the lateral earth pressure coefficient. Accuracy of this model is based on the ability to accurately estimate or determine the  $K_s$  coefficient. The net uplift capacity is determined using the following formula:

$$P_{nu} = \frac{\pi}{2} K_s d \gamma L^2 \tan \delta \quad (2.11)$$

Truncate Cone Model: Is based on the inverted trunk slip planes where the ultimate capacity consists of the weight of soil contained within the zone. Determined by the following formula:

$$P_{nu} = \frac{\pi}{3} L^3 \tan^2 \frac{\phi}{2} \gamma \quad (2.12)$$

Myerhof's Model: "Ignoring the weight of the pile he suggested an expression for the pull-out resistance assuming that under axial pull the failed soil mass has a roughly similar shape as for a shallow anchor." (Shanker et al 2007) Thus,

$$P_{nu} = \frac{\pi}{2} K_u d \gamma L^2 \tan \delta \quad (2.13)$$

---

# USQ Physical Testing Facilities



## 3.1 Introduction

During the physical investigations conducted as part of this project, a number of testing facilities were utilised to conduct experimentation. The main testing equipment included the soil loading machine, the accompanying software and the shear box test equipment. The soil loading machine was used to induce required uplift loads whilst the computer and appropriate software recorded the relevant data. Shear box tests were also conducted to determine the soil cohesion and soil friction angle. It is noted that other equipment was used throughout this investigation and is further mentioned in Chapter 4, however this chapter gives details of the ‘main’ components of experimentation.

## 3.2 Testing Equipment

### 3.2.1 Soil Loading Machine

The soil loading machine consists of a steel ram that is attached to a large steel frame containing a large loading platform and can be viewed below in figure 3-1. The ram is a form of linear actuator and is used to apply the uplift force to the buried anchors to replicate the uplift forces imposed on ground anchors in reality. The linear actuator is run by an electric motor that is capable of running in both directions, i.e. upwards vertical and downwards vertical directions respectively. This electric motor is connected through a series of gears which in turn move the steel ram accordingly in the required direction. The particular ram system used for experimentation is capable of delivering a force of 27kN if required. This piece of equipment is generally used for compression loading, therefore an important aspect of the loading machine is the ability of the machine to operate in both

directions. This is achieved by selecting the required type of loading with the attached switch to either tensile force or compression forces.



**Figure 3-1.** Overview of Soil Loading Machine

The ram further requires devices to actually measure the required information such as applied load and anchor displacement. To accomplish this a load cell and linear variable differential transformer (LVDT) transducers are employed. The load cell is used to detect the force that is being applied to the ram at any given time, whilst the LVDT transducer is able to determine the vertical displacement of the ram at any time. The underside of the load cell then has attached to it a plate that attaches to the anchors to perform the uplift function. This plate consists of a threaded joint to attach to the load cell and ram on the top side whilst containing a hook on the bottom side to attach anchors to as required. Figure 3-2 below provides an overview of all the sections of the loading machine including the linear actuator, the load cell, transducer and the attachment plate.

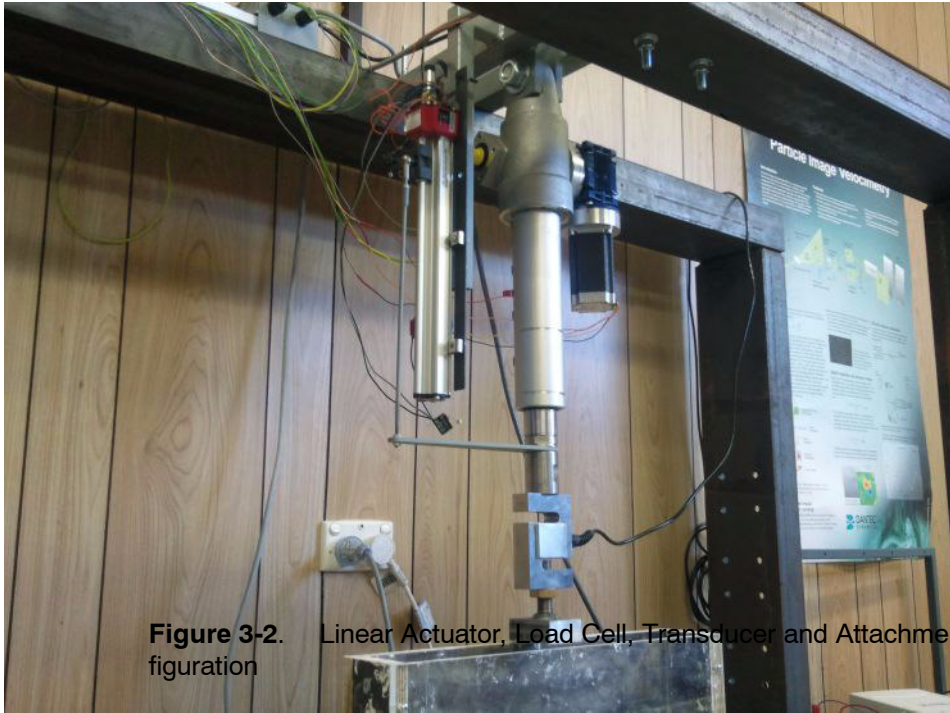


**Figure 3-2.** Linear Actuator, Load Cell, Transducer and Attachment Plate Configuration

### 3.2.2 Load Frame Software

In 3.2.2 above the soil loading machine and its elements were described, however this is only half of the testing facilities required for physical investigations. The linear actuator, load cell and transducer described above only determine that data. It is also required that data that is provided by the load frame is recorded and presented in an obtainable and useful format. A program is used that receives and records the signals that represent the data from the load cell and transducer, therefore recording data for the load induced by the ram and the displacement that occurs. This same program is used to set the test parameters before each investigation 'run' is conducted. The program interface is depicted below in figure 3-3.

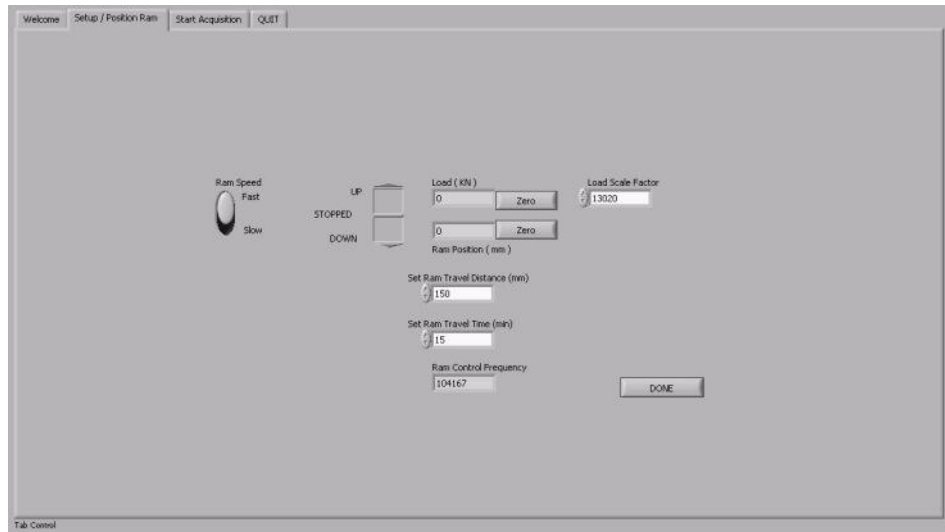


**Figure 3-3.** Load Machine Software - User Interface

It is seen above that the program software is presented in a easy to use and user-friendly format that both sets up the test parameters and records the required data output. To begin a test the switch is set to the desired testing conditions of either tensile testing or compression testing, therefore deciding whether the ram will move in an upwards fashion or downwards. The next step is to set the ram into the desired initial position either by raising or lowering its location by using the slider that contains the controls ‘up,’ ‘down’ and ‘stopped’ in the above figure 3-3. Once the ram is put into the desired initial position the ‘Set Ram Travel Distance (mm)’ and ‘Set Ram Travel Time (min)’ are set to desired values. These parameters tell the program how long or how far to run the ram during experimentation. For example, the above conditions in figure 3-3 would allow the test to run for either 15 minutes or a total ram displacement of 150mm which ever is met first, then the test would be complete and the machine would stop. The next step in the process is ensuring the appropriate load scale factor is entered into the parameters. This load scale factor is dependant on the particular load cell that is to be used during experimentation and is determined using a proofing ring. The factor used with the program allows for the data signal that are obtained from the load cell to be converted to useful and accurate data. The final step before beginning the test is zeroing the load and displacement values by pushing both of the zero buttons respectively. The test can then be started by clicking ‘done’ then ‘start’ on the subsequent page that appears. The test will then run according to the parameters that have been set, receive and record data and produce plots of the data on screen as the data is captured.

### 3.2.3 Shear Box Test Equipment

The shear box test equipment used during this research project was a Geocomps Products Shear Trac II and is depicted below. Figure 3-4 gives an overview of the entire test equipment rig, whilst figure 3-5 focuses on the ‘box’ section itself. Please note that this section only displays the equipment used, for an explanation of procedures please see Chapter 4.

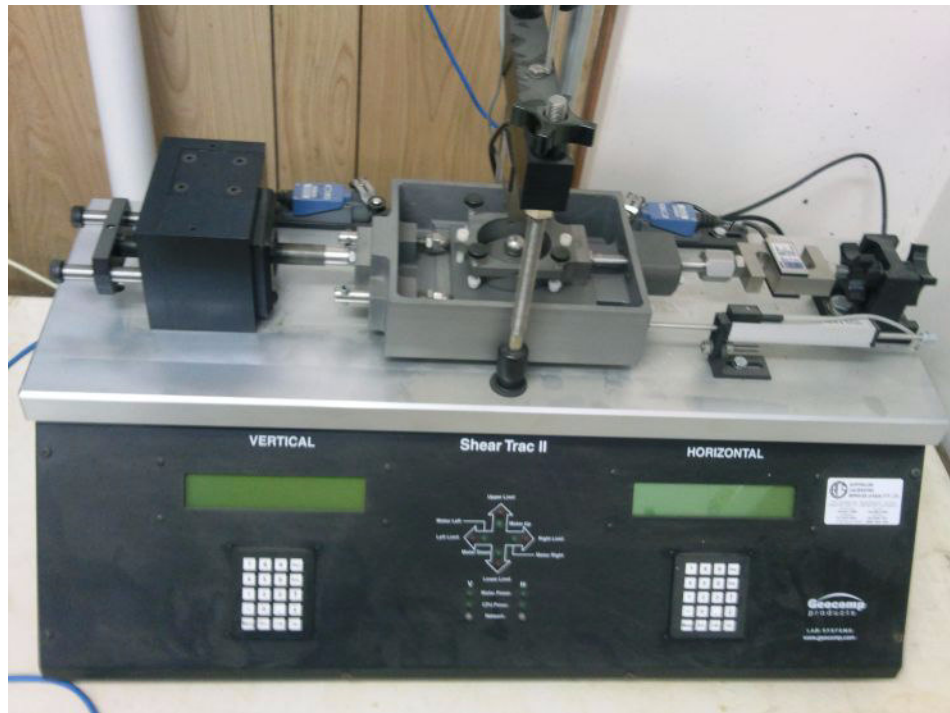


**Figure 3-4.** Shear Box Testing Equipment

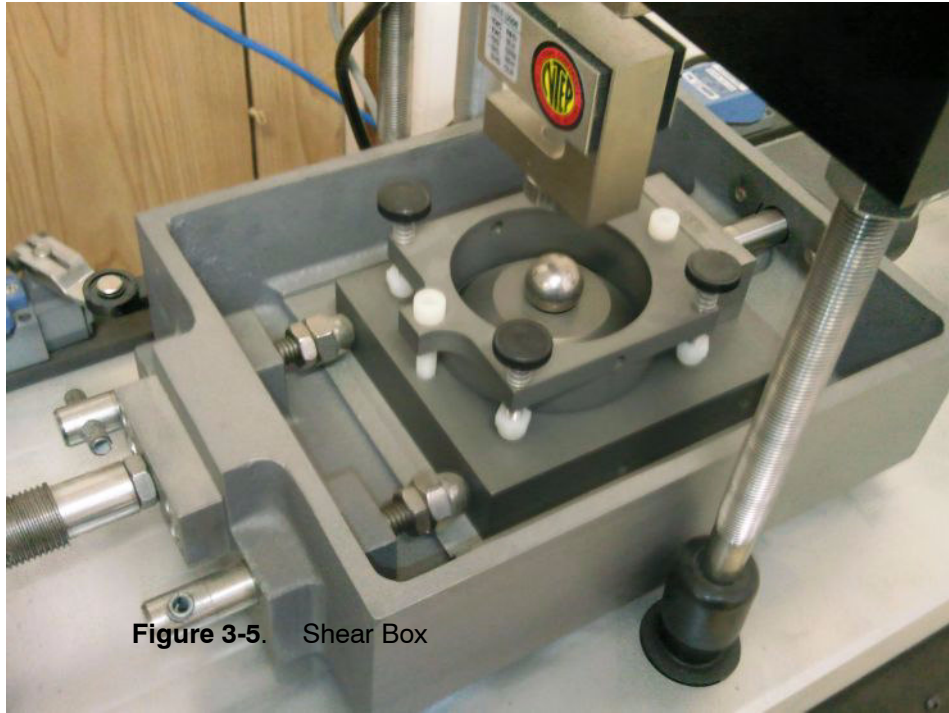


**Figure 3-5.** Shear Box

### 3.3 Summary

This chapter has provided an insight into the testing equipment that was used as part of this research project and subsequent dissertation. The main facilities used including the linear actuator, data recording equipment and the shear box machine have been investigated to display how they work and what they were used for. Subsequent chapters of this dissertation explain further the procedures used to prepare materials and tests, this chapter has just demonstrated the actual testing equipment.

---

# Experimental Material



## 4

### 4.1 Introduction

Chapter 4 introduces the properties of the materials that were used for all of the experiments conducted as part of this research. This chapter introduces a brief background to each of the concepts and the methods employed to obtain reproducible material parameters for each of the experiments conducted.

### 4.2 Density & Unit Weight of Soil

#### 4.2.1 Background

Throughout the experimentation process it was noted that it was an important aspect of this project that many of the experimental parameters would need to be kept constant throughout the investigation process so as to provide results that could be easily compared to one another. The density of the sand material was one of the parameters that was determined to be very important to keep consistent throughout each of the experiments. Therefore, a suitable sand deposition and compaction method was established that provided homogenous sand beds and provided reproducible sand densities. Thus, after trials and testing a density value was determined that could be assumed to be correct for any of the cases after following the method.

Density is determined from the mass of the soil and the volume of the soil or space in which contains the soil specimen. Knowing these values the density can be determined from  $\rho = \frac{M}{V}$  where  $\rho$  is the density typically represented in  $kg/m^3$ ;  $M$  is the mass of the sample in  $kg$ ; whilst  $V$  represents the volume of the soil or contained space in  $m^3$ . After the density of a soil is determined it is possible to convert this value to be a representation of the unit

weight of soil. The unit weight of soil is determined using  $\gamma = \frac{M \times g}{V} = \rho \times g$  where  $\gamma$  is the unit weight of soil in  $N/m^3$ ;  $M$  is the mass of the sample in  $kg$ ;  $g$  represents acceleration due to gravity which is taken as  $9.81 \text{ m/s}^2$ ;  $V$  is the volume of the soil and is measured in  $m^3$ ;  $\rho$  is the density of the soil measured in  $kg/m^3$ .

#### **4.2.2 Previous Works Control Methods**

It is noted in literature that it is important to keep sand densities consistent throughout experimentation and can prove to be difficult without following a consistent method. Many authors convey the importance of creating a method of sand deposition that proves to be reproducible soil properties. From the literature investigated as part of this project, there is two notable methods that discussed in papers. These methods include the use of sand raining devices or drop weights used in conjunction with steel plates and are best explained in literature by Merifield et al (1999) and Ilamparuthi et al (2002) respectively.

Merifield et al (1999) sets out the use of a raining device to deposit the sand into each of the experimental cases to achieve the same sand density throughout. The following method was used in this investigation: “(1) Sand was rained into the chamber using a hopper to a predetermined height; (2) The anchor was then placed horizontally on a levelled out area of sand in the center of the chamber; (3) Sand was then rained into the chamber until the anchor was buried slightly deeper than the required depth; (4) The excess sand was then removed. ...The minimum height from which the sand was rained from was  $550mm$ , thus providing a uniform density throughout the sample. The average density thus obtained for all tests was around  $\gamma = 17.87kN/m^3$ .” (Merifield et al 1999)

Ilamparuthi et al (2002) uses a method similar to that which was adopted for this project based on the use of steel plate and tamping using a drop weight. Ilamparuthi et al (2002) extends this method to also include close control of the size of sand particles that were included in the examination. The following extract represents the method used in the Ilamparuthi et al (2002) investigation. “Uniformly graded medium Palar River sand... was used. Preparation of homogeneous sand beds was achieved by controlled pouring and tamping techniques, which provided reproducible densities. Controlled pulviation in tests on full-shaped models was carried out using a  $1.45m$  diameter sieve with  $18mm$  diameter holes at  $30mm$  centers. Medium-dense and dense sand beds were prepared in layers using a  $25N$  drop weight falling on a  $150mm$  square mild steel plate. Average unit weights  $\gamma'$  were  $15.5$ ,  $16.5$  and  $17.0kN/m^3$  for loose, medium-dense, and dense conditions respectively.” (Ilamparuthi et al 2002)

### 4.2.3 Implemented Control Methods

As mentioned above a similar method to Ilamparuthi et al (2002) was implemented to obtain consistent and reproducible sand density values suitable for experimentation. The method of this project implemented a similar theory to preparing homogeneous sand beds by controlling pouring and tampering techniques. The following section describes the methodology behind the sand preparation for each of the anchor cases. The horizontal plate anchor and pipeline cases were prepared in the exact same fashion, however the pile anchor cases were prepared a little different.

The horizontal plate anchors and pipelines were prepared in the following manner. The sand was deposited into the testing tanks in layers. A sand scoop was used to pour the sand into the tanks where one layer consisted of three full sand scoops. This layer was then even dispersed across the bottom of the tank providing a basic bed layer that was yet to receive any form of compaction. To induce compaction to the layer a wooden plate with the exact dimensions of the tank is then placed over the sand layer. A drop weight of approximately \_\_\_\_\_N was applied a total of 30 blows to the plate in the form of 15 blows per half of the tank. This would approximately provide a compacted sand layer of about 50mm – 75mm depth. Further layers were then deposited on top of each other following the same method until a predetermined height was achieved. The next step was to place the anchor (plate or pipeline) on the levelled out area of sand in tank with the attaching wires leaving vertically out the top of the tank to be connected to the ram. This predetermined height represents the required level of burial for the anchor so as to achieve the desired embedment ratio of the current investigation. Another layer of sand is then deposited on top of the anchor and compacted as described above. There is however a slight variation in sand compaction after the anchor is placed into the required position. After the anchor is in position and the next layer of sand is placed over the top of the anchor, the wooden board is again placed on top of the layer to be compacted. The board has a rectangular section removed that allows for the attaching anchor wires to pass through the board undisturbed but still allowing for adequate and equal tampering measures to be applied. These layer steps are then again repeated until the final predetermined surface level is met.

The preparation method for pile anchors was very similar to that of the plate anchors and pipeline investigations. The sand is deposited again in layers of 3 scoops of sand and then compressed. In this case the wooden ‘compression’ plate is used until the predetermined level is achieved at which the pile is placed into position. Once the pile is in position sand is deposited on either side half of the tank in intervals of 1.5 sand scoops per half. The sand is then compressed either side of the pile by inflicting 15 blows per side using the compaction weight. These compaction blows are inflicted straight to the sand in this case as the wooden plate is disregarded for all layers after the pile is placed into the tank. This

occurs as the plate cannot possibly fit over or around the pile once into position and is therefore neglected. The sand is still deposited in layers until the final height of the sand surface is reached.

#### **4.2.4 Results**

Therefore following the sand deposition and compaction methods explained above in section 4.2.3 suitable sand densities were created for each of the cases that proved to be reproducible. Through investigations it was therefore possible to determine the assumed density and therefore unit weight of soil for each of the cases. This was completed by using the above formula of  $\rho = \frac{M}{V}$  where the mass of sand was known and the volume of the tank was also known. The tanks used during experimentation had internal experimental zone dimensions of 240mm high, 450mm wide and 70mm deep and therefore had an internal volume of 7560000mm<sup>3</sup> or 0.00756m<sup>3</sup>. A value for the mass of sand was determined after following the above procedures and adhering to the appropriate actions, therefore taking the following measurements. The tanks self mass was 2.754kg, the mass of the tank and the contained sand was 14.407kg, therefore providing a mass of sand to be 11.653kg. Therefore the density could be calculated as 1541.40kg/m<sup>3</sup>. The sand density can then be converted to a value to represent unit weight of soil from  $\gamma = \frac{M \times g}{V} = \rho \times g$ . Therefore the unit weight of soil for all cases was assumed to be  $\gamma = 15121.15N/m^3 = 15.121kN/m^3$ .

### **4.3 Moisture Content**

#### **4.3.1 Background**

The moisture content of the sand material that was used for the anchor experiments was also determined through simple investigation. Just as with the density explained above, it is important to determine the level of moisture contained within the sand product so that each test can be conducted under the same conditions with reproducible parameters.

The moisture content of a sample represents the amount of water that is contained within the soil and is usually represented as a percentage ranging from completely dry soil at 0% to completely saturated soil at 100%. The moisture content of the soil can have an affect on other soil properties such as density and cohesion, so it is important that each of the experiments are conducted using sand with the same moisture content.

During experimentation of each of the three separate test cases, plate anchors, pipelines and pile anchors; the moisture content conditions employed were constant for each of these

cases respectively. This meaning that each of the plate anchor experiments were conducted using sand with the same moisture content for each of the respective embedment depths, the pipeline experiments had the same moisture content for each of the relative embedment ratios and finally the pile anchor tests used consistent moisture content levels for each of the experiments conducted within this case. These conditions were achieved by using sand that was stored in the same room under similar conditions over a short testing period of three full days. All of the plate anchor experiments were conducted on day one allowing for the same moisture content to be employed for each of these investigations. Day two involved all of the pipeline testing allowing the same moisture content to be used for each of the pipeline experiments. Finally day three concluded experimentation with all of the pile cases being tested and therefore allowing the same moisture content to be utilised for each of the pile cases respectively. Therefore, it is assumed that a similar sand moisture content was employed throughout each of the three cases as very little change would have occurred to the moisture content over a three day time period under given storage conditions.

#### 4.3.2 Methodology

The following methodology was used to investigate the moisture content of the test material used for each of the experimental cases. First an appropriate sample of sand was selected from storage that was representative of the soil under consideration that was to be used for physical experimentation. The next step was to select a suitable dish to contain the specimen that would also be appropriate to withstand drying in the microwave. The selected dish is then weighed and recorded and therefore the mass of the dish is known as  $M_1$ . It is essential that the selected dish is completely empty, clean of debris and dry. Next, the sample of selected to sand is added and also weighed to give the mass of the dish and the sand sample which is known as  $M_2$ . The sample is then placed into the microwave and heated until the sand is completely dry or at 0% moisture content. After the drying period is complete and the sample is allowed to cool, the dish is once more weighed. This final weight represents the dry sand and the dish and is recorded as  $M_3$ . The moisture content is then determined using the definition of moisture contents as follows:

$$m = \frac{\text{mass of water}}{\text{mass of solid matter}} \times 100\% \quad (4.1)$$

$$m = \frac{M_2 - M_3}{M_3 - M_1} \times 100\% \quad (4.2)$$

### 4.3.3 Results

The moisture content of the material used for each of the anchor cases was therefore determined by following the procedure set out in the above section 4.3.2 Methodology and using equation 4.9 above. The following measurements for the sand material following the above procedure:

$$M_1 = 0.267kg$$

$$M_2 = 0.850kg$$

$$M_3 = 0.842kg$$

Therefore the moisture content of the sand used for each of the three anchor cases is assumed to be  $1.3913\% \approx 1.4\%$ .

## 4.4 Shear Box Test

### 4.4.1 Background

Shear box tests were necessary to determine certain soil properties of the test materials, namely the soil cohesion and soil friction angle. The shear box test can often be called the direct shear test as the focus of the evaluation is to relate the shear stress at failure directly to the normal stress and therefore defining the Mohr-Columb failure. This is achieved by making a sample of soil subject to a constant normal stress whilst shear stress is induced along a predetermined plane until shear failure occurs.

The normal load is applied to the sample vertically to the sample at a consistent rate whilst the shear load is applied horizontally along the predetermined plane. The shear box is divided into two section of a upper and lower half through which the shear load is applied until after shear failure occurs. To allow for free movement of the two halves the box is mounted on ball-bearing slides. During experimentation at minimum the shear load and horizontal displacement are recorded. Below in figure 4-1 is a typical configuration of a shear box testing apparatus.

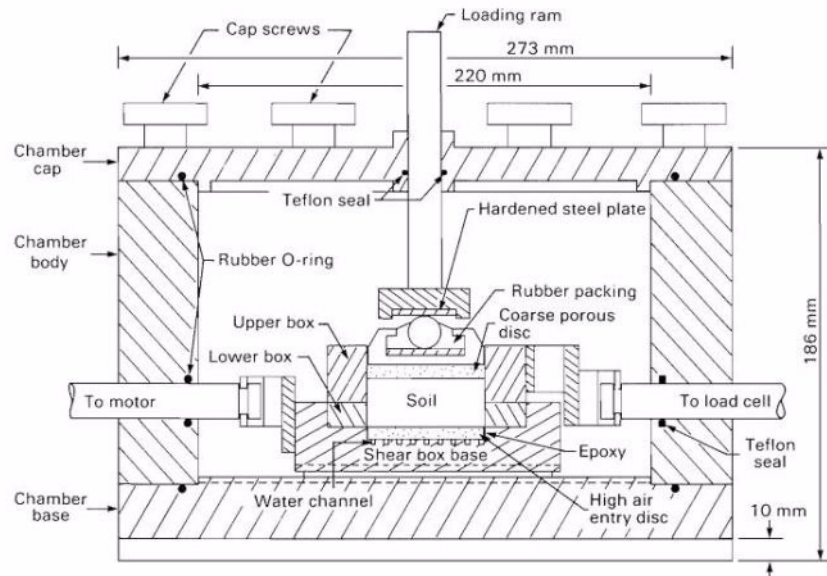


**Figure 4-1.** Typical Configuration of Shear Box Testing Apparatus  
(Source: Gan, Fredlund & Rahardjo 1988)

#### 4.4.2 Experimental Set-up

As explained earlier, an important aspect of this physical investigation is creating reproducible experimental parameters. This is especially true for soil parameters such as density and moisture content. Therefore, the reproducible density and moisture content were determined as per the methods set out above in sections 4.2 and 4.3 respectively. It is also an important aspect of conducting shear box tests, that the material to be tested displays the same properties as is expected in other situational testing. This means that “care must be taken to ensure that the tested samples are prepared at bulk unit weight and moisture content values relevant to the problem under consideration” (University of Southern Queensland 2008). Therefore, incredible care went into reproducing the soil density and moisture content determined in the above sections for the shear box experimentations.

The shear box test requires that the moisture content of the sample to be approximately 1.4% as discovered above and have a soil unit weight of  $\gamma = 15117.21 \text{ N/m}^3$  or a density of approximately  $1541 \text{ kg/m}^3$ . The moisture content requirements were achieved by using the same material that was prepared in the same way as the testing material. The density of the sample however proved to be more complicated. The exact volume of the shear container was determined, then knowing the required density the mass could be back-calculated using  $\rho = \frac{M}{V}$  rearranging for the required mass  $M = \rho \times V$ .

### 4.4.3 Experimental Procedure

As mentioned just above, the first step in preparing a sample investigation was to determine the correct mass of sand to place into the shear box. The sand is then tamped or receives blows until the shear box is filled to the correct level at the required density therefore fulfilling the required sample condition. The box is then held together with plastic screws and put into position into the apparatus. After being placed within the apparatus the vertical normal stress is determined and set to the correct load. The test parameters are set, the plastic screws are removed and the test is begun. The plastic screws are used so if in the case that the screws are forgotten to be removed before the test is started, the machine only has to attempt to shear plastic screws rather than steel screws which cause a large amount of damage. The test is then conducted applying a constant vertical normal stress and an increasing shear stress applied horizontally until after shear failure occurs. During experimentation the shearing load, horizontal displacement and time are recorded. For this particular shear box investigation the vertical normal loads that were applied to the test samples were 50 *kPa*, 100 *kPa* and 200 *kPa*.

### 4.4.4 Results

The testing apparatus records values for the horizontal load in newtons, horizontal displacement in millimeters and time in seconds. This horizontal load is converted to a horizontal stress or shear stress by dividing this value by the appropriate shear box surface area. This will give a horizontal stress or shear stress which can be presented in kilopascals. Figure 4-2 below demonstrates the achieved results for the shear stress (*kPa*) plotted against the horizontal displacement (*mm*). The graph represents the data achieved for each of the three separate normal loads that were induced on the sample. As mentioned above, three different normal loads applied vertically were tested including 50 *kPa*, 100 *kPa* and 200 *kPa*. Figure 4-2 represents the shear stress versus the horizontal displacement for each of the vertical normal loads respectively. It can be seen that a peak shear stress load is achieved for each of the tests, where the test for induced normal load of 50 *kPa* clearly demonstrates a peak failure shear stress value. The failure shear stress load for each of the investigations is tabulated below in table 4-1.

Vertical Pressure - Normal Load	Maximum Shear Stress
50 kPa	47.95 kPa
100 kPa	78.84 kPa
200 kPa	148.63 kPa

Table 4-1: Maximum Shear Stress Values

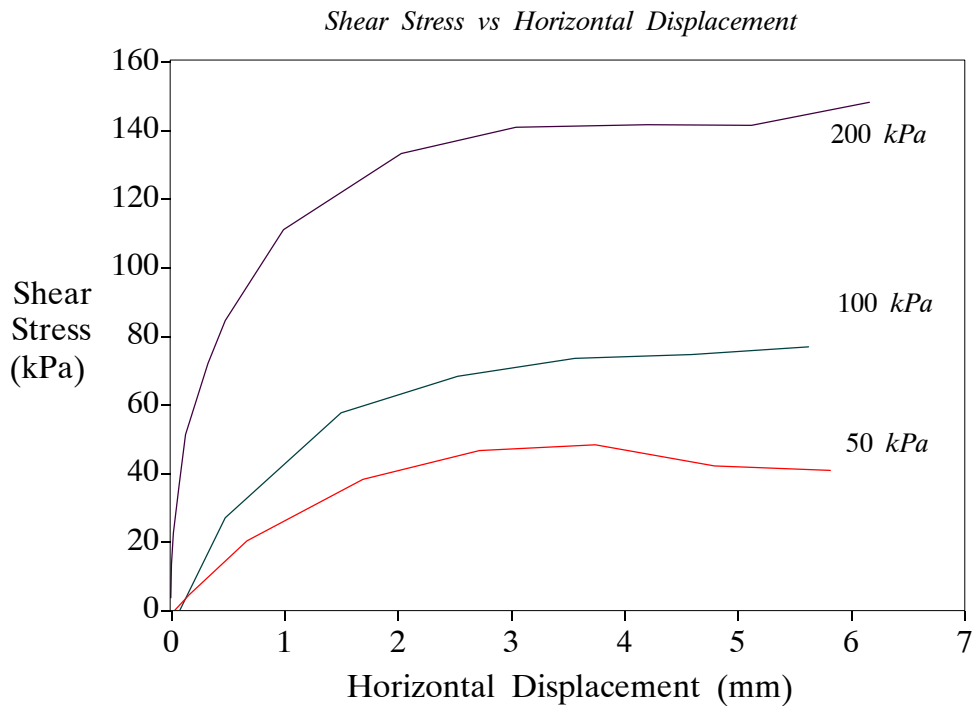


**Figure 4-2.** Shear Stress vs Horizontal Displacement for Relative Normal Stresses

The final stage in the shear box testing is to convert these known failure shear stress values and normal stress values to the required information of the soil cohesion and soil friction angle. This is done by plotting the failure horizontal shear stress loads against the corresponding vertical pressure values as seen below in figure 4-3. A line of best fit is then placed to include each of the determined points where the line will intersect the y-axis. The angle that occurs between the x-axis and the line of best fit represents the soil friction angle whilst the value of the y-intercept represents the soil cohesion. From figure 4-3 below it can be seen that the approximate value for soil cohesion is 12 *kPa* whilst the value for soil friction is determined to be  $\phi = 35.8^\circ$ .

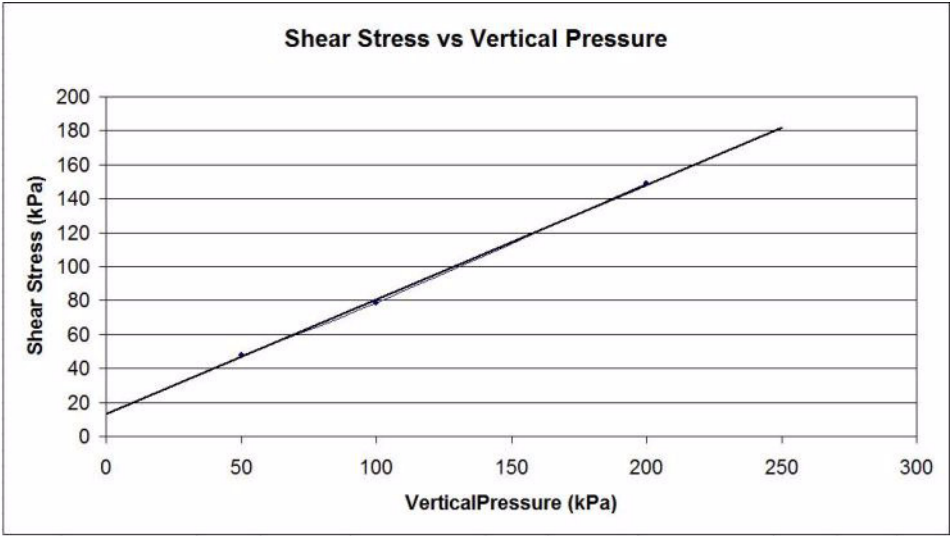


Figure 4-3. Shear Stress vs Vertical Pressure

---

# Plate Anchor



## 5.1 Introduction

Chapter 5 presents the investigation conducted on the uplift of horizontal plate anchors. This chapter includes the methodology explanation for the set-up and preparation of the experiments. The experimental results are then presented including the observed failure mechanisms, load-displacement relationship, ultimate load compared to embedment ratio and the break-out factor in comparison to the embedment ratio. These results that are obtained are then compared with existing results in this field. Also included within the results section is some PIV analysis results conducted by fellow student Michael Hobson which provide further understanding of this topic.

## 5.2 Methodology

### 5.2.1 Background

A series of uplift experiments were conducted on horizontal plate anchors to investigate a number of different factors related to this topic including failure mechanisms, embedment ratios and break-out factors. These tests were conducted using scale sized testing tanks and anchors and utilised a linear actuator in reverse to induce uplift loads. As mentioned in previous chapters, it was a focal point of this investigation to keep a number of parameters constant throughout testing for each of the horizontal plate anchor experiments as well as the pipeline and pile anchor cases. Therefore, this project kept factors such as soil parameters (soil density, soil cohesion, soil friction angle and moisture contents), pull-out rate, anchor width and preparation methods exactly the same for each of the cases whilst changing the anchor depth and therefore embedment ratio  $H/B$ . Methods

were developed so as each of these factors could be reproduced in each of the testing apparatus' time and time again.

The main factor that changed between each of the test cases was the embedment ratio of the anchor relating the depth of anchor burial to the width of the plate anchor. The same width anchors were used throughout each of the investigation, therefore the embedment ratio was altered by burying each of the anchors at different depths. This project focussed on the uplift capacity of shallow anchors that are typically defined from literature to have an embedment ratio of  $H/B \leq 6$  or when the failure mechanism reaches and disturbs the soil surface. Therefore the embedment ratios investigated for horizontal plate anchors as part of this investigation included  $H/B = 2, 3, 4 \text{ \& } 5$ .

### **5.2.2 Experimental Set-up**

Experimentation conducted on horizontal plate anchors were completed using scale model anchors were subjected to pullout loads within testing tanks. The testing tanks used during experimentation were constructed of marine ply wood and have a front screen of perspex to allow for easy observations. The internal dimensions of the box, meaning the experimentation area of the box, were 240mm height, 450mm width and 70mm depth. Figure 4-1 below depicts the testing tanks used throughout experimentation for each of the cases. The model anchors were constructed of steel with a width of 45mm, height of 20mm and a depth just slightly smaller than the testing tank depth at approximately 68mm. The anchors and connecting shaft were separate entities and were attached using hook joints. The shaft consisted of 3.25mm diameter wire and utilised hook joints where the wire passed and looped through the anchor to connect the two pieces. It was decided to use wire to represent shafts and connections as it was thought wire would have the least effect on the overall failure compared to large rectangular shafts. It was decided to use two wire shafts to attach to each plate, where one shaft looped on one side of the plate's top surface whilst the other shaft attached to the opposing side of the plate's top surface. This shaft and anchor layout was selected so as to ensure equal distribution of the uplift forces occurred. These two shafts were then attached to a single pulling point connected to the load cell and linear actuator also through using a similar hook joint arrangement. See Figure 4-2 below for a view of the anchor plates and connecting shafts used throughout experimentation.

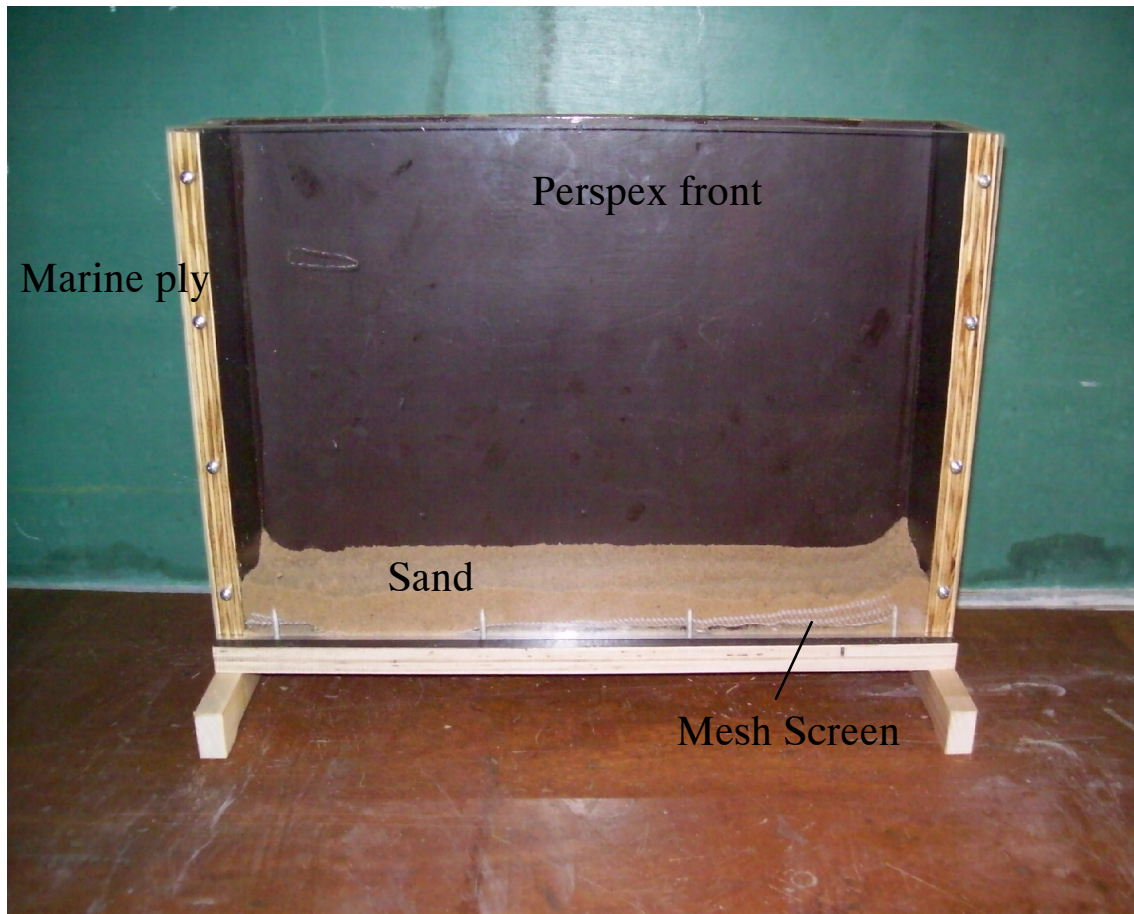


**Figure 5-1.** Overview of Testing Tank  
(Source: Cole, A.J.S 2009)

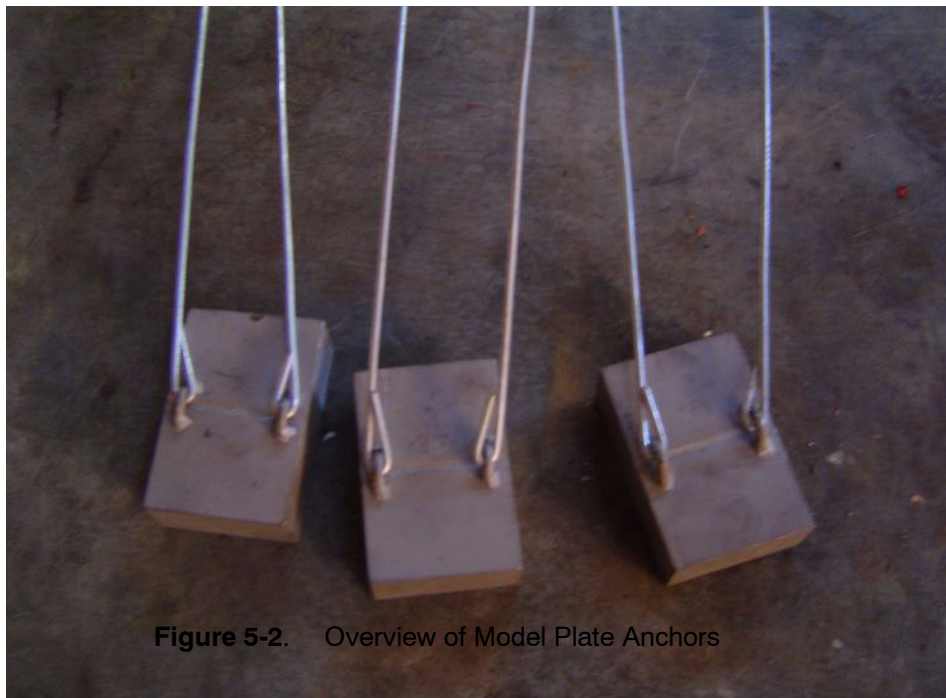


**Figure 5-2.** Overview of Model Plate Anchors

The sand material that was used for all cases of experimentation has been discussed in Chapter 4 Experimental Material. It was determined that the sand used for investigations

had the following reproducible properties:

Density:  $\rho = 1541.40\text{kg}/\text{m}^3$

Unit weight of soil:  $\gamma = 15.121\text{kN}/\text{m}^3$

Moisture content: 1.4%

Soil cohesion:  $c = 12\text{kPa}$

Soil friction angle:  $\phi = 35.8^\circ$

### **5.2.3 Experimental Procedure**

The following represents the procedure employed to conduct experimentation on horizontal plate anchors. This section will refer back to both Chapters 3 and 4 to relate to USQ testing facilities and testing materials.

1. First the required embedment depth was decided, whether this would be for  $H/B = 2, 3, 4$  or 5. As the width of the anchors is kept at a constant of  $B = 45\text{mm}$  the burial depth  $H$  is altered to obtain the desired embedment ratio  $H$ . Therefore the required anchor location and final soil surface location are marked onto the perspex screen using a marker.
2. The sand is placed into the testing tank in layers following the procedure set out in Chapter 4 in particular section 4.2.3. This involves placing 3 scoops of sand into the tank per layer, evening out the added sand into an even layer, placing the wooden compression plate into position over the layer, applying 30 blows (15 blows per half of testing tank) with the compression weight. This deposition of sand layers is continued until the depth of sand is equal to the required depth of the anchor.
3. The horizontal plate anchor is then placed into position in the center of the tank on a levelled out section of sand. The anchor is checked to be in a good position and a completely horizontal arrangement. The connecting shafts or wires are then guided out the top of the tank at a completely vertical fashion.
4. Sand is then again deposited in layers into the testing tank over the plate anchor. The sand layers are created into the same manner as mentioned above, except the wooden plate has a small rectangular section missing that allows the plate to be passed over the top of the attached wire shafts. Once the plate is in position, again 30 blows are applied with the compression weight. Layers are continued to be applied until the required surface level is reached. The first layer to be applied after the anchor is put into place requires great care not to disturb the anchor position. This is important when adding the sand with the scoop, placing the compression plate into position around the wire shafts and when administering blows for sand compaction.

5. After the tank is prepared with anchor buried at correct depth and having the desired embedment ratio, the testing tank is placed on the loading frame. The tank is positioned correctly underneath the linear actuator. The ram is lowered to the correct position where the anchor shafts are connected to the pullout hook that is attached to the load cell and ram. This is done by using a small D-link piece that loops through both wire shafts and the pullout hook and then tightened.

6. Once the tank is in position and the shafts and anchor are attached to the ram, the next step is to enter the test parameters into the computer as discussed in Chapter 3. The desired running time, total anchor displacement and load scale factor are all entered into the computer and the test begins.

7. The test continues after failure occurs to observe both failure and post-failure mechanism. At this stage the data is also recorded by the program including load, vertical displacement and time.

## **5.3 Testing Results**

### **5.3.1 Introduction**

The following section represents the results obtained during experimentation including observations, graphs, calculations and comparisons. The observations made relating to the failure mechanism is noted whilst the load-displacement behaviour of the anchors is also discussed. Furthermore, the effects of the embedment ratio on both the ultimate load and the break-out factor are also investigated. Some results obtained in this project are compared to existing literature results whilst a small look at PIV analysis is also included.

### **5.3.2 Results of Failure Mechanism**

During experimentation each of the plate anchors were loaded until failure occurred and then were continued to be loaded to observe post-failure behaviour also. For each of the embedment ratios typical shallow anchor failure mechanisms were observed. Uplift loading of the plate anchors caused conical slip planes to form beginning at the anchor and continue to develop until reaching the soil surface. The rupture surface is first observed at the edges of the plate anchor and continues to form vertically in a convex fashion until the soil surface is reached. This observed failure plane can be seen below in figure 5-3 and 5-4, where the plate anchor tests for embedment ratios  $H/B = 2$  and  $H/B = 5$  have been depicted respectively (Further failure diagrams are presented for horizontal plate anchors in Appendix B). In the diagrams below the slip plane has been highlighted in red to easily

identify its location. As the failure plane reaches the soil surface, it is understood that shallow anchor conditions have been tested.

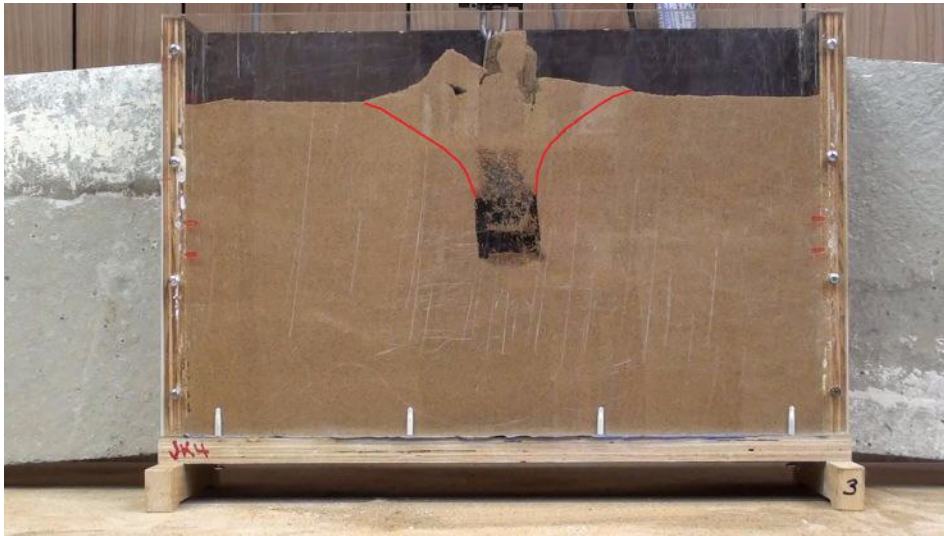


**Figure 5-3.** Horizontal Plate Anchor Failure  $H/B = 2$



**Figure 5-4.** Horizontal Plate Anchor Failure  $H/B = 5$

The rupture surface is seen to emerge at the soil surface as expected for shallow anchors. The following measurements apply to the total width of the failure plane at the soil surface for each of the corresponding embedment ratios:

$$H/B = 2: 200\text{mm} \approx 4.44B$$

$$H/B = 3: 210\text{mm} \approx 4.67B$$

$$H/B = 4: 250\text{mm} \approx 5.56B$$

$$H/B = 5: 280\text{mm} \approx 6.22B$$

It can be seen that only a small in the size of the rupture size at the soil surface between embedment ratio  $H/B = 2$  and  $H/B = 3$ , whilst a stead increase is witnessed from  $H/B = 3$  to  $H/B = 5$ .

### 5.3.3 Load-Displacement Behaviour

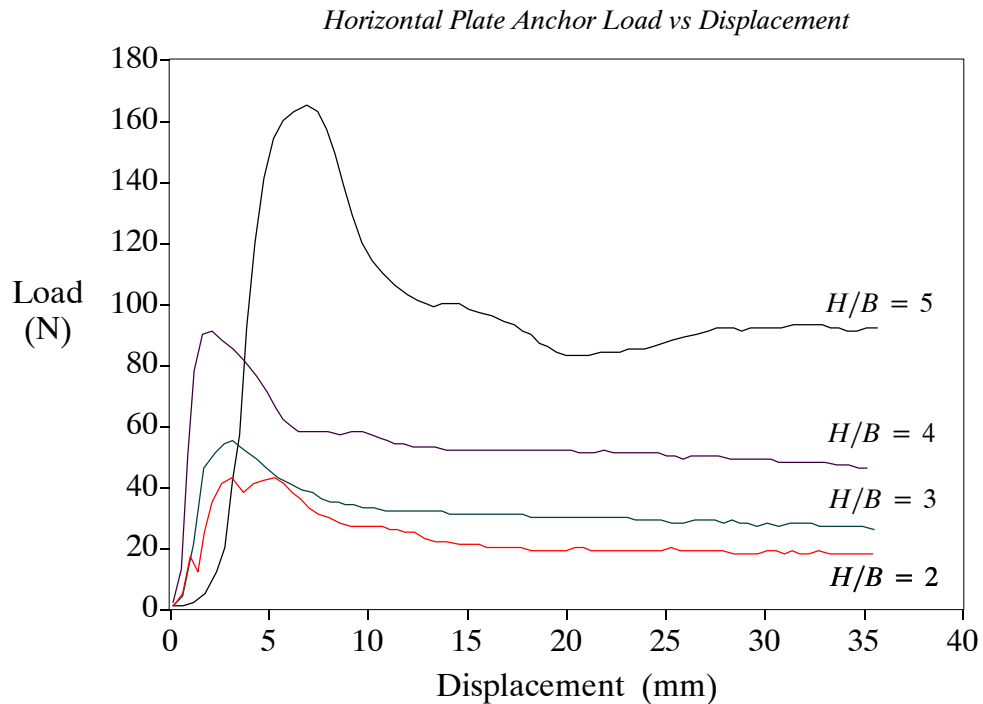


**Figure 5-5.** Horizontal Plate Anchor Load vs Displacement Diagram

Figure 5-5 displays typical load displacement response for horizontal plate anchors that were placed using different embedment ratios. In this diagram load-displacement relationships are demonstrated for shallow anchors of embedment ratios of  $H/B = 2, 3, 4$  &  $5$ . Further load-displacement diagrams are presented in Appendix B that demonstrate each of the results for individual embedment ratios clearly.

From figure 5-5 above it is noted that there is a distinct peak load hump, where a very large peak load is reached within a small displacement then quickly drops off and finally settles to an approximate constant load. This peak load that is achieved after a short period of displacement represents the failure of the plate anchor and the maximum load of the peak can be taken to be the ultimate load  $Q_u$ . It is observed that three phases of loading can be observed from the above figure. Those phases can be categorised as:

1. Pre-peak behaviour where a rapid increase in load occurs over a small displacement area.
2. Post-peak behaviour where a rapid decrease in load occurs over increasing displacement.

3. Residual behaviour where load is approximately constant at large displacement values. These observations are consistent with the results and definitions described in both Merifield et al (1999) and Ilamparuthi et al (2002) for shallow anchor results.

After failure has occurred the plate continues to be loaded causing post-failure load-displacement relationship to be observed as the load quickly drops after peak load is reached to plateau out to an approximate linear load. This residual constant load is observed to be approximately 50% of the peak load achieved for each of the embedment ratios. The following represents the percentage of the constant post failure load compared to the peak failure load for each of the individual embedment cases:

$H/B = 2$ : 40.7% of the peak load  $Q_u$

$H/B = 3$ : 49.1% of the peak load  $Q_u$

$H/B = 4$ : 47.25% of the peak load  $Q_u$

$H/B = 5$ : 52.7% of the peak load  $Q_u$

#### 5.3.4 Variation of Peak Uplift Load with Embedment Ratio

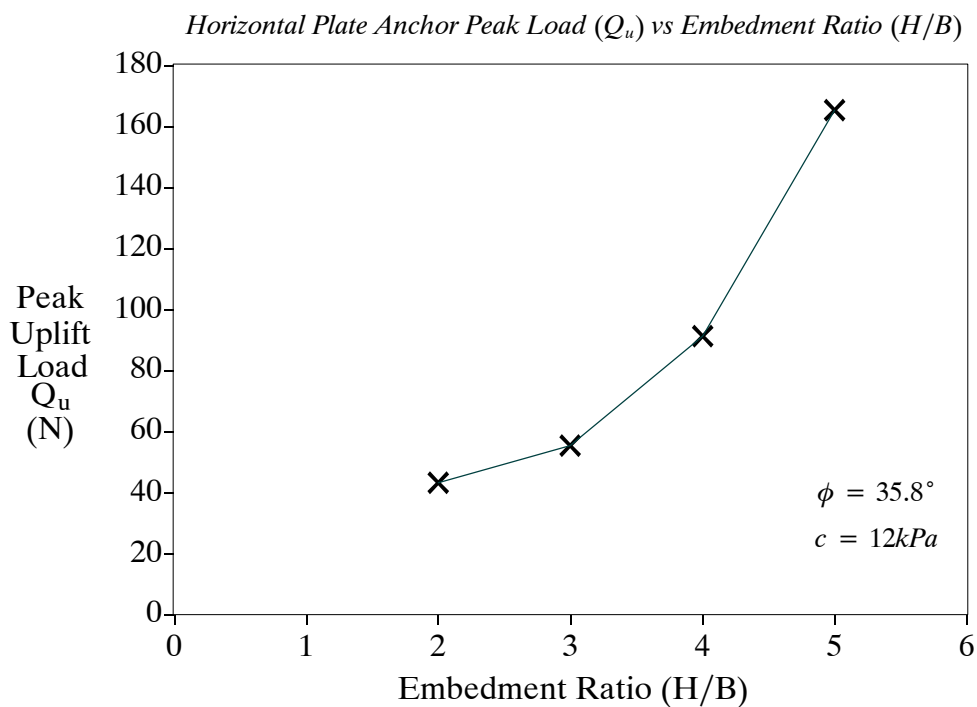


**Figure 5-6.** Horizontal Plate Anchor Peak Load vs Embedment Ratio

The variation of peak uplift load  $Q_u$  compared to relative embedment depths  $H/B$  is presented above in figure 5-6. From the above graph it can be seen that the peak load  $Q_u$  increases at a higher rate with an increase in embedment ratio. This is observed as the graph beginning to resemble an exponential form of increase in load. Therefore as embedment

ratio  $H/B$  increases the greater the increase in peak load  $Q_u$ . Obviously this also represents increased peak load with an increased embedment ratio as would be expected. These results obtained are again similar to trends presented in both Merifield et al (1999) and Ilamparuthi et al (2002).

### 5.3.5 Variation of Break-out Factor with Embedment Ratio

The break-out factor is calculated using equation 2.3 rearranged into the form presented in both Merifield et al (1999) and Ilamparuthi (2002).

$$N_\gamma = \frac{Q_u}{\gamma AH}$$

Where:  $N_\gamma$  = Break-out factor.

$Q_u$  = Ultimate load determined from as the peak load hump.

$\gamma$  = Unit weight of soil defined in Chapter 4 Experiment Material.

$A$  = Area of the anchor =  $0.045 \times 0.068 = 0.00306m^2$

$H$  = Depth of Anchor

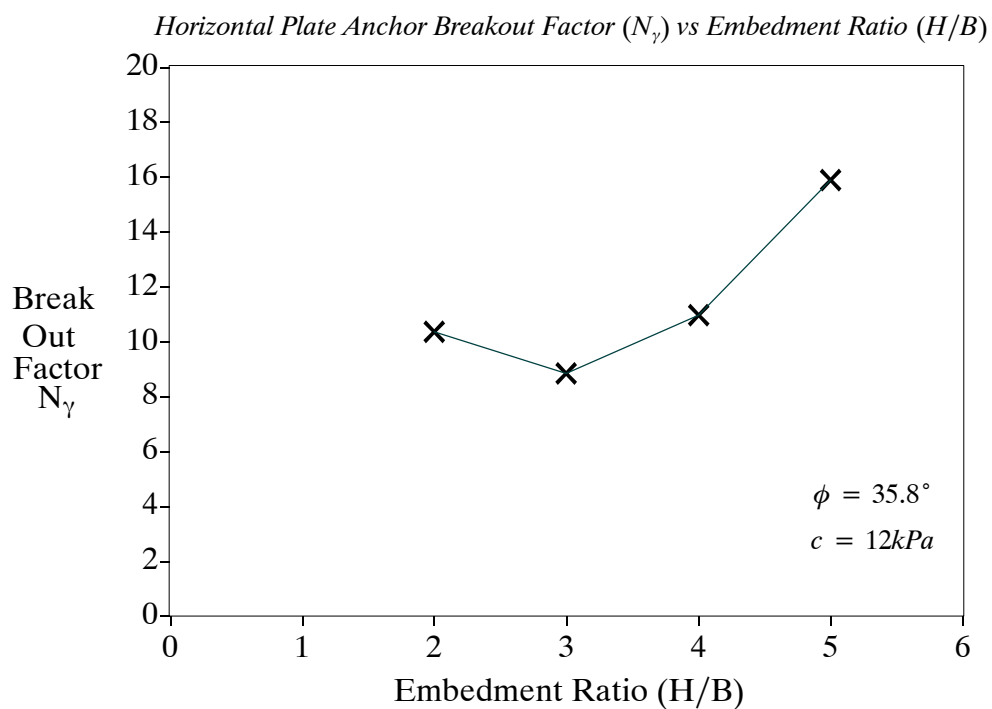


**Figure 5-7.** Horizontal Plate Anchor Break-out Factor vs Embedment Ratio

From figure 5-7 above it can be seen that the general trend for the break-out factor is to increase with increased embedment ratio. It is noted that for  $H/B = 3$  the break-out factor decreases and does not fit the expected trend. Merifield et al (1999) and Ilamparuthi (2002) both comment on the trend of the break-out factor against embedment ratio and suggest

that the break-out factor should increase with increased embedment ratio until it plateaus out at an approximate constant value. Therefore, viewing the above figure it would be expected that larger values of break-out factor should be obtained for embedment ratios of  $H/B = 2$  and 3.

### 5.3.6 Comparison to Existing Studies

It is appropriate to compare results obtained within this investigation to existing published results to evaluate the trends observed as part of this paper compared to other works. For horizontal plate anchors results shall be compared to Merifield et al (1999) experimentation that was conducted on circular plate anchor of diameter  $75mm$  and embedment ratio of  $H/B = 4$ . The results presented and discussed above are therefore compared with the existing study conducted by Merifield et al (1999) including load-displacement relationship, peak load  $Q_u$  vs embedment ratio  $H/B$  and break-out factor  $N_y$  vs embedment ratio  $H/B$ .

Figure 5-8 and 5-9 represent the load-displacement curves presented by Merifield et al (1999) and this paper respectively. For both cases demonstrated the embedment ratio presented is  $H/B = 4$ . It is noted that both sets of results produce the typical load-displacement curve expected for shallow anchor results, where the early peak failure load is reached after small displacement before reducing to an approximate constant value for increasing displacement. The ultimate load  $Q_u$  reached in Merifield et al (1999) is approximately  $500N$ , whilst this project investigation had an ultimate uplift load of  $Q_u = 91N$ . Therefore meaning that the results achieved within this paper have a much smaller uplift capacity to those produced by Merifield et al (1999) where the ultimate load is approximately 5 times larger for this particular case.

There are a number of reasons that these results may differ by such a degree. First of all it is noted that the particular investigation conducted for these project used a sand that was not cohesionless and in fact had a cohesion value of  $c = 12kPa$  and a soil friction angle of  $\phi = 35.8^\circ$ . Merifield et al (1999) does not actually provide relevant values for either soil cohesion nor soil friction angle, so direct comparison cannot be made between each of the studies. A further reason for the differences could be the size of the both the anchors and testing tanks with which were used to conduct experimentations. Merifield et al (1999) used much larger apparatus to conduct testing when compared to this investigation; in fact the tank used by Merifield et al (1999) was approximately 220% larger and the anchor was about 166% larger in width. This could lead to the possibility of scale effects having an affect on this particular investigation, as this is noted to be a possible problem in literature. One final point for result comparison is that it is particularly difficult to find any results

that were conducted under the same conditions using the same parameters as this research, in fact near on impossible. It is therefore impossible to completely exclude the results obtained in either of these papers as neither can really be directly related to one another. Although from reviewing the results obtained for load-displacement relationships, although expressing the exact same form it would be thought that the results displayed in this paper would be a little low for typical ultimate load  $Q_u$  values relative to particular embedment ratios  $H/B$ .

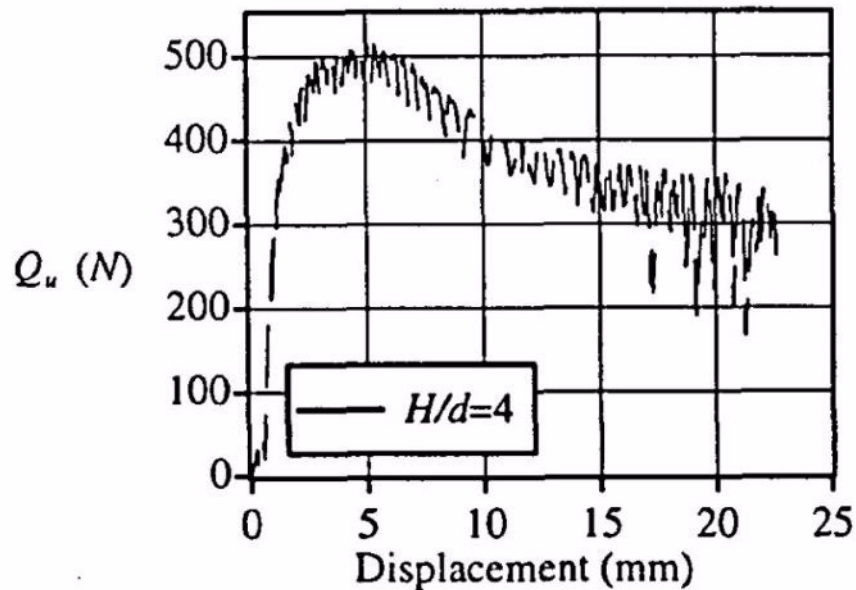


**Figure 5-8.** Horizontal Plate Anchor: Load vs Displacement Merifield et al (1999)  $H/B = 4$

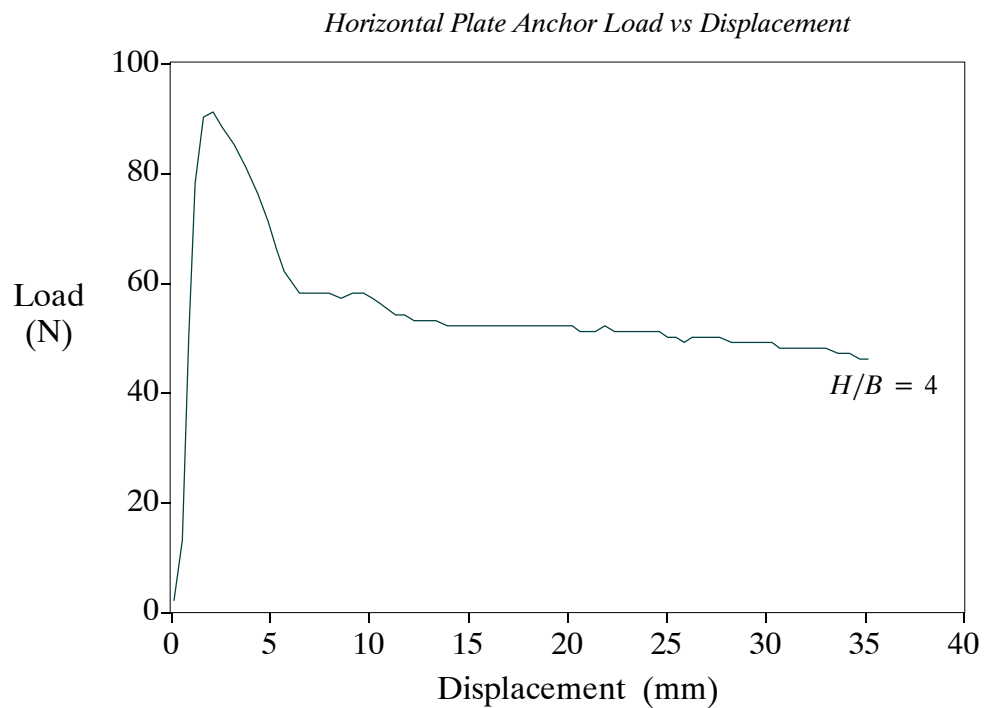


**Figure 5-9.** Horizontal Plate Anchor: Load vs Displacement  $H/B = 4$  Comparison to Merifield et al (1999)

Figure 5-10 below compares the peak uplift load 500N for each of the relative embedment depths and compares once again results obtained as part of this project to the investigation conducted by Merifield et al (1999). Once more, the same factors that contribute to some of the inaccuracies of direct comparison between papers and the difficulty of finding relative papers for comparison still apply.

From figure 5-10 it can be seen that a more extensive investigation had been conducted by Merifield et al (1999) as deep anchor conditions have also been investigated. The same general trend is again observed between the results of both investigations of an increasing ultimate pullout load with increasing embedment ratio as would be expected. However, once again it would appear that the loading results obtained as a result of this investigation are a little less than those obtained by Merifield et al (1999), possibly for the same reasons mentioned already. It is seen that for an embedment ratio of  $H/B = 2$  the results between the investigations are fairly similar, but with increasing anchor depth the results grow further apart. For an embedment ratio of  $H/B = 5$ , the results presented in Merifield et al (1999) are approximately 3 times larger.

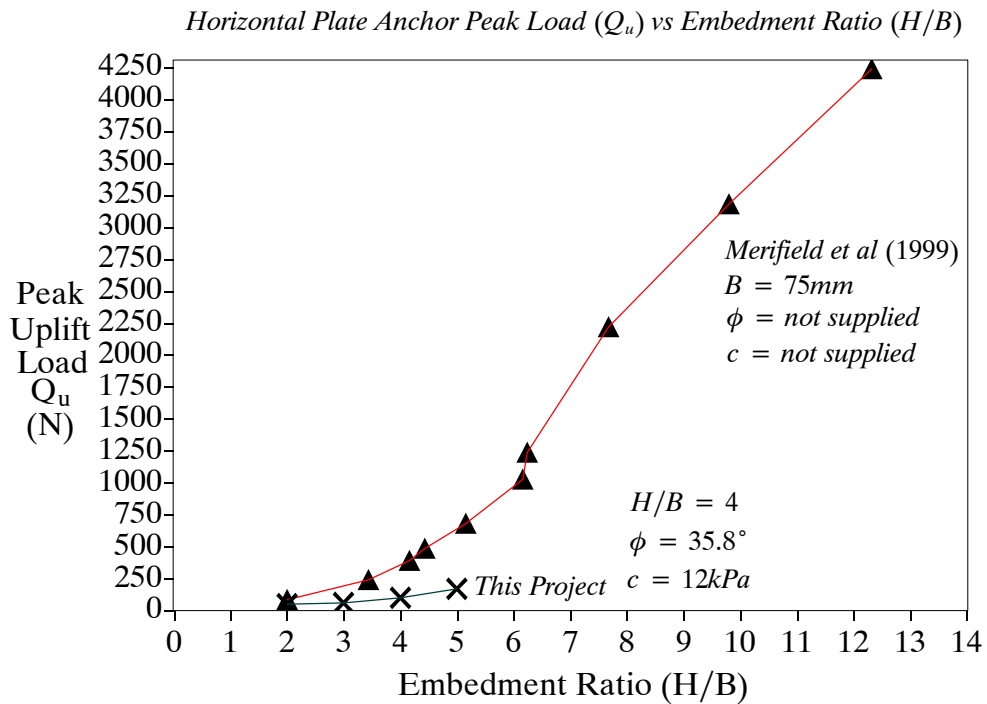


**Figure 5-10.** Horizontal Plate Anchor: Peak Uplift Load vs Displacement Compared to Merifield et al (1999)

Finally the break-out factor and embedment ratio relationships are compared between this project and Merifield et al (1999) and are depicted below in figure 5-11. It is observed that although producing the closest results in comparison of the two papers; similar trends are not exactly seen in regards to break-out factor and embedment ratio relationships. It is apparent that the results obtained for this project for embedment ratio  $H/B = 3$  are a little low and if increased would produce a similar trend of increasing embedment ratio with increasing embedment ratio.

It is a possibility that the reason behind the break-out factors being the closest results when considering comparison between the two papers of this project and Merifield et al (1999) is the fact that the break-out factor is a dimensionless entity. During calculations for determining the break-out factor for each of the anchors all the dimensions are cancelled out, possibly allowing the fact of different parameters used during different investigations to have less of an affect. Basically, because all the parameters are cancelled out during conversion, having differing investigation parameters such as soil cohesion and soil friction angle appears to have a lessened effect on the overall results. This is observed below as previous comparisons being different by factors of 3, whereas the largest factor difference in this break-out factor comparison is approximately 0.8.

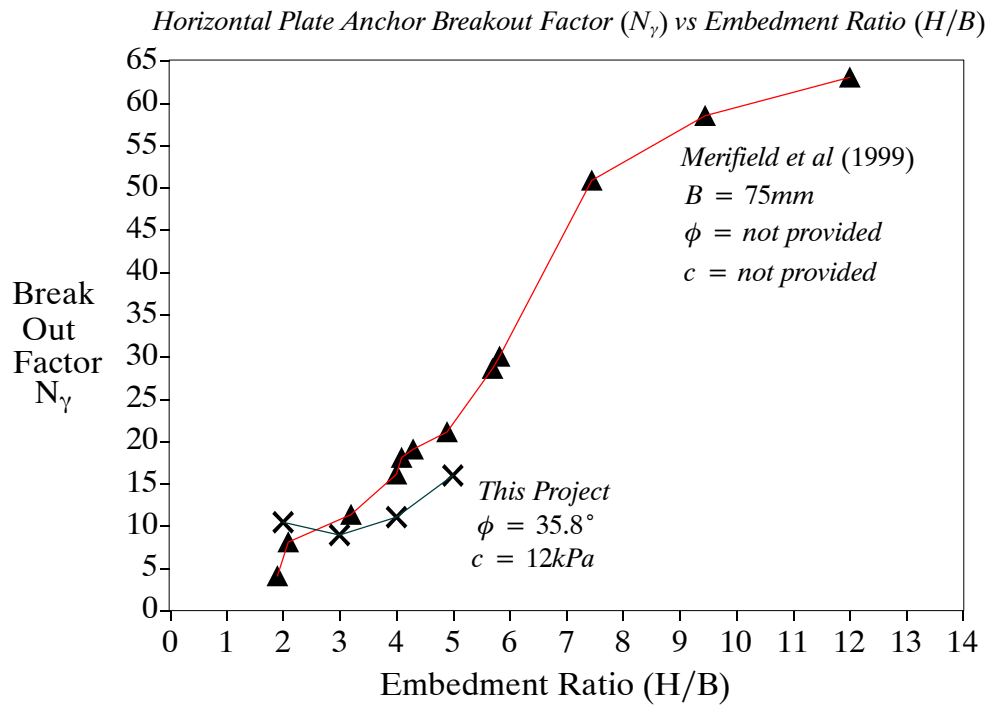


**Figure 5-11.** Horizontal Plate Anchor: Break-out Factor vs Embedment Ratio Compared to Merifield et al (1999)

### 5.3.7 PIV Analysis

PIV analysis is Particle Image Velocimetry analysis and provides vector plots that represent particle movement that occurs and is observed during experimentation. A PIV analysis was carried out by Michael Hobson for the horizontal plate anchor experiments conducted as part of this research paper. The research paper ‘An Analysis of Retaining Wall Failure Using Particle Image Velocimetry’ completed by Michael Hobson explains the PIV analysis conducted in conjunction with this research project in great detail. Some results from Hobson (2010) have been included within this research paper as PIV analysis can provide a great insight to the failure mechanisms observed during experimentation.

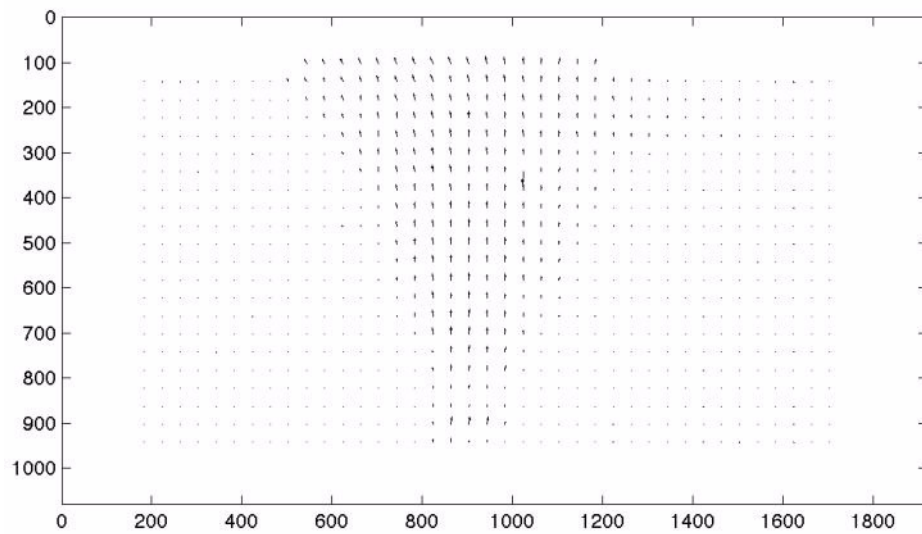


**Figure 5-12.** PIV Analysis Vector Plot - Plate Anchor  $H/B = 5$   
(Source: Hobson 2010)

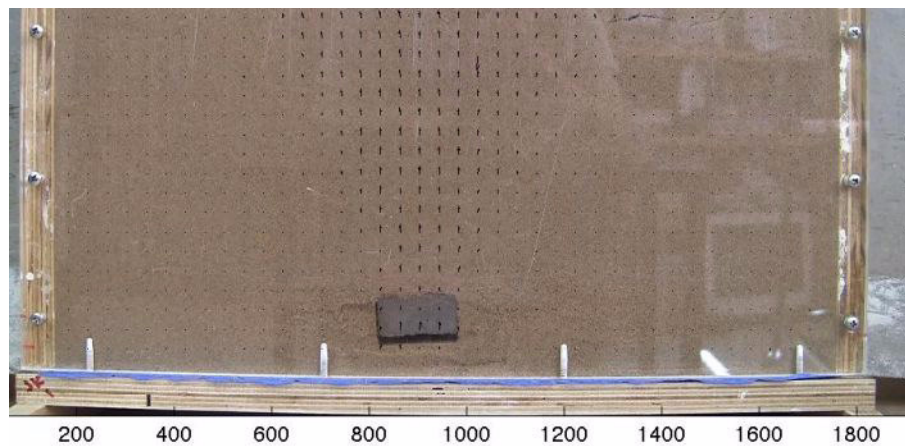


**Figure 5-13.** PIV Analysis Superimposed Image - Plate Anchor  $H/B = 5$   
(Source: Hobson 2010)

Figures 5-12 and 5-13 above demonstrates PIV results obtained for a horizontal plate anchor buried at an embedment ratio of  $H/B = 5$ . The vector plots obtained are very useful when investigating the failure mechanisms of these anchors. It can be seen that when compared with figure 5-4 that the exact same conical rupture surface is observed that extends to the surface. This research thus confirms the observations and statements made above in section 5.3.2 regarding the failure mechanism of horizontal plate anchors.

---

# Buried Pipeline



## 6.1 Introduction

Chapter 6 presents the investigation conducted on the uplift of buried pipelines. This chapter includes the methodology explanation for the set-up and preparation of the experiments. The experimental results are then presented including the observed failure mechanisms, load-displacement relationship and ultimate load compared to embedment ratio. Also included within the results section is some PIV analysis results conducted by fellow student Michael Hobson which provide further understanding of this topic.

## 6.2 Methodology

### 6.2.1 Background

A series of experiments were conducted on model pipelines in sand that were subject to uplift forces where the failure mechanism, embedment ratio and break-out factor were the focus of investigation. These tests were conducted in a similar method to the horizontal plate anchors where scale testing tanks and pipelines were tested under uplift conditions until failure where a linear actuator was used to induce the required uplift forces. The same requirements applied to the pipeline investigations as to the plate anchor tests where efforts were made to keep a number of parameters constant throughout the testing process as described in the previous chapters. Therefore again parameters such as soil properties (soil density, soil cohesion, soil friction angle and moisture content), pull-out rate anchor dimensions and testing procedure exactly the same for each of the pipeline tests whilst the pipeline burial depth was altered to investigate desired embedment ratios. Preparation

methods were developed to allow each of these parameters to be reproduced at the same value for each of the tests.

As with the plate anchors, a primary focal point of the pipeline investigation was performing uplift tests that modelled alternate embedment ratios  $H/B$ . As the width, or diameter, of the pipeline remained constant through each of the tests, alternate embedment ratios were achieved by burying the pipeline at differing depths  $H$ . The focus once more was to investigate pipelines buried under shallow conditions and therefore the embedment ratios investigated in this project were  $H/B = 2, 3 \text{ \& } 4$ .

### 6.2.2 Experimental Set-up

Experimentation conducted on pipelines buried in sand were completed using scale model pipelines that were subjected to pullout loads within testing tanks. The testing tanks used during experimentation were constructed of marine ply wood and have a front screen of perspex to allow for easy observations. The internal dimensions of the box, meaning the experimental area of the box, was  $240\text{mm}$  height,  $450\text{mm}$  width and  $70\text{mm}$  depth. Figure 4-1 in the previous chapter depicts the testing tanks used throughout experimentation for each of the cases. The pipelines were PVC pipe of  $50\text{mm}$  diameter therefore providing width of  $50\text{mm}$ , height of  $50\text{mm}$  and a depth just slightly smaller than the testing tank depth at approximately  $68\text{mm}$ . Again the pipelines and shaft were separate entities where the shaft consisted of  $3.25\text{mm}$  diameter wire and was connected on either side of the pipeline using hook arrangements as was completed with the plate anchors. See figure 6-1 below for an overview of the pipeline setup.

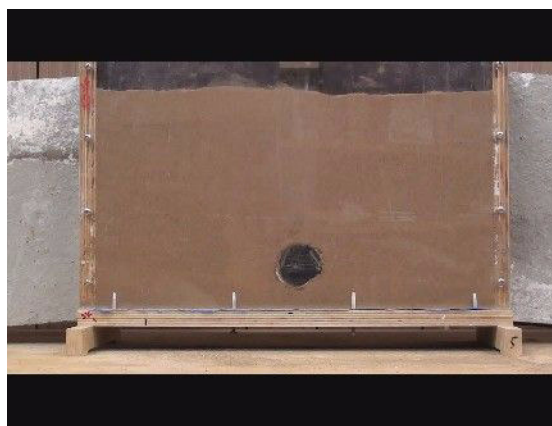


**Figure 6-1.** Overview of Pipeline Test Layout

The sand material that was used for all cases of experimentation has been discussed in Chapter 4 Experimental Material. It was determined that the sand used for investigations had the following reproducible properties:

$$\text{Density: } \rho = 1541.40\text{kg/m}^3$$

Unit weight of soil:  $\gamma = 15.121kN/m^3$

Moisture content: 1.4%

Soil cohesion:  $c = 12kPa$

Soil friction angle:  $\phi = 35.8^\circ$

### 6.2.3 Experimental Procedure

The experimental procedure used for the pipeline testing was very similar to that of the horizontal plate anchor experiments and the following represents the procedure employed to conduct this experimentation on pipelines. This section will refer back to both Chapters 3 and 4 to relate to USQ testing facilities and testing materials.

1. First the required embedment depth was decided, whether this would be for  $H/B = 2, 3, \text{ or } 4$ . As the diameter of the pipeline is kept at a constant of  $B = 50mm$  the burial depth  $H$  is altered to obtain the desired embedment ratio  $H$ . Therefore the required anchor location and final soil surface location are determined and then marked onto the perspex screen using a marker.
2. The sand is placed into the testing tank in layers following the procedure set out in Chapter 4 in particular section 4.2.3. This involves placing 3 scoops of sand into the tank per layer, evening out the added sand into an level layer, placing the wooden compression plate into position over the layer, and then applying 30 blows (15 blows per half of testing tank) with the compression weight. This deposition of sand layers is continued until the depth of sand is equal to the required depth of the pipeline.
3. The pipeline is then seated into position in the center of the tank on a levelled out section of sand. The pipeline is checked to be in a good position where minimal to no movement will occur from this position. The connecting shafts or wires are then guided out the top of the tank in a completely vertical fashion.
4. Sand is then again deposited in layers into the testing tank over the pipe. The sand layers are created in the same manner as mentioned above, except the wooden plate has a small rectangular section removed that allows the plate to be passed over the top of the attached wire shafts. Once the plate is in position, again 30 blows are applied with the compression weight. Layers are continually applied until the required soil surface level is reached. The first layer to be applied after the pipeline is put into place requires great care not to disturb the its position. This is important when adding the sand with the scoop, placing the compression plate into position around the wire shafts and when administering blows for sand compaction.

5. After the tank is prepared with the pipe buried at the correct depth and having the desired embedment ratio, the testing tank is placed on the loading frame. The tank is positioned correctly underneath the linear actuator. The ram is lowered to the correct position where the anchor shafts are connected to the pullout hook that is attached to the load cell and ram. This is done by using a small D-link piece that loops through both of the wire shafts and the pullout hook and then tightened.
6. Once the tank is in position and the shafts connected to the pipeline are attached to the ram, the next step is to enter the test parameters into the computer as discussed in Chapter 3. The desired running time, total anchor displacement and load scale factor are all entered into the computer and the test begins.
7. The test continues after failure occurs to observe both failure and post-failure mechanisms. At this stage the data is recorded by the program including load, vertical displacement and time values.

## **6.3 Test Results**

### **6.3.1 Results of Failure Mechanism**

During experimentation each of the pipes were loaded until failure occurred and then continued to have load applies so as to observe post-failure behaviour also. For each of the pipeline cases shear planes developed from along side the pipe and developed to reach the soil surface. It is suggested that as these shear planes did infact continue to rupture at the soil surface that shallow conditions have been displayed for pipelines. Each of the embedment ratios developed the shear planes in a conical shape and thus can be related to the inverse trapezoidal failure mechanisms discussed within section 2.3.2 of the literature review. Figure 6-2 and 6-3 below give examples of the failure plains observed during pipeline experimentation for embedment ratios of  $H/B = 2$  & 4. In these figure the identified slip planes have been highlighted in red to easily identify its location.

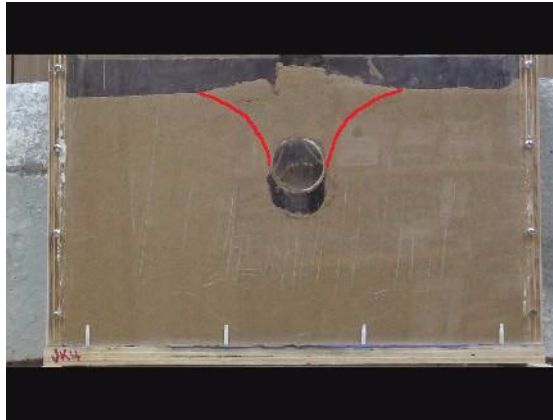


**Figure 6-2.** Buried Pipeline Failure  $H/B = 2$

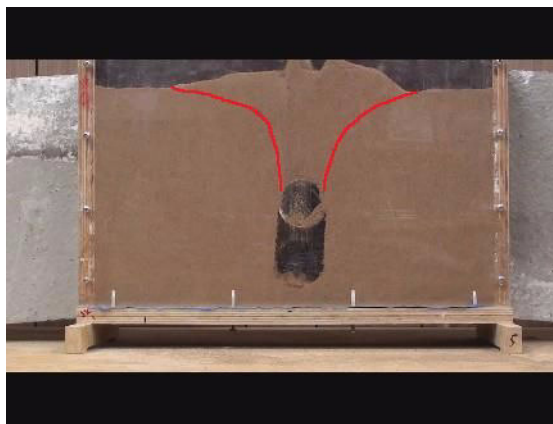


**Figure 6-3.** Buried Pipeline Failure  $H/B = 4$

Downward soil movement or infilling mechanism was observed as part of this investigation also. Figure 6-4 and 6-5 represent a pipeline buried at  $H/B = 4$  where figure 6-4 is seen to show the pipe before downward movement has occurred whilst figure 6-5 demonstrates the pipe after the infilling mechanisms has occurred. During experimentation, it was noted that initially heaving of the soil occurred before collapse of sand occurred to fill the void underneath the pipeline.



**Figure 6-4.** Buried Pipeline  $H/B = 2$  Before Downward Soil Movement



**Figure 6-5.** Buried Pipeline  $H/B = 2$  After Downward Soil Movement

### 6.3.2 Load-Displacement Behaviour

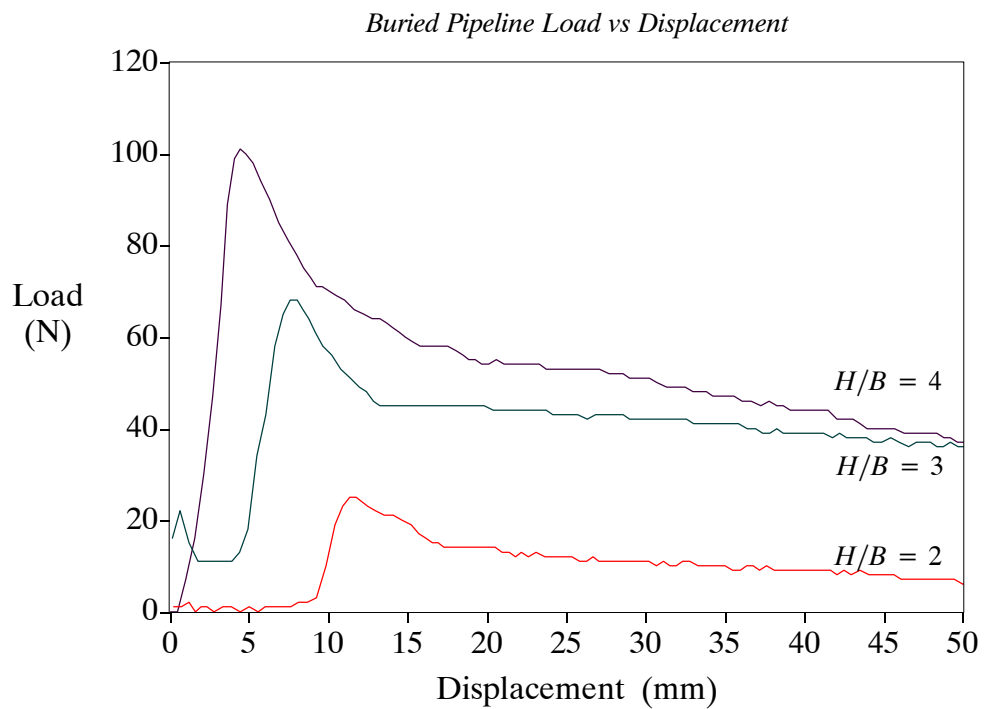


**Figure 6-6.** Buried Pipeline Load vs Displacement Diagram

Figure 6-6 displays typical load displacement response for pipelines that were placed using different embedment ratios. In this diagram load-displacement relationships are demonstrated for shallow conditions of embedment ratios of  $H/B = 2, 3$  &  $4$ . Further load-displacement diagrams are presented in Appendix C that demonstrate each of the results for individual embedment ratios clearly.

From figure 6-6 above it is noted to display the distinct peak load hump just as demonstrated with plate anchors, where a very large peak load is reached within a small

displacement then quickly drops off and finally settles to an approximate constant load. It is noted however that although closely resembling the load curve produced by the plate anchors there is a greater displacement of the pipeline before the peak load is reached in the pipeline case compared to the plate anchors. This peak load that is achieved after a short period of displacement represents the failure of the pipeline and the maximum load of the peak hump can be taken to be the ultimate load  $Q_u$ . It is observed that three phases of loading can be observed from the above figure again just as was observed for plate anchors. Those phases can be categorised as:

1. Pre-peak behaviour where a rapid increase in load occurs over a small displacement area.
2. Post-peak behaviour where a rapid decrease in load occurs over increasing displacement.
3. Residual behaviour where load is approximately constant at large displacement values.

After failure has occurred the pipeline continues to be loaded causing post-failure load-displacement relationship to be observed as the load quickly drops after peak load is reached to plateau out to an approximate linear load. This residual constant load is observed to be in the vicinity of 30% to 45% of the peak load achieved for the pipeline investigations. The following represents the percentage of the constant post failure load compared to the peak failure load for each of the individual embedment cases:

$H/B = 2$ : 28% of the peak load  $Q_u$

$H/B = 3$ : 44% of the peak load  $Q_u$

$H/B = 4$ : 29.7% of the peak load  $Q_u$

### 6.3.3 Variation of Peak Uplift Load with Embedment Ratio

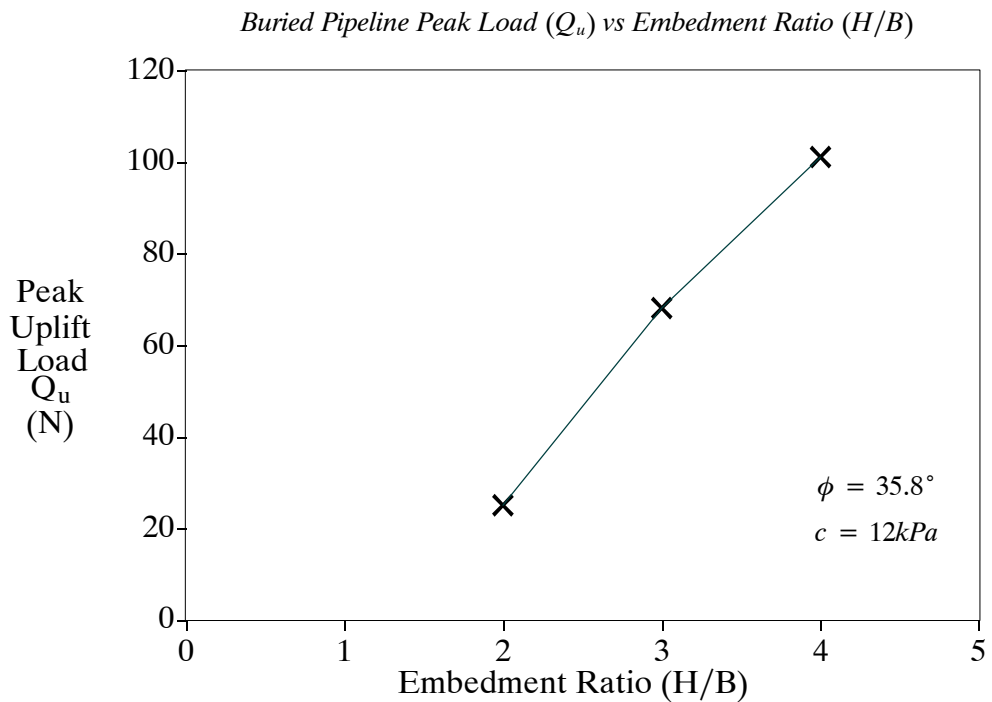


**Figure 6-7.** Buried Pipeline Peak Uplift Load  $Q_u$  vs Embedment Ratio  $H/B$

The variation of peak uplift load  $Q_u$  compared to relative embedment depths  $H/B$  is presented above in figure 6-7. From the above graph it can be seen that the peak load  $Q_u$  increases steadily with an increase in embedment ratio. From these few investigations, it would be investigated that for low values of  $H/B$  that a linear relationship occurs between  $Q_u$  and  $H/B$ .

### 6.3.4 PIV Analysis

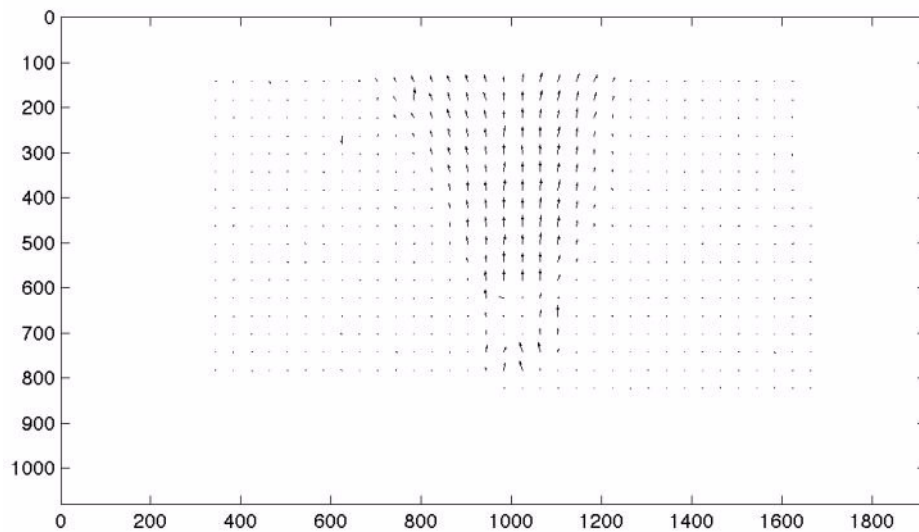


**Figure 6-8.** PIV Analysis Pipeline  $H/B = 4$  Vector Plot

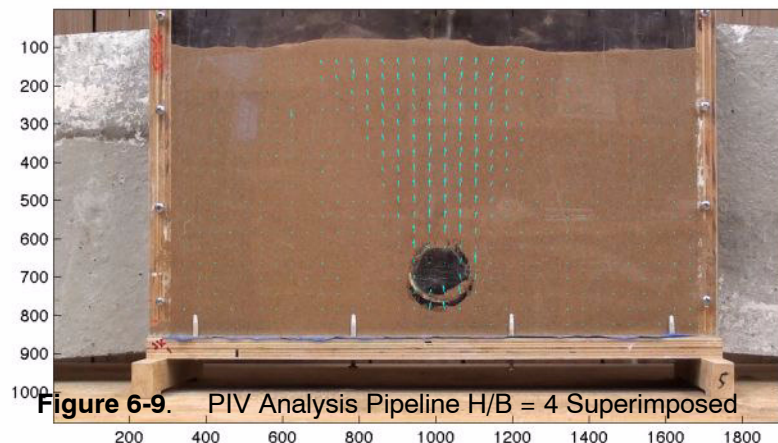


**Figure 6-9.** PIV Analysis Pipeline  $H/B = 4$  Superimposed

As mentioned earlier in Chapter 5, a PIV analysis has been completed for some cases of this project by Michael Hobson in conjunction with the paper ‘An Analysis of Retaining Wall Failure Using Particle Image Velocimetry’ by Michael Hobson. Figures 6-8 and 6-9 above demonstrates PIV results obtained for a pipeline buried at an embedment ratio of  $H/B = 4$ . The vector plots obtained are very useful when investigating the failure mechanisms of these pipelines and can be compared to the observed results displayed earlier. It can be seen that when compared with figure 6-2 and 6-3 that the exact same conical rupture surface is observed that extends to the surface demonstrating the shear planes that form during failure. This PIV research thus confirms the observations and statements made above in section 6.3.1 regarding the failure mechanism of pipelines

---

# Pile Anchor



## 7.1 Introduction

Chapter 7 presents the investigation conducted on the uplift of buried pipelines. This chapter includes the methodology explanation for the set-up and preparation of the experiments. The experimental results are then presented including the observed failure mechanisms, load-displacement relationship and ultimate load compared to embedment ratio. Also included within the results section is some PIV analysis results conducted by fellow student Michael Hobson which provide further understanding of this topic.

## 7.2 Methodology

### 7.2.1 Background

A series of experiments were conducted on model pile anchors in sand that were subject to uplift forces where the failure mechanism, embedment ratio and break-out factor were the focus of investigation. A further section of this pile investigation involved testing both smooth piles and rough piles. These tests were conducted in a similar method to both the horizontal plate anchors and buried pipeline investigations where scale testing tanks and piles were tested under uplift conditions until failure where a linear actuator was used to induce the required uplift forces. The same requirements applied to the pile investigations as to the previous investigations where efforts were made to keep a number of parameters constant throughout the testing process as described in the previous chapters. Therefore parameters such as soil properties (soil density, soil cohesion, soil friction angle and moisture content), pull-out rate anchor dimensions and testing procedure exactly the same for each of the pile tests whilst the burial depth of the pile was altered to investigate desired

embedment ratios. Preparation methods were developed to allow each of these parameters to be reproduced at the same value for each of the tests.

Once more the primary focal point of these was performing uplift tests that investigate the effects that alternate embedment ratios  $H/B$  have on different parameters of pile anchors. As the width of the pile remained constant throughout each of the tests, alternate embedment ratios were achieved by burying the base of the pile anchor at differing depths  $H$ . The embedment ratios investigated as part of the pile section of this project were  $H/B = 5, 7.5, 10$  &  $13$ .

### 7.2.2 Experimental Set-up

Experimentation conducted on pile anchors were completed using scale model piles that were subjected to pullout loads within testing tanks. The testing tanks used during experimentation were constructed of marine ply wood and have a front screen of perspex to allow for easy observations. The internal dimensions of the box, meaning the experimental area of the box, was  $240\text{mm}$  height,  $450\text{mm}$  width and  $70\text{mm}$  depth. Figure 4-1 in the depicts the testing tanks used throughout experimentation for each of the cases. The piles were constructed of marine ply timber  $20\text{mm}$  in width, a depth just slightly smaller than the testing tank depth at approximately  $68\text{mm}$  and differing heights that all protruded from the top of the tanks. The pile anchors also included a further aspect not tested in the plate or pipeline examples. Piles were tested in both a smooth form and a rough form. Initial experiments were conducted on piles that had a smooth marine waterproof layer, however it was decided to run the experiments again with a pile surface that would produce greater friction. Therefore a second bath of piles were created that removed the smooth waterproof layer to provide a rough wooden outer layer. Finally, the piles were directly connected using D-links to the hook attachment on the linear actuator just below the load cell. See figure 7-1 below for an overview of the pile experimentation setup.



**Figure 7-1.** Overview of Pile Anchor Test Layout

The sand material that was used for all cases of experimentation has been discussed in Chapter 4 Experimental Material. It was determined that the sand used for investigations had the following reproducible properties:

Density:  $\rho = 1541.40\text{kg}/\text{m}^3$

Unit weight of soil:  $\gamma = 15.121\text{kN}/\text{m}^3$

Moisture content: 1.4%

Soil cohesion:  $c = 12\text{kPa}$

Soil friction angle:  $\phi = 35.8^\circ$

### 7.2.3 Experimental Procedure

The experimental procedure used for the pile testing was similar to that of the previous investigations of horizontal plate anchors and buried pipeline experiments and the following represents the procedure employed to conduct this experimentation. This section will refer back to both Chapters 3 and 4 to relate to USQ testing facilities and testing materials.

1. First the required embedment depth was decided, whether this would be for  $H/B = 5, 7.5, 10$  or 13. The height of the pile changes accordingly to allow for the correct burial depth  $H$  to be obtained so as to achieve the desired embedment ratio  $H/B$ . Therefore the required pile depth location and final soil surface location are determined and then marked onto the perspex screen using a marker.
2. The sand is placed into the testing tank in layers following the procedure set out in Chapter 4 in particular section 4.2.3. This involves placing 3 scoops of sand into the tank per layer, evening out the added sand into an level layer, placing the wooden compression plate into position over the layer, and then applying 30 blows (15 blows per half of testing tank) with the compression weight. This deposition of sand layers is continued until the depth of sand is equal to the required depth of the base of the pile.
3. The pile is then placed into position in the center of the tank on a levelled out section of sand. The pile is checked to be in a good position where no movement will occur from this position.
4. Sand is then again deposited in layers into the testing tank either side of the pile. The sand layers are created in similar manner as explained above, except the wooden plate is no longer used as part of the compression process. Three scoops of sand were evenly distributed either side of the pile before 15 blows are applied with the compression weight on each half of soil. Layers are continually applied following this method until the required soil surface level is reached. It is important that the first layer to be applied after the pile

is put into place is added with care not to disturb the locality of the pile. This is important when both adding the sand with the scoop and whilst administering blows with the drop weight.

5. After the tank is prepared with the pile buried at the correct depth and having the desired embedment ratio, the testing tank is placed on the loading frame. The tank is positioned correctly underneath the linear actuator. The ram is lowered to the correct position where the pile is connected to the pullout hook that is attached to the load cell and ram. This is done by using a small D-link piece that loops through both the pile and the pullout hook and then tightened.

6. Once the tank is in position and the pile is connected to the to the ram, the next step is to enter the test parameters into the computer as discussed in Chapter 3. The desired running time, total pile anchor displacement and load scale factor are all entered into the computer and the test begins.

7. The test continues after failure occurs to observe both failure and post-failure mechanisms. At this stage the data is recorded by the program including load, vertical displacement and time values.

## **7.3 Test Results**

### **7.3.1 Results of Failure Mechanism**

During experimentation each of the piles were loaded until failure occurred and then continued to have load applies so as to observe post-failure behaviour also. For each of the pile cases, both smooth and rough surfaces, shear planes did not form and were not observed. It is suggested that these shear planes did not form for two reasons. The first is that in both the smooth and rough piles cases the pile friction angle is too small. Therefore the pile does not create enough friction along the pile-soil plane and thus only achieves small pullout capacities that do not produce shear planes. The second reason could be the moisture and cohesion of the sand used during experimentation. This is evident as the experiments just appeared to remove from the testing area easily without causing any soil disruptions. Figure 7-2 and 7-3 below give typical examples of the observations made of the pile and testing tank after failure has occurred for an embedment ratio of  $H/B = 5$  &  $10$ .



**Figure 7-2.** Pile Anchor Observed Failure  $H/B = 5$



**Figure 7-3.** Pile Anchor Observed Failure  $H/B = 10$

### 7.3.2 Load-Displacement Behaviour

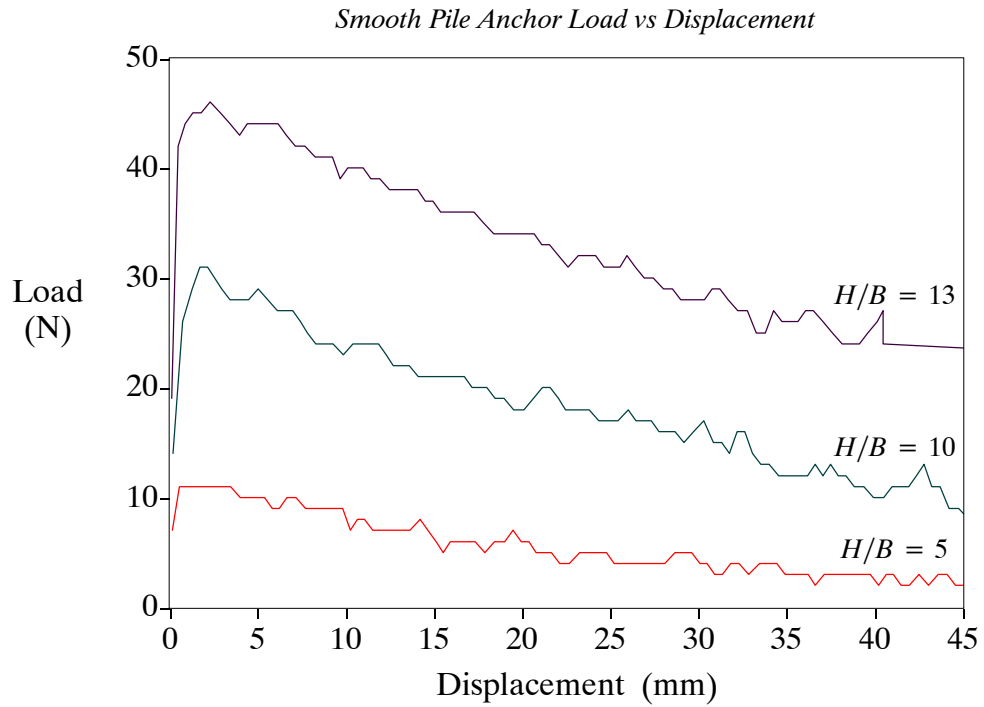


**Figure 7-4.** Smooth Pile Anchor Load vs Displacement Diagram

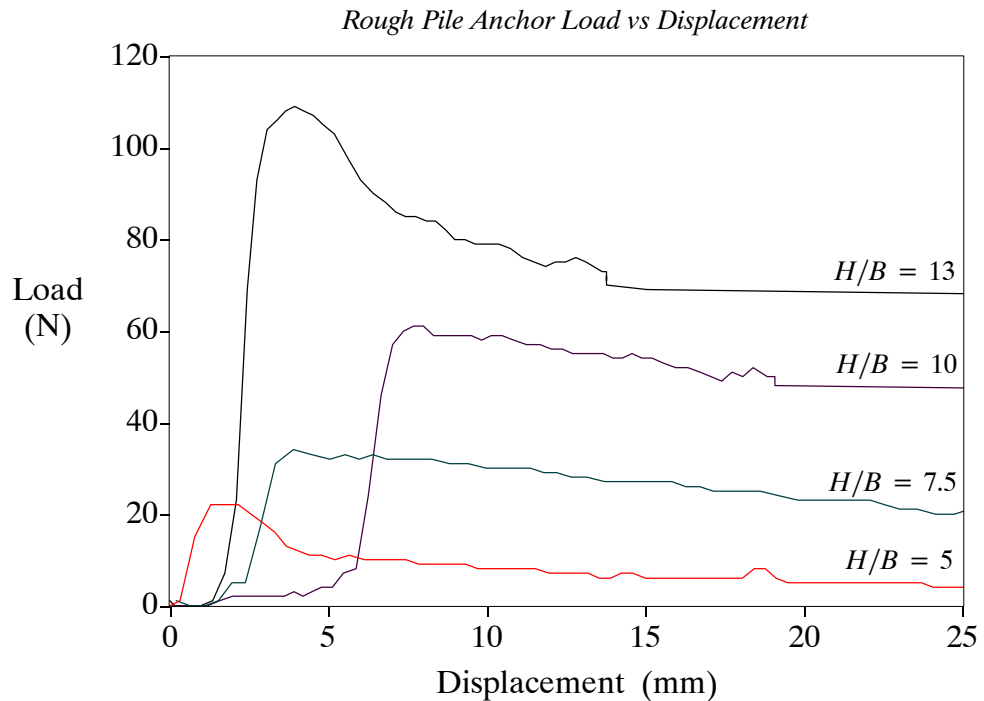


**Figure 7-5.** Rough Pile Anchor Load vs Displacement Diagram

Figure 7-4 and 7-5 display typical load–displacement responses for piles that were placed using different embedment ratios. Further load–displacement diagrams are presented in Appendix D that demonstrate each of the results for individual embedment ratios clearly.

From figure 7-4 and 7-5 above it is noted again that the load–displacement relationship displays the distinct peak load hump just as demonstrated with plate anchors and pipelines, where a very large peak load is reached within a small displacement then quickly drops off and finally settles to an approximate constant load. This phenomena is evident in both smooth pile and rough pile cases. This peak load that is achieved after a short period of displacement represents the failure of the pile and the maximum load of the peak hump can be taken to be the ultimate load  $Q_u$ . It is observed that three phases of loading can be observed from the above figure again just as was observed for plate anchors and pipelines. Those phases can be categorised as:

1. Pre–peak behaviour where a rapid increase in load occurs over a small displacement area.
2. Post–peak behaviour where a rapid decrease in load occurs over increasing displacement.
3. Residual behaviour where load is approximately constant at large displacement values.

A further observation of the above graphs can be made when comparing peak load of smooth pile anchors to that of rough pile anchors. It can be seen for each of the embedment ratios that the rough piles demonstrate a peak pullout load to be approximately double each of the smooth pile anchor results.

### 7.3.3 Variation of Peak Uplift Load with Embedment Ratio

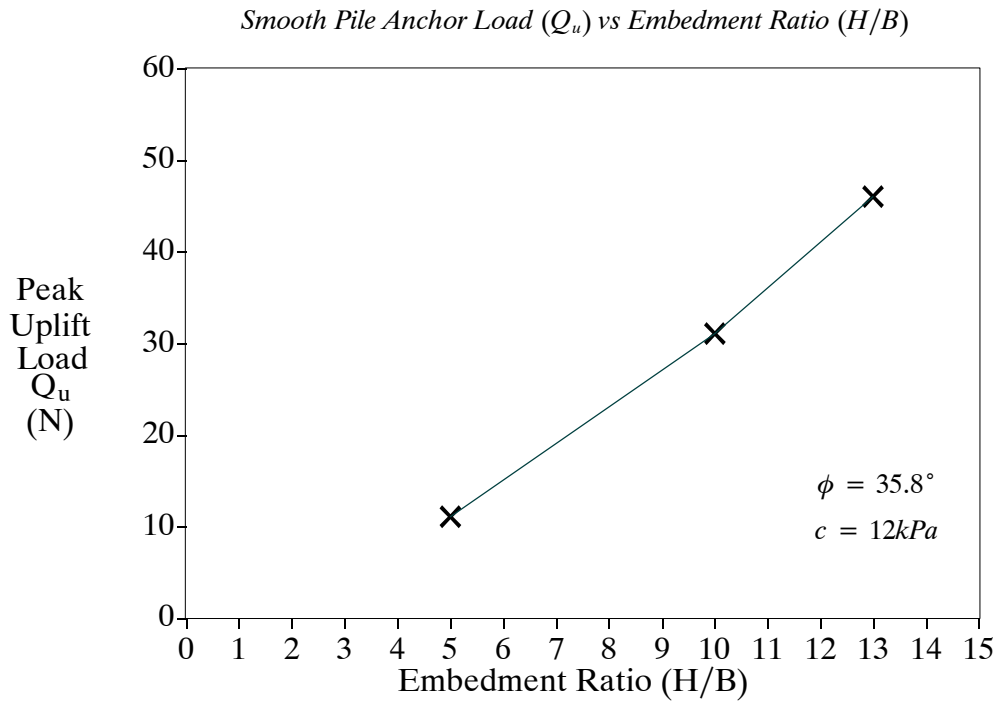


**Figure 7-6.** Smooth Pile Anchor Peak Load vs Embedment Ratio

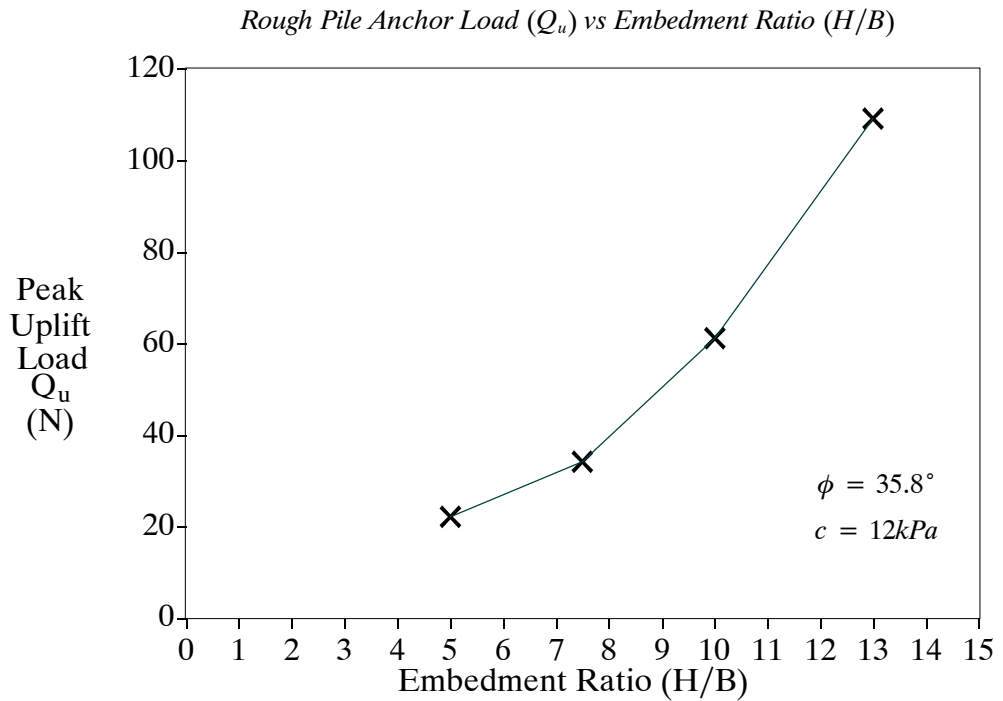


**Figure 7-7.** Rough Pile Anchor Peak Load vs Embedment Ratio

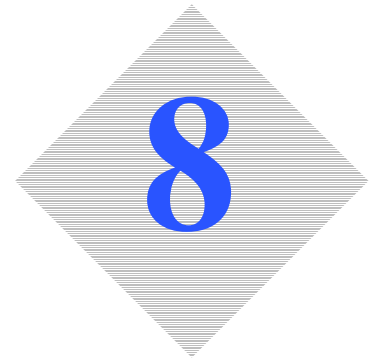
The variation of peak uplift load  $Q_u$  compared to relative embedment depths  $H/B$  is presented above in figure 7-6 and 7-7. From the above graph it can be seen that the peak load  $Q_u$  increases steadily with an increase in embedment ratio.

#### **7.3.4 PIV Analysis**

No PIV analysis has been completed for any of the pile anchor examples to this date. It would very interesting to perform a PIV analysis on the pile anchor data that has been collected to see if formation of shear failure planes can be determined.

---

# Conclusion & Future Work



## 8.1 Conclusions

### 8.1.1 Failure Mechanisms

Through literature review it is noted that the failure mechanisms for each of the three cases investigated within this project, plate anchors, buried pipelines and pile anchors, that each of the cases should demonstrate fairly similar failure mechanisms. All of these cases form slip planes that should take the form of an inverted trapezoid. Of course each of these cases will express this failure phenomena slightly differently, however the same basic principle is behind all of these examples.

The plate anchors and buried pipelines displayed the expected failure mechanism throughout experimentation consistently. These results can be viewed in Chapters 5 and 6 respectively and also some further results are included within the Appendix chapter. It was seen in Chapter 7 that the pile anchors tested did not display observable failure mechanisms, it would be interesting to complete a PIV analysis on the results obtained for the pile anchors to see if the failure mechanism is in fact observable from this perspective.

### 8.1.2 Load-Displacement Behaviour

It was observed for all three investigation cases that there is a distinct peak load hump, where a very large peak load is reached within a small displacement then quickly drops off and finally settles to an approximate constant load result obtained for all experiments. This peak load that is achieved after a short period of displacement represents the failure of the particular anchor and the maximum load of the peak can be taken to be the ultimate load  $Q_u$ . It is observed that three phases of loading can be observed from these results. Those

phases can be categorised as:

1. Pre-peak behaviour where a rapid increase in load occurs over a small displacement area.
2. Post-peak behaviour where a rapid decrease in load occurs over increasing displacement.
3. Residual behaviour where load is approximately constant at large displacement values.

These observations are consistent with the results and definitions described in both existing literature.

### 8.1.3 Variation of Peak Uplift Load with Embedment Ratio

The variation of peak uplift load  $Q_u$  compared to relative embedment depths  $H/B$  is observed and documented for each of the cases and displayed within the respective chapters. It is noted that it can be seen that the peak load  $Q_u$  increases at a higher rate with an increase in embedment ratio. Therefore as embedment ratio  $H/B$  increases the greater the increase in peak load  $Q_u$ . Obviously this also represents increased peak load with an increased embedment ratio as would be expected. These results obtained are again similar existing literature.

### 8.1.4 Variation of Break-out Factor with Embedment Ratio

The break-out factor calculations were only conducted the plate anchor results. It is observed that the general trend for the break-out factor is to increase with increased embedment ratio. It is noted that for  $H/B = 3$  the break-out factor decreases and does not fit the expected trend. Merifield et al (1999) and Ilamparuthi (2002) both comment on the trend of the break-out factor against embedment ratio and suggest that the break-out factor should increase with increased embedment ratio until it plateaus out at an approximate constant value. Therefore, viewing the results obtained in this paper it would be expected that larger values of break-out factor should be obtained for embedment ratios of  $H/B = 2$  and 3. Therefore suggesting that some of the results obtained are a little smaller than should be expected.

### 8.1.5 PIV Analysis

The PIV analysis completed for the plate anchors and buried pipelines were all produced by Michael Hobson as part of research that was cooperatively conducted in conjunction with this research project. The results displayed are very good and display the expected

failure mechanisms, thus providing better understanding of the topic and giving creditation to the research conducted.

## **8.2 Future Work**

### **8.2.1 Plate Anchor**

There are a few options available for future research in this field. Trial test that were conducted as part of this research accidentally induced a layered soil profile and provided some interesting results. It would therefore be appropriate and interesting to further investigate this, whether the layers were made of differing solid (gravel and sand) or differing moisture contents between levels.

As mentioned, if time permitted extended investigations into group anchors and three drimensional anchors was to be conducted. However, this provides a great opportunity for future work to be conducted in these fields. An introductory literature review for group anchors has been conducted and included as part of this research paper.

### **8.2.2 Pile Anchor**

As mentioned, the failure mechanisms for pile anchors have not been able to be observed as part of this research and therefore PIV analysis could provide this solution. It is also possible just to take the research conducted in this paper in regards to pile anchors and take it further and obtain the desirable results. Just as with plate anchors it is also possible to extend pile anchor research into including three dimensional results and/or group piles.

---

# References



1. Abbo, A.J. 1997. 'Finite element algorithms for elastoplasticity and consolidation', PhD. thesis, Department of Civil, Surveying and Environmental Engineering, University of Newcastle, Callaghan, NSW, Australia.
2. Abbo, A.J. & Sloan, S.W. 1998. SNAC (solid nonlinear analysis code), a finite element program for the analysis of elastoplasticity and consolidation. User manual version 1.0. Department of Civil, Surveying and Environmental Engineering, University of Newcastle, Callaghan, NSW, Australia.
3. Balla, A. 1961. 'The resistance of breaking-out of mushroom foundations for pylons', Proceedings of the 5th International Conference on Soil Mechanics and Foundation Engineering, Paris, France. A.A. Balkema, Rotterdam, The Netherlands. Vol. 1, pp. 569-576.
4. Bouazza, A. 1996, 'Pull Out Resistance of a Plate Anchor in a Three Layered Sand', 7th Australia New Zealand Conference on Geomechanics: Geomechanics in a Changing World Conference Proceedings, Barton, ACT, Institution of Engineers, Australia, pp. 601-603.
5. Bouazza, A., Dickin, E., Subba Rao, K.S. & Kumar, J. 1996, 'Vertical Uplift Capacity of Horizontal Anchors', Journal of Geotechnical Engineering, vol. 122, no. 2, pp.163-165.
6. Bransby, M.F., Newson, T.A., Brunning, P. & Davies, M.C.R. 2001, 'Numerical and Centrifuge Modelling of the Upheaval resistance of Buried Pipelines', Proceedings of OMAE '01 20th International Conference on Offshore Mechanics and Arctic Engineering, Rio de Janeiro, Brazil, pp. 1- 8.

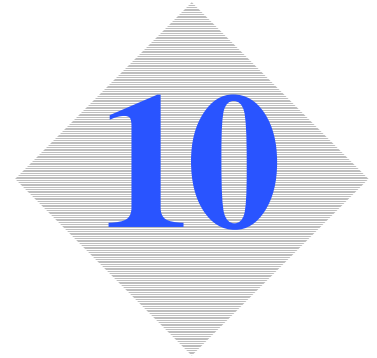
- 
7. Bransby, M.F., Newson, T.A. & Brunning, P. 2002a, 'Centrifuge modelling of upheaval capacity of pipelines in liquefied clay', ISOPE 2002 Conference, Kita-Kyushu, Japan, (Paper #: 02-JSC-243).
  8. Bransby, M.F., Newson, T.A., Davies, M.C.R. & Brunning, P. 2002b, 'Physical Modelling of Upheaval Resistance of Buried Offshore Pipelines', 4th Int Conf. Physical Modelling in Geomechanics, St. Johns, Newfoundland, pp. 899-904.
  9. Chattopadhyay, B.C. & Pise, P.J. 1986, 'Uplift capacity of Piles in Sand', Journal of Geotechnical Engineering, vol. 112, no. 9, pp. 888-904.
  10. Cheuk, C.Y., White, D.J. & Bolton, M.D. 2008, 'Uplift Mechanics of Pipes Buried in Sand', Journal of Geotechnical and Geoenvironmental Engineering, vol.134, no. 2, pp. 154-163.
  11. Clemence, S.P. (ed.) 1985, 'Uplift Behaviour of Anchor Foundations in Soil', American Society of Civil Engineers, New York, United States of America.
  12. Clemence, S.P. & Veesaert, C.J. 1997. 'Dynamic pullout resistance of anchors in sand', In Proceedings of the International Conference on Soil-Structure Interaction, Roorkee, India, pp. 389-397.
  13. Cole, A.J.S. 2009, 'A Comprehensive Study of Footing on  $c - \phi$  Soil Slopes - Numerical and Physical Modelling', Student Project, University of Southern Queensland, Toowoomba, Australia.
  14. Das, B.M. 1990, 'Development in Geotechnical Engineering', vol. 50: Earth Anchors, Elsevier Science Publishers B.V., Amsterdam, Netherlands.
  15. Das, B.M. 1999, 'Shallow Foundations: Bearing Capacity and Settlement', CRC Press LLC, Boca Raton, Florida, United States of America.
  16. Das, B.M. 2004, 'Foundation Engineering', 5th edn, Brooks/Cole - Thomson Learning, Pacific Grove, California, United States of America.
  17. De Nicola, A. & Randolph, M.F., 1993. 'Tensile and Compressive Shaft Capacity of Piles in Sand', Journal of Geotechnical Engineering, ASCE, Vol 119, No. 12, pp. 1952-1973.
  18. Dickin, E.A. 1988, 'Uplift Behavior of Horizontal Anchor Plates in Sand', Journal of Geotechnical Engineering, vol. 114, no.11, pp. 1300-1316.
  19. Gan, J.K.M., Fredlund, D.G. & Rahardjo, H. 1988. 'Determination of the shear strength parameters of an unsaturated soil using the direct shear test', Canadian Geotechnical Journal, 25(3) pp. 500-510.
  20. Geddes, J.D. & Murray, E.J. 1996, 'Plate Anchor Groups Pulled Vertically in Sand', Journal of Geotechnical Engineering, vol. 122, no. 7, pp. 509-515.
  21. Gerrard, C.M. & Cameron, D.A. 1988, 'Inclined Uplift capacity of various Ground Anchors', Fifth Australian-New Zealand Conference on Geomechanics, Sydney, Australia, pp. 497-502.

- 
22. Hobson, M.A. 2010, 'An Analysis of Retaining Wall Failure Using Particle Image Velocimetry', Student Project, University of Southern Queensland, Toowoomba, Australia.
  23. Ilamparuthi, E.A., Dickin, E.A. & Muthukrisnaiah K. 2002, 'Experimental investigation of the uplift behaviour of circle plate anchors embedded in sand', *Canadian Geotechnical Journal*, vol 39, no. 3, pp. 648-664.
  24. Kouzer, K.M., & Kumar, J. 2009, 'Vertical Uplift Capacity of Equally Spaced Horizontal Strip Anchors in Sand', *International Journal of Geomechanics*, vol.9, no.5, pp. 230-236.
  25. Merifield, R.S., Pearce, A., Yu, H.S. & Sloan, S.W. 1999, 'Stability of Anchor Plates', *Proceedings 8th Australia New Zealand Conference on Geomechanics*, Hobart, Hobart, Australia, pp. 553-559.
  26. Merifield, R.S. & Sloan, S.W. 2006, 'The ultimate pullout capacity of anchors in frictional soils', *Proceedings of the Tenth International Conference on Computer Methods and Advances in Geomechanics*, Rotterdam, pp. 852-868.
  27. Merifield, R.S., Lyamin, A.V. & Sloan, S.W. 2005, 'Stability of Inclined Strip Anchors in Purely Cohesive Soil', *Journal of Geotechnical and Geoenvironmental Engineering*, vol. 131, no. 6, pp.792-799.
  28. Mors, H. 1959. 'The behaviour of mast foundations subject to tensile forces. *Bautechnik*, 10: 367-378.
  29. Murray, E.J. and Geddes, J.D. 1987. 'Uplift of anchor plates in sand.', *Journal of Geotechnical Engineering*, ASCE, 113(3): 202-215.
  30. Narasimha Rao, S. & Prasad, Y.V.S.N., 1993. 'Uplift of Pile Anchors Subjected to Lateral Cyclic Loading', *Journal of Geotechnical Engineering*, ASCE, Vol. 119, No. 4. pp. 786-790.
  31. Periera Pinto, C. & Mahler, C.F. 1988, 'Behaviour of Anchors in Residual Soils', *Fifth Australia-New Zealand Conference of Geomechanics*, Sydney, Australia, pp. 309-313.
  32. Rowe, R.K. & Davis, E.H. 1982, 'The behaviour of anchor plates in sand', *Geotechnique*, vol. 32, no.1, pp. 25-41.
  33. Saran, S., Ranjan, G. & Nene, A.S. 1986. 'Soil anchors and constitutive laws', *Journal of Geotechnical Engineering*, ASCE, 112(12): 1084-1100.
  34. Schupp, J., Byrne, B.W., Eacott, N., Martin, C.M., Oliphant, J., Maconochie, A. & Cathie, D. 2006. 'Pipeline Unburial Behaviour in Loose Sand', *Proceedings of OMAE'06 - 25th International Conference on Offshore Mechanics and Arctic Engineering*, Hamburg, Germany.
  35. Shahin, M.A. & Jaksa, M.B. 2006, 'Pullout capacity of small ground anchors by direct cone penetration test methods and neural networks', *Canadian Geotechnical Journal*, vol. 43, no. 6, pp. 626-637.

- 
36. Shanker, K., Basudhar, P.K, & Patra, N.R., 2007. 'Uplift Capacity of Single Piles: Predictions and Performance', *Geotech Geol Eng*, 25. pp. 151-161.
  37. Smith, C.S., 1998. 'Limit loads for an anchor/trapdoor embedded in an associated coulomb soil'. *International Journal for Numerical and Analytical Methods in Geomechanics*, 22: 855-865.
  38. Su, W. & Fragaszy, J. 1987, 'Uplift Testing of Model Anchors', *Journal of Geotechnical Engineering*, vol.114, no.9, pp. 961-983.
  39. Subba Rao, K.S. & Kumar, J. 1994, 'Vertical Uplift Capacity of Horizontal Anchors', *Journal of Geotechnical Engineering*, vol. 120, no. 7, pp. 1134-1147.
  40. Sutherland, H.B. 1965. 'Model studies of shaft raising through cohesionless soils', In *Proceedings of the 6th International Conference on Soil Mechanics and Foundation Engineering*, Montreal, Vol. 2, pp. 410-413.
  41. Sutherland, H.B., Finlay, T.W. & Fadl, M.O. 1982. 'Uplift capacity of embedded anchors in sand', In *Proceedings of the 3rd International Conference on the Behaviour of Offshore Structures*, Cambridge, Mass., Vol. 2, pp. 451-463.
  42. Trautmann, C.H., O'Rourke, T.D. & Kulhawy, F.H., 1985. 'Uplift Force-Displacement Response of Buried Pipe', *Journal of Geotechnical Engineering*, Vol. 111, No. 9, pp. 1061-1076.
  43. University of Southern Queensland, 2008. 'Shear-strenght Tests', ENV2901 Soil and water engineering practice 1 - (2) Laboratory works in soil mechanics, University of Southern Queensland, Toowoomba, pp. 73-78.
  44. White, D.J., Cheuk, C.Y. & Bolton, M.D., 2008. 'The Uplift Resistance of Pipes and Plate Anchors Buried in Sand', *Geotechnique* 58, No. 10, pp. 771 - 779.

---

# Appendices



## **10.1 Appendix A - Project Specification**



Examiner/Co-examiner: \_\_\_\_\_

## 10.2 Appendix B - Plate Anchor Results



**Figure 10-1.** Horizontal Plate Anchor Failure  $H/B = 2$

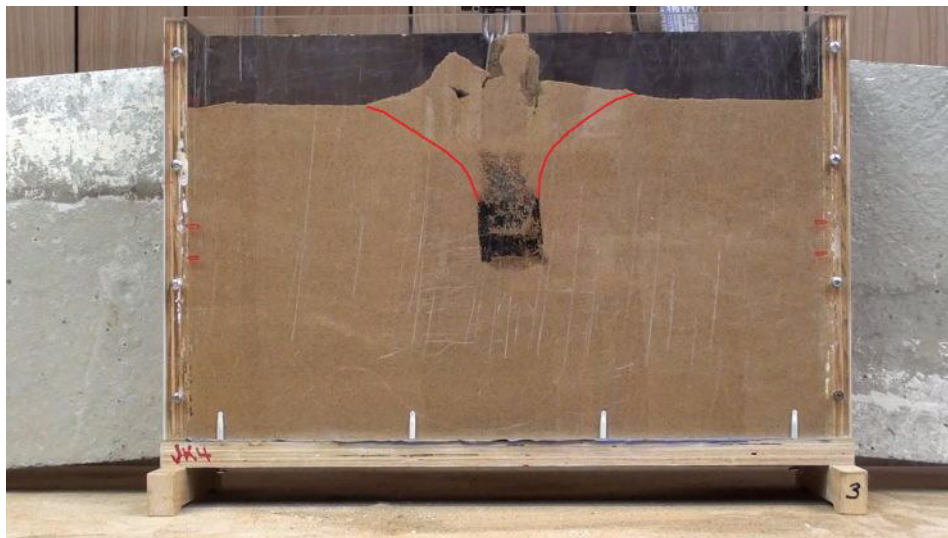


**Figure 10-2.** Horizontal Plate Anchor Failure  $H/B = 2$  - Highlighted Failure Plane



**Figure 10-3.** Horizontal Plate Anchor Failure  $H/B = 3$

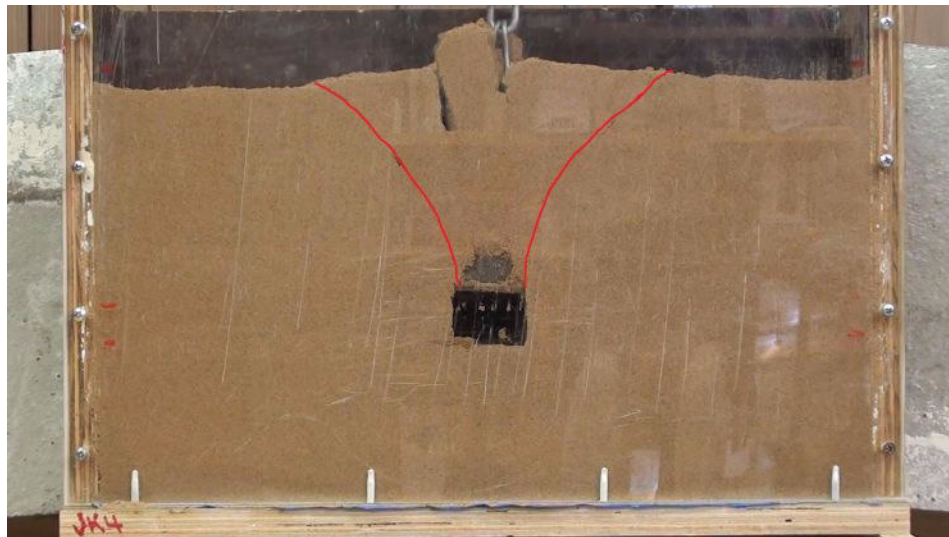


**Figure 10-4.** Horizontal Plate Anchor Failure  $H/B = 3$  - Highlighted Failure Plane



**Figure 10-5.** Horizontal Plate Anchor Failure  $H/B = 4$

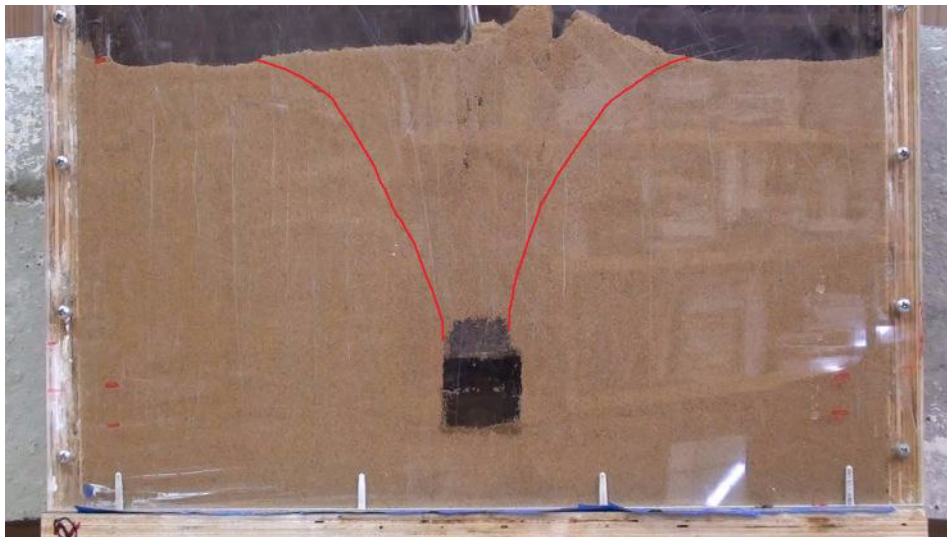


**Figure 10-6.** Horizontal Plate Anchor Failure  $H/B = 4$  - Highlighted Failure Plane



**Figure 10-7.** Horizontal Plate Anchor Failure  $H/B = 5$



**Figure 10-8.** Horizontal Plate Anchor Failure  $H/B = 5$  - Highlighted Failure Plane

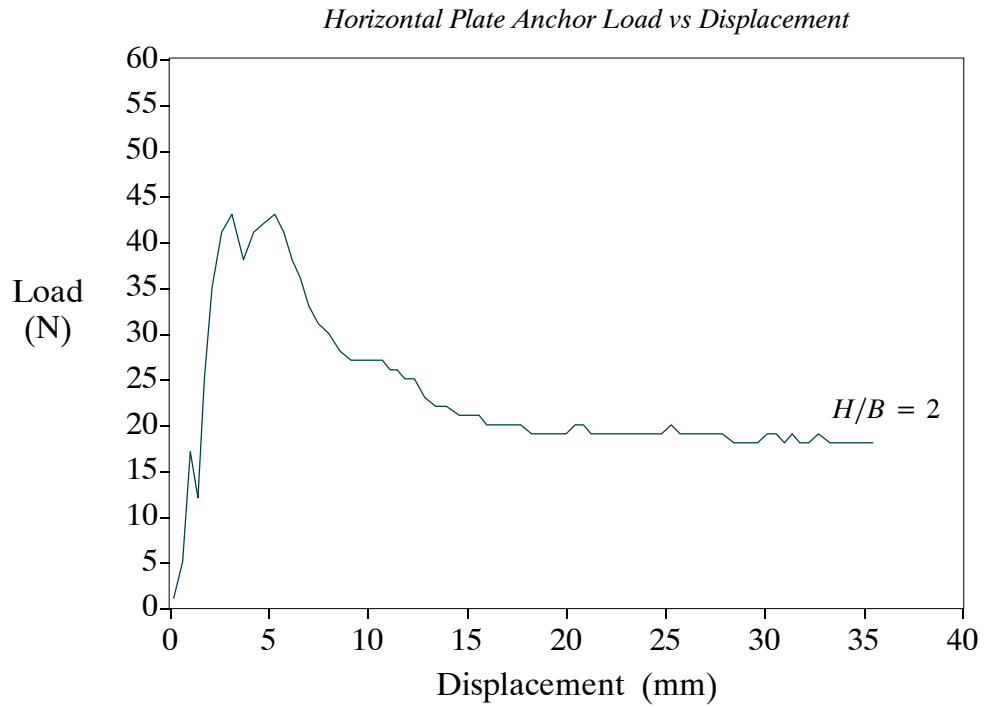


**Figure 10-9.** Horizontal Plate Anchor Load vs Displacement Diagram H/B = 2

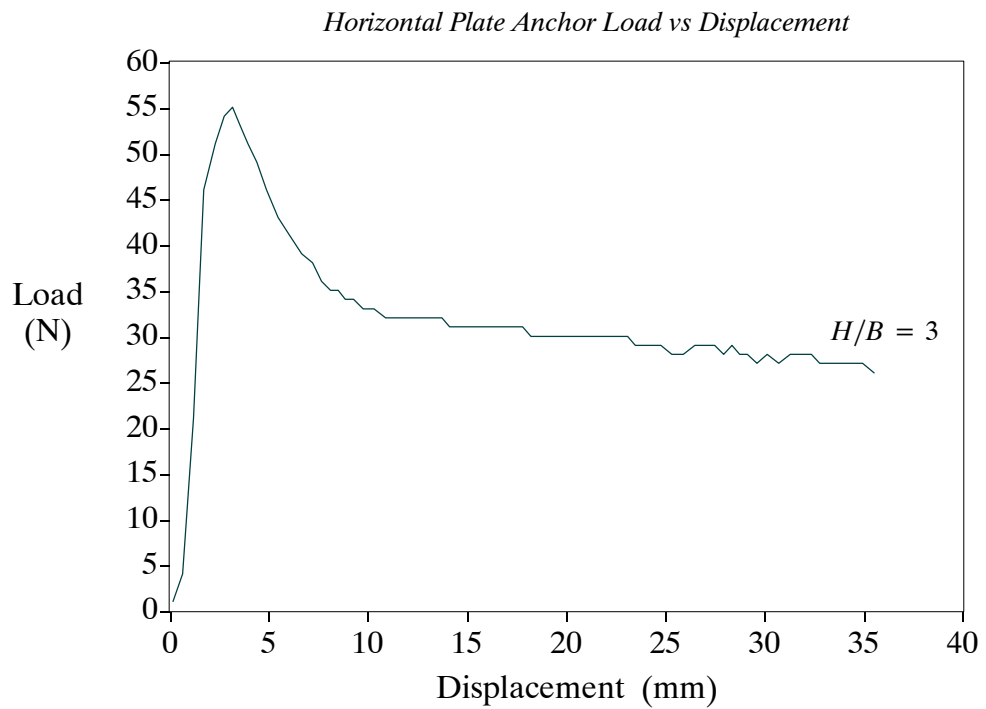


**Figure 10-10.** Horizontal Plate Anchor Load vs Displacement Diagram H/B = 3

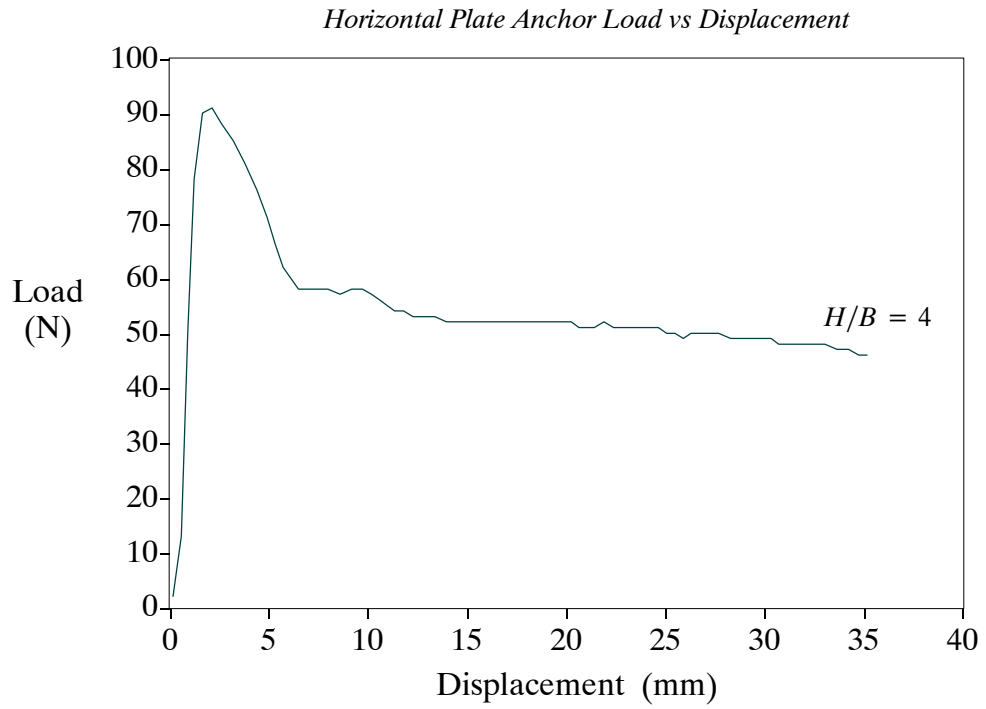


**Figure 10-11.** Horizontal Plate Anchor Load vs Displacement Diagram H/B = 4

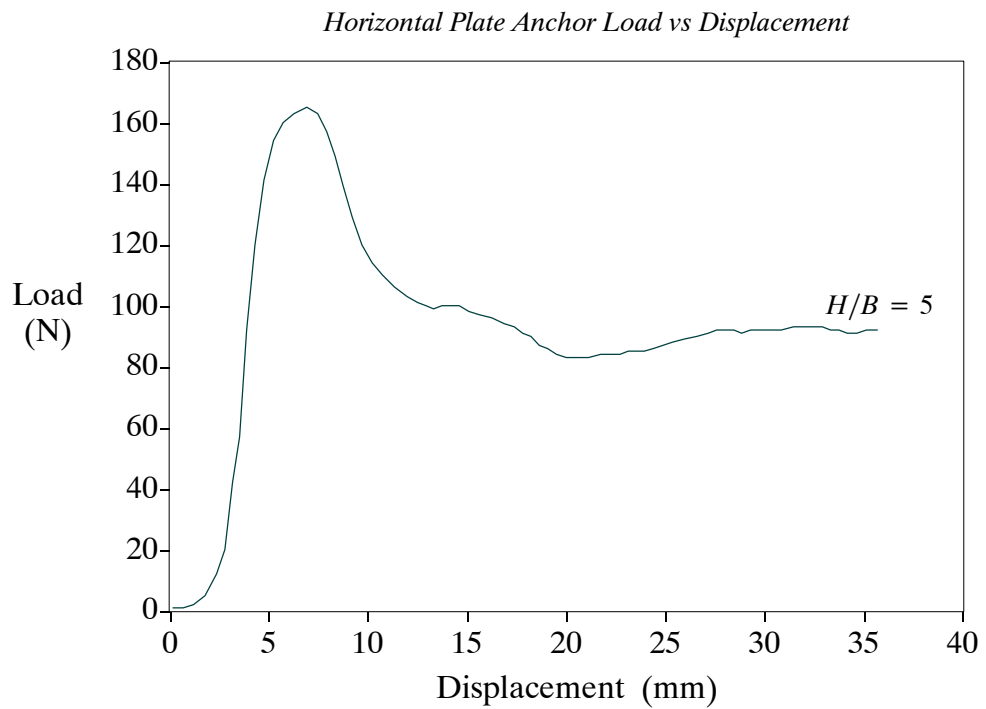


**Figure 10-12.** Horizontal Plate Anchor Load vs Displacement Diagram H/B = 5

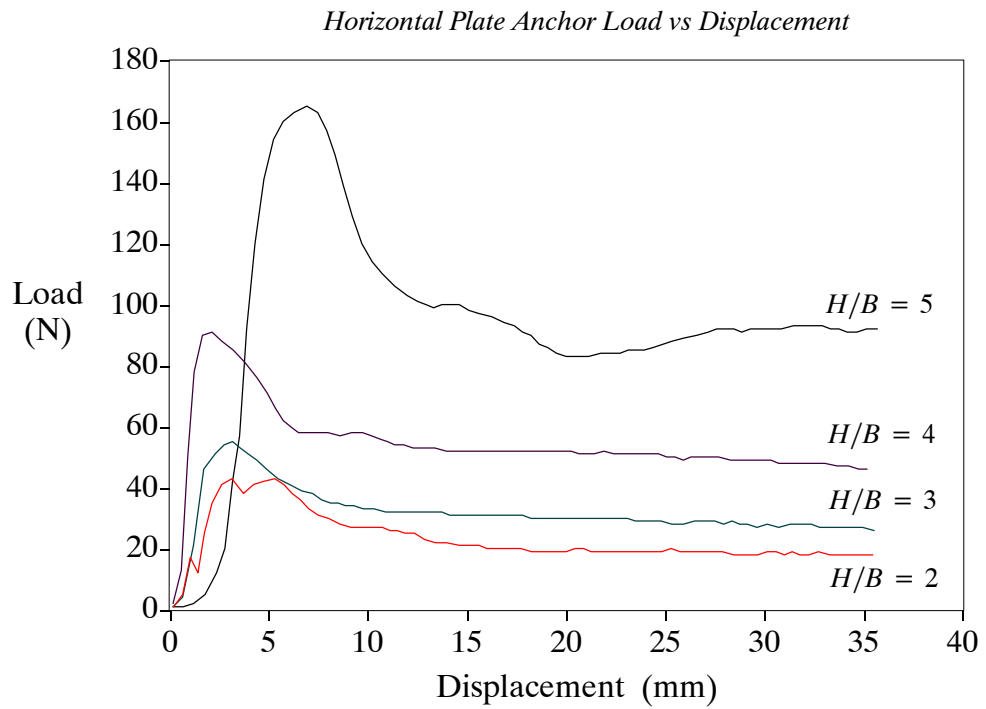


**Figure 10-13.** Horizontal Plate Anchor Load vs Displacement Diagram Combined Results

### 10.3 Appendix C - Buried Pipeline Results



**Figure 10-14.** Buried Pipeline Failure H/B = 2

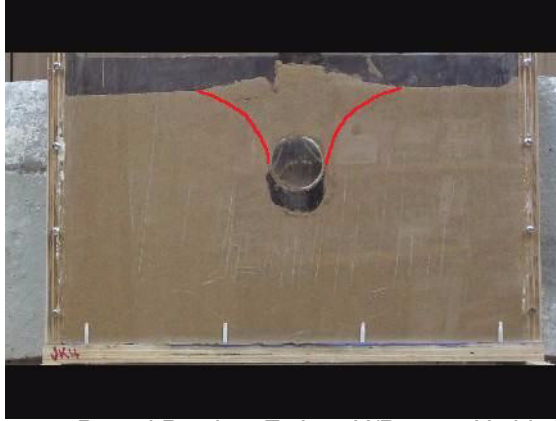


Figure 10-15. Buried Pipeline Failure  $H/B = 2$  - Highlighted Failure



Figure 10-16. Buried Pipeline Failure  $H/B = 3$

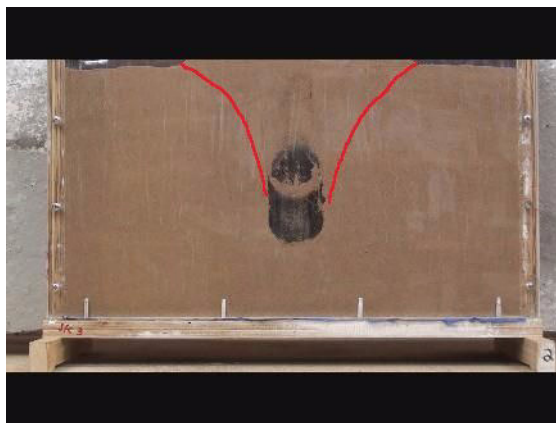


Figure 10-17. Buried Pipeline Failure  $H/B = 3$  - Highlighted Failure



Figure 10-18. Buried Pipeline Failure  $H/B = 4$

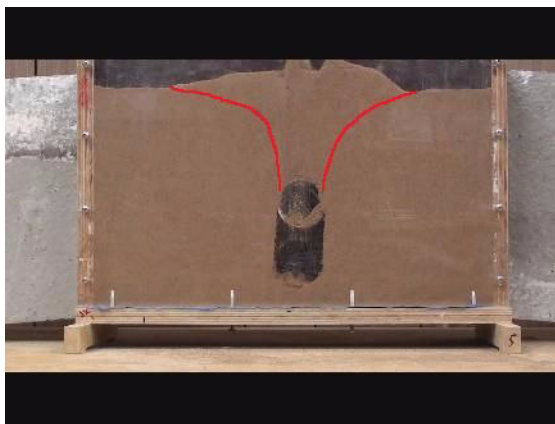


Figure 10-19. Buried Pipeline Failure  $H/B = 4$  - Highlighted Failure

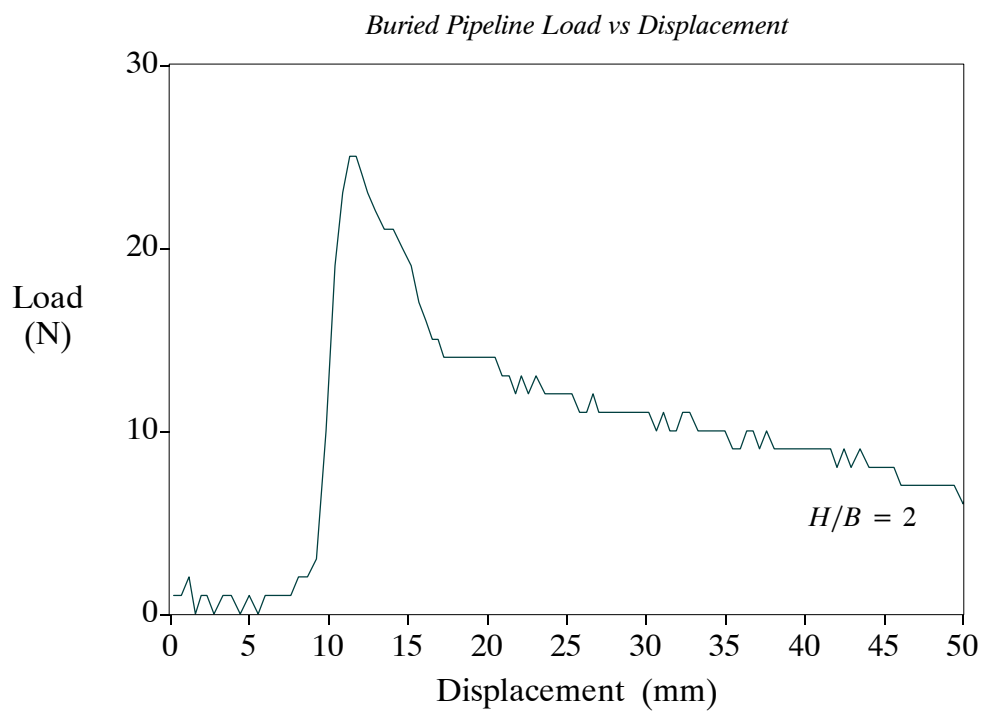
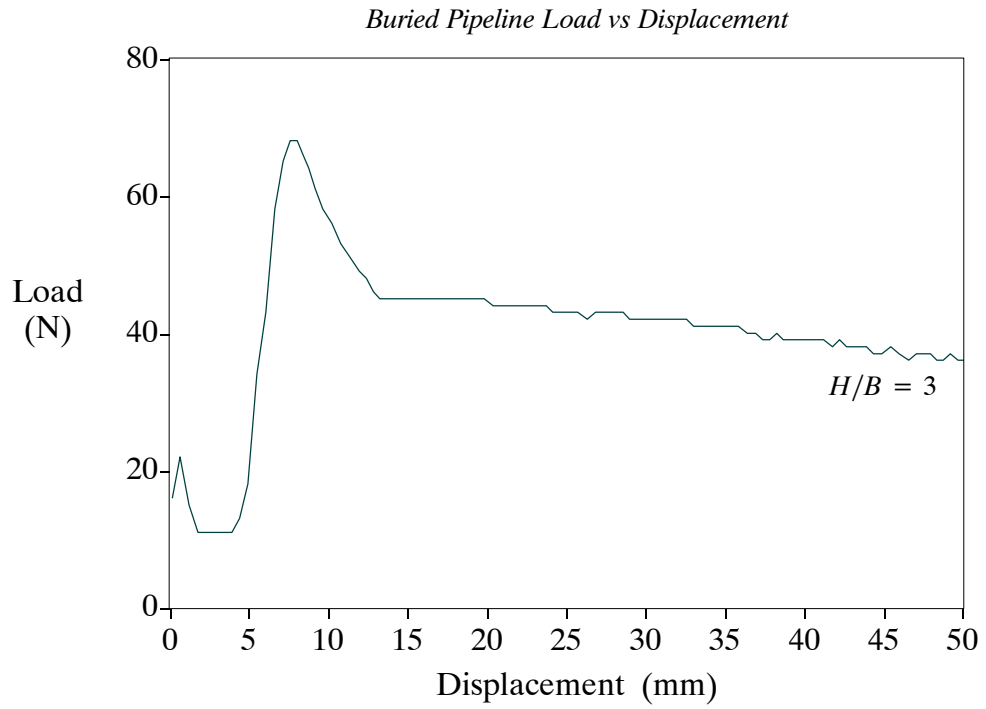
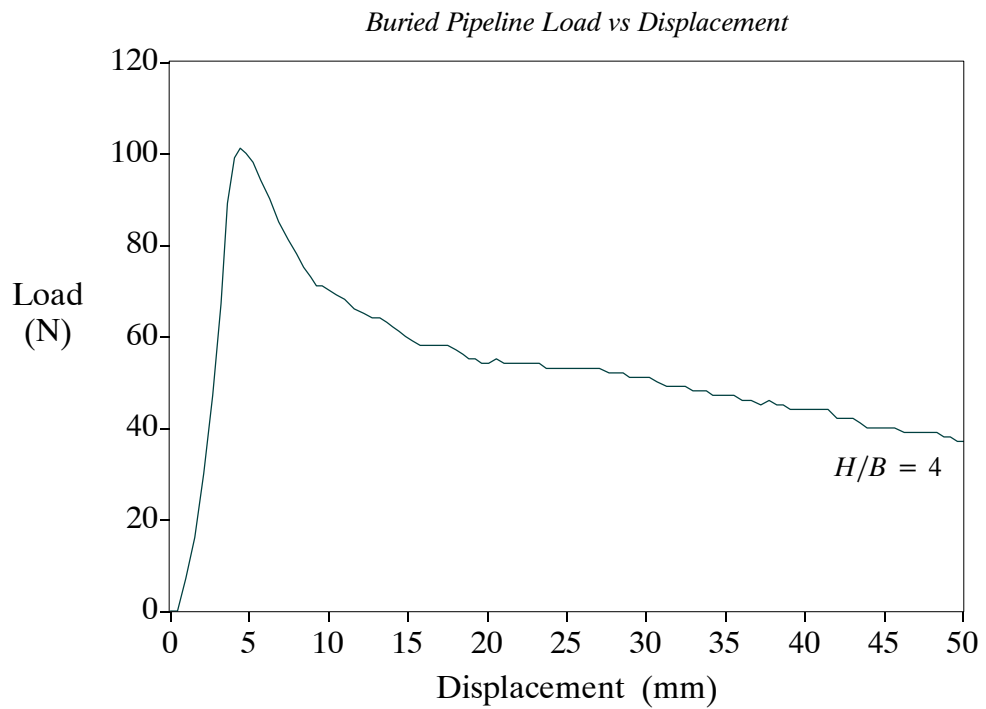


Figure 10-20. Buried Pipeline Load vs Displacement Diagram  $H/B = 2$



**Figure 10-21.** Buried Pipeline Load vs Displacement Diagram H/B = 3



**Figure 10-22.** Buried Pipeline Load vs Displacement Diagram H/B = 4

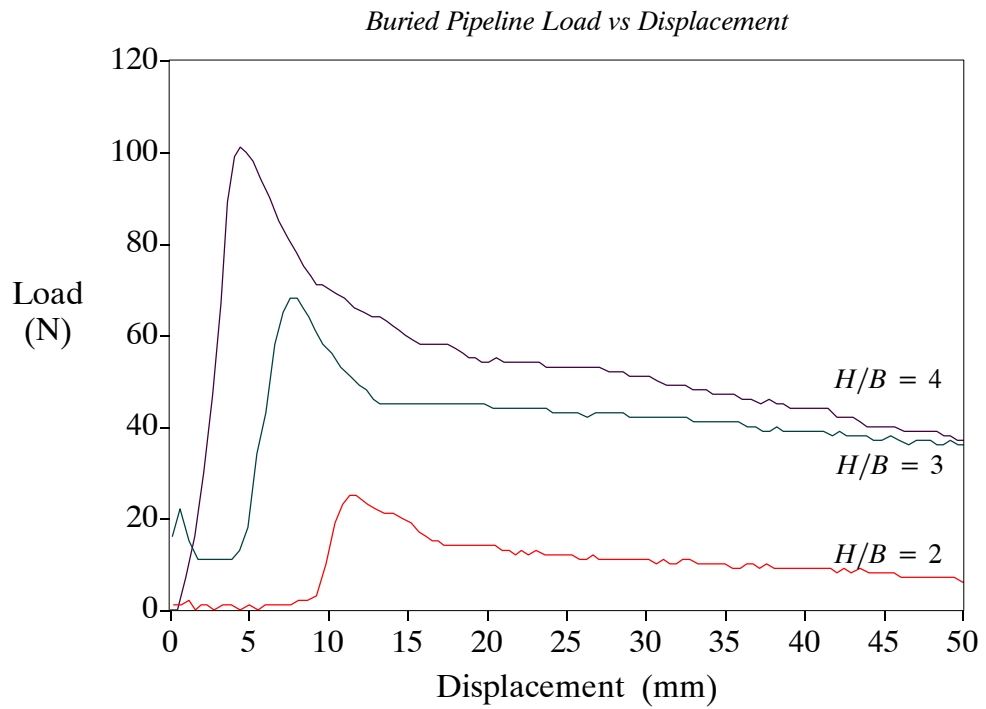


**Figure 10-23.** Buried Pipeline Load vs Displacement Diagram Combined Results

### 10.4 Appendix D - Pile Anchor Results

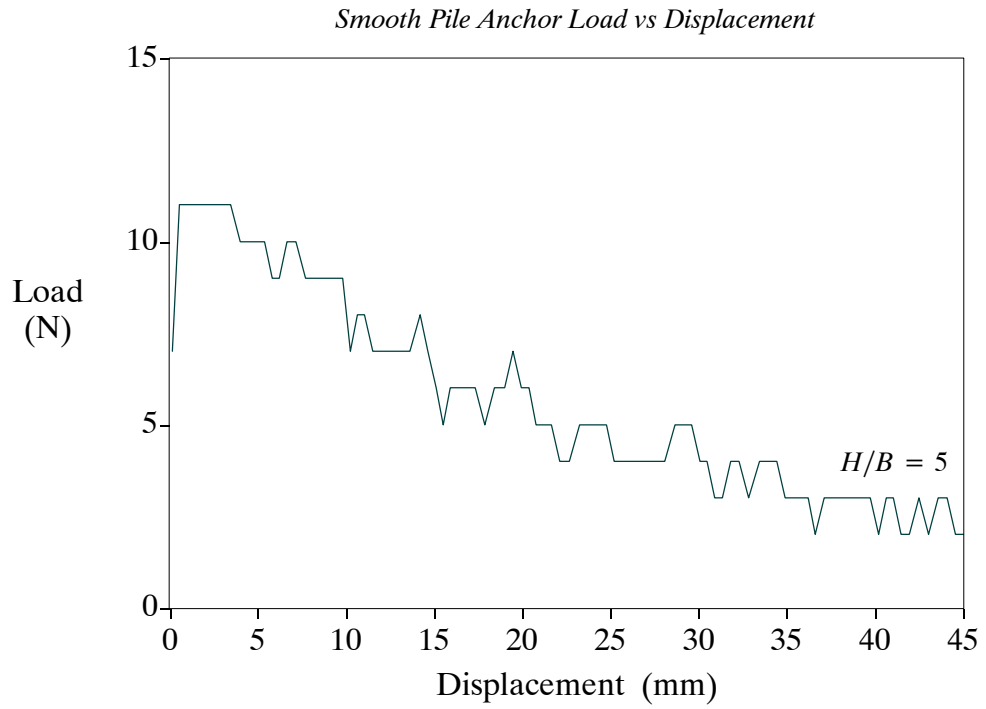


**Figure 10-24.** Smooth Pile Anchor Load vs Displacement  $H/B = 5$

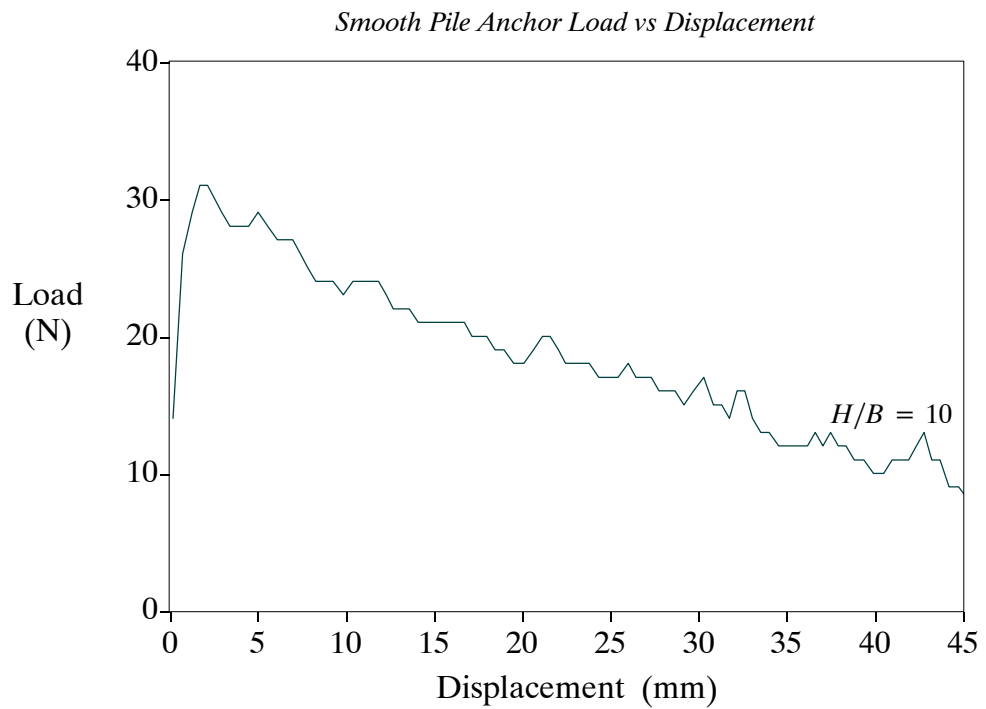


**Figure 10-25.** Smooth Pile Anchor Load vs Displacement  $H/B = 10$

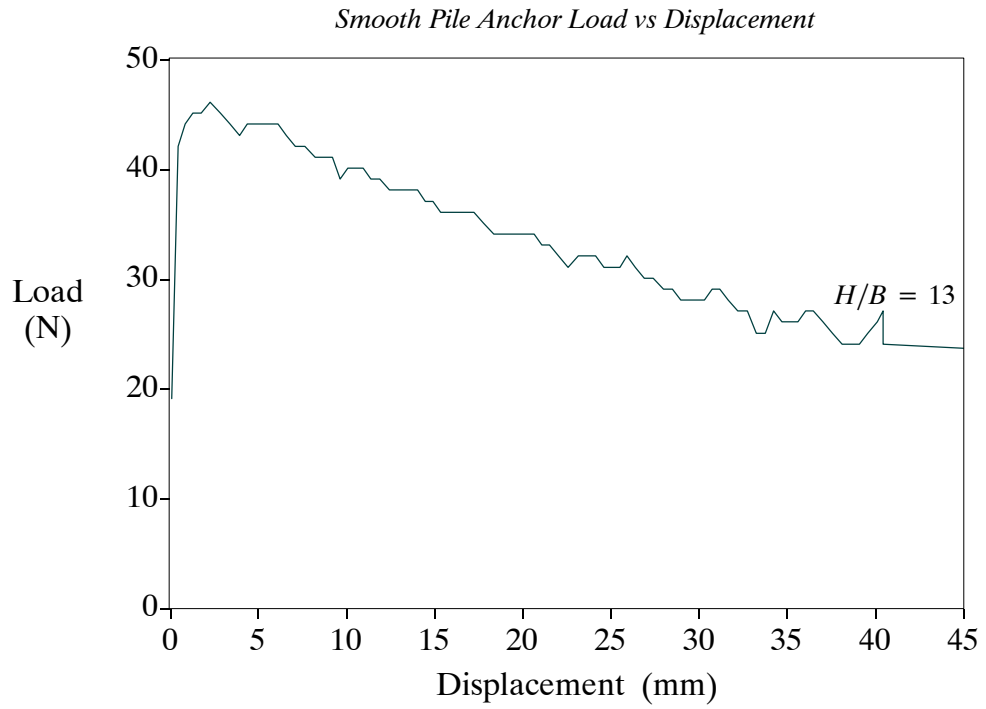


**Figure 10-26.** Smooth Pile Anchor Load vs Displacement  $H/B = 13$

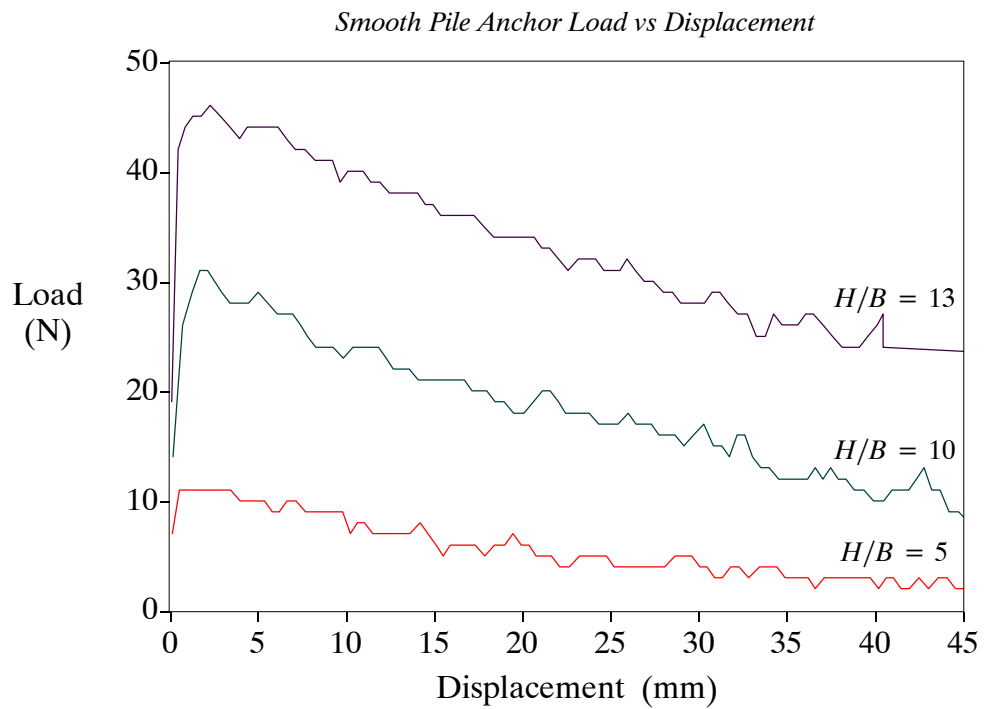


**Figure 10-27.** Smooth Pile Anchor Load vs Displacement Combined

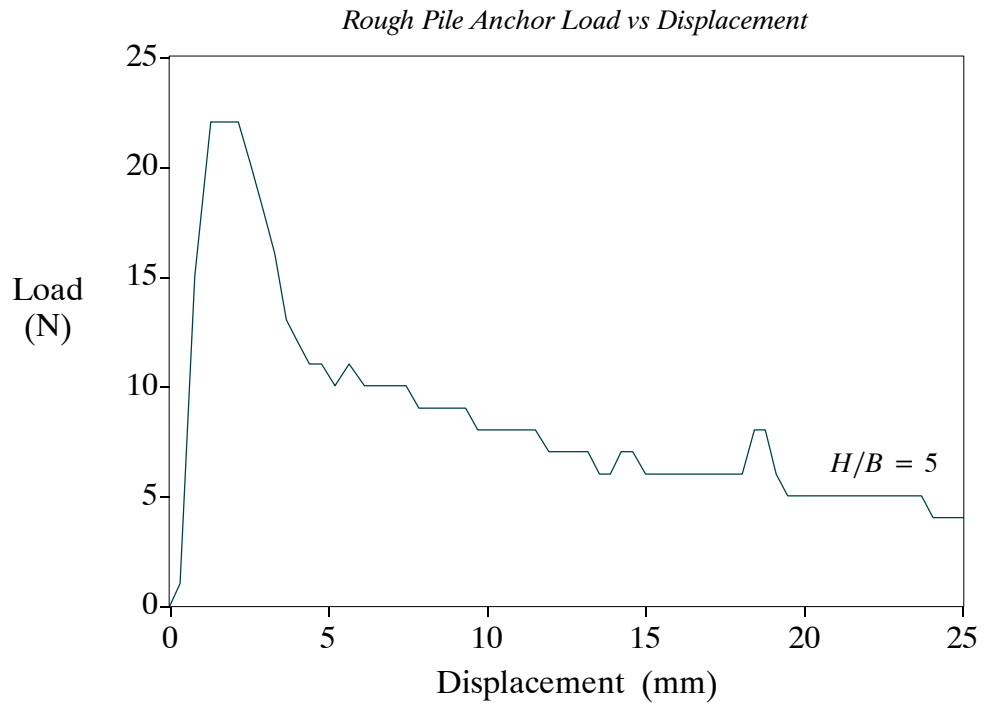


**Figure 10-28.** Rough Pile Anchor Load vs Displacement H/B = 5

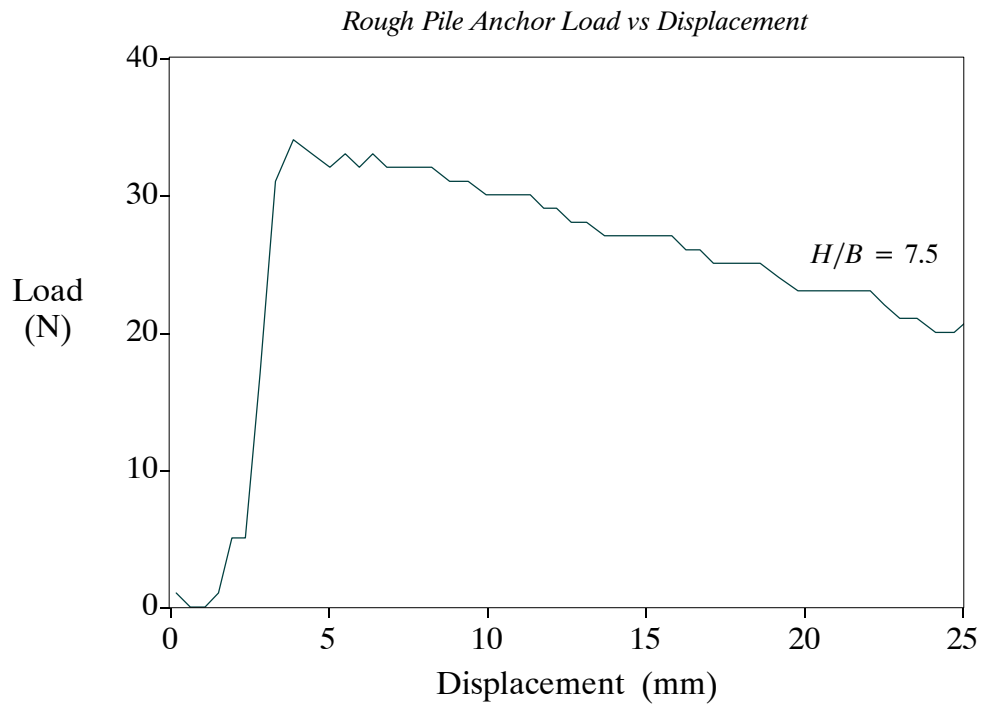


**Figure 10-29.** Rough Pile Anchor Load vs Displacement H/B = 7.5

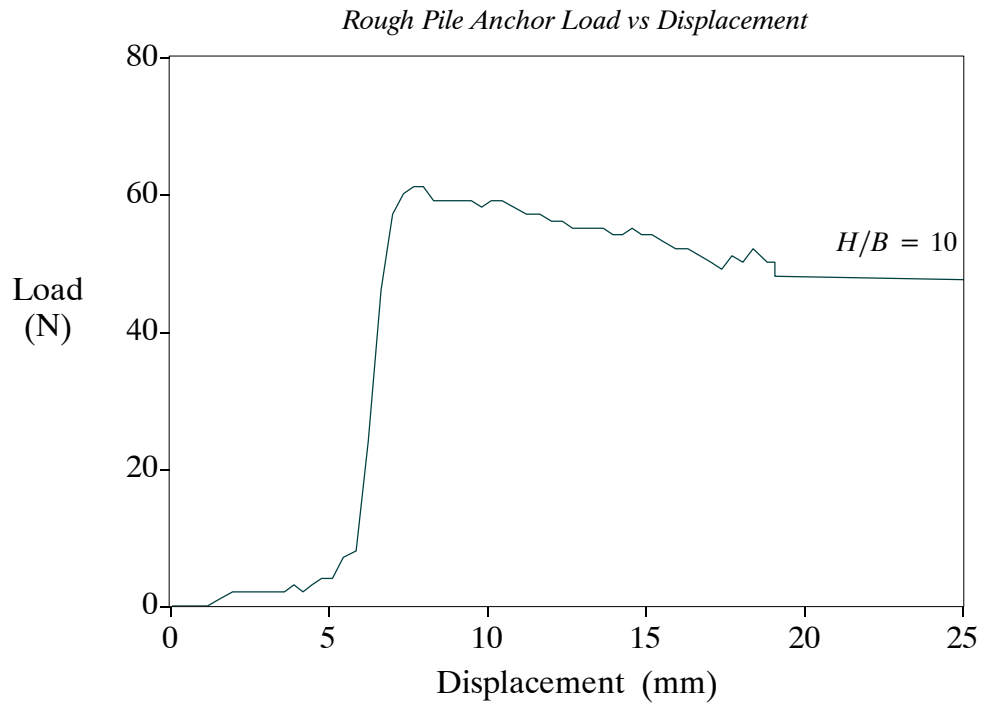


**Figure 10-30.** Rough Pile Anchor Load vs Displacement H/B = 10

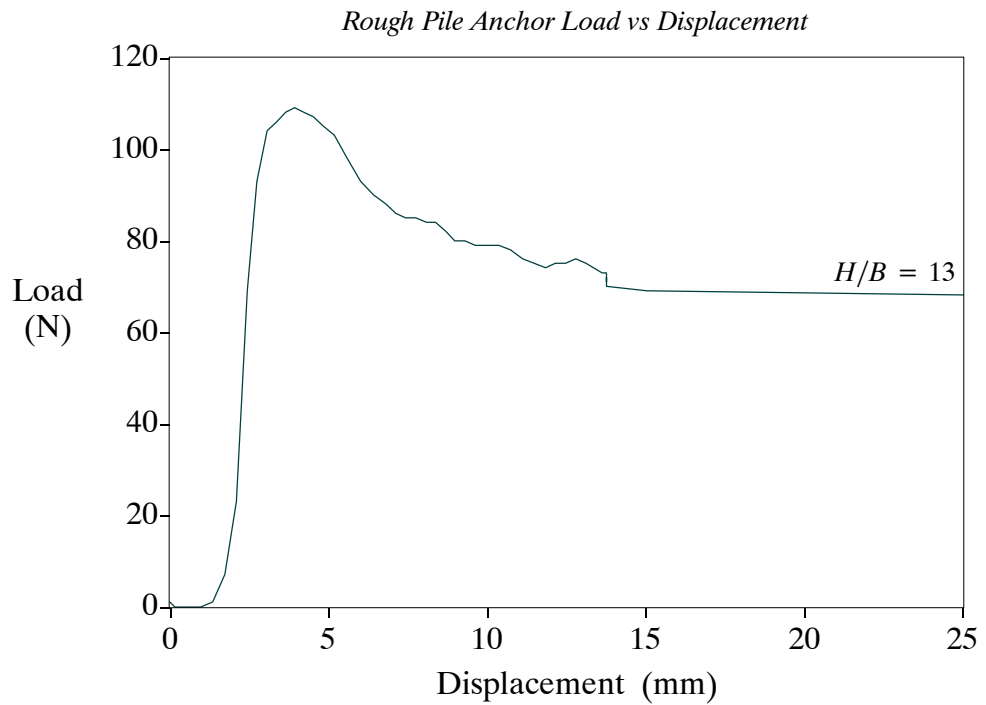


**Figure 10-31.** Rough Pile Anchor Load vs Displacement H/B = 13

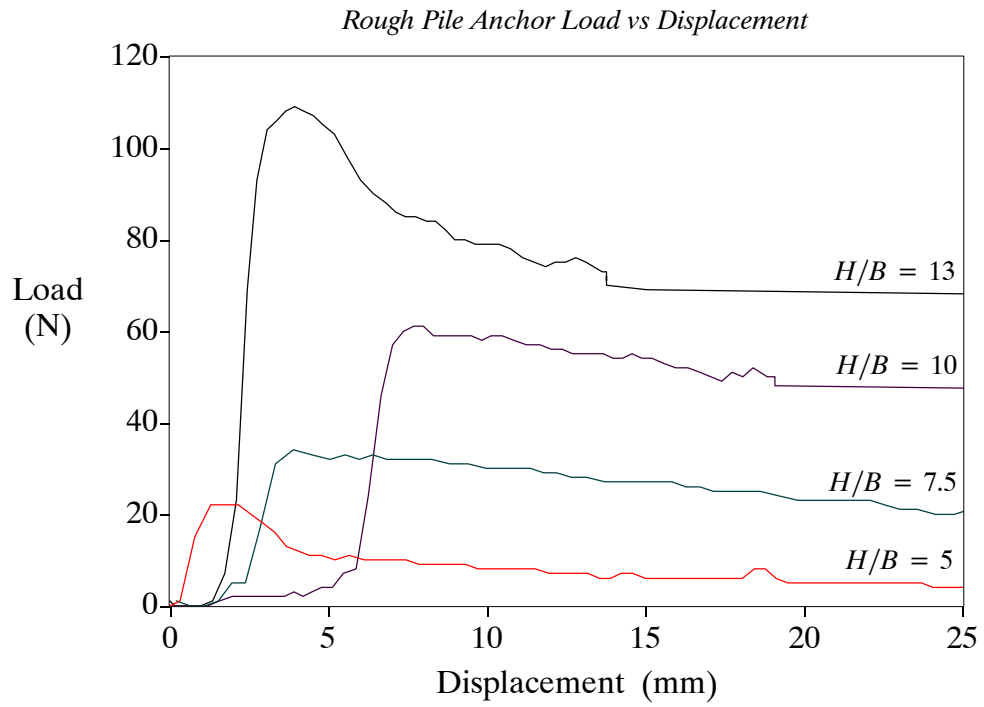


**Figure 10-32.** Rough Pile Anchor Load vs Displacement Combined